

## CLASSICAL QUANTUM MECHANICS

Randell L. Mills, BlackLight Power, Inc., 493 Old Trenton Road, Cranbury, NJ 08512  
(609)490-1090, rmills@blacklightpower.com, www.blacklightpower.com

Despite its successes, quantum mechanics (QM) has remained mysterious to all who have encountered it. Starting with Bohr and progressing into the present, the departure from intuitive, physical reality has widened. The connection between quantum mechanics and reality is more than just a “philosophical” issue. It reveals that quantum mechanics is not a correct or complete theory of the physical world and that inescapable internal inconsistencies and incongruities arise when attempts are made to treat it as a physical as opposed to a purely mathematical “tool.” Some of these issues are discussed in a review by Laloë [1]. In an attempt to provide some physical insight into atomic problems and starting with the same essential physics as Bohr of  $e^-$  moving in the Coulombic field of the proton and the wave equation as modified by Schrödinger, a classical approach is explored which yields a model which is remarkably accurate and provides insight into physics on the atomic level. The proverbial view deeply seated in the wave-particle duality notion that there is no large-scale physical counterpart to the nature of the electron may not be correct. Physical laws and intuition may be restored when dealing with the wave equation and quantum mechanical problems. Specifically, a theory of classical quantum mechanics (CQM) is derived from first principles that successfully applies physical laws on all scales. Rather than use the postulated Schrödinger boundary condition: “ $\Psi \rightarrow 0$  as  $r \rightarrow \infty$ “, which leads to a purely mathematical model of the electron, the constraint is based on experimental observation. Using Maxwell’s equations, *the classical wave equation is solved with the constraint that the bound  $n = 1$ -state electron cannot radiate energy.* By further application of Maxwell’s equations to electromagnetic and gravitational fields at particle production, the Schwarzschild metric (SM) is derived from the classical wave equation which modifies general relativity to include conservation of spacetime in addition to momentum and matter/energy. The result gives a natural relationship between Maxwell’s equations, special relativity, and general relativity. CQM holds over a scale of spacetime of 85 orders of magnitude—it correctly predicts the nature of the universe from the scale of the quarks to that of the cosmos. A review is given by Landvøgt [2].

Key Words: Maxwell’s equations, nonradiation, quantum theory, special and general relativity, particle masses, cosmology, wave equation

## INTRODUCTION

The hydrogen atom is the only real problem for which the Schrödinger equation can be solved without approximations; however, it only provides three quantum numbers—not four, and inescapable disagreements between observation and predictions arise from the later postulated Dirac equation as well as the Schrödinger equation [3-5]. Furthermore, unlike physical laws such as Maxwell's equations, it is always disconcerting to those that study quantum mechanics that both must be accepted without any underlying physical basis for fundamental observables such as the stability of the hydrogen atom in the first place. In this instance, a circular argument regarding definitions for parameters in the wave equation solutions and the Rydberg series of spectral lines replaces a first-principles-based prediction of those lines [3-5]. Nevertheless, the application of the Schrödinger equation to real problems has provided useful approximations for physicists and chemists. Schrödinger interpreted  $e\Psi^*(x)\Psi(x)$  as the charge-density or the amount of charge between  $x$  and  $x + dx$  ( $\Psi^*$  is the complex conjugate of  $\Psi$ ). Presumably, then, he pictured the electron to be spread over large regions of space. After Schrödinger's interpretation, Max Born, who was working with scattering theory, found that this interpretation led to inconsistencies and he replaced the Schrödinger interpretation with the probability of finding the electron between  $x$  and  $x + dx$  as

$$\int \Psi(x)\Psi^*(x)dx \quad (1)$$

Born's interpretation is generally accepted. Nonetheless, interpretation of the wave function is a never-ending source of confusion and conflict. Many scientists have solved this problem by conveniently adopting the Schrödinger interpretation for some problems and the Born interpretation for others. This duality allows the electron to be everywhere at one time—yet have no volume. Alternatively, the electron can be viewed as a discrete particle that moves here and there (from  $r = 0$  to  $r = \infty$ ), and  $\Psi\Psi^*$  gives the time average of this motion. Despite its successes, after decades of futility, QM and the intrinsic Heisenberg Uncertainty Principle have not yielded a unified theory, are still purely mathematical, and have yet to be shown to be based in reality [5]. Both are based on circular arguments that the electron is a point with no volume with a vague probability wave requiring that the electron have multiple positions and energies including negative and infinite energies simultaneously. It may be time to revisit the 75 year old notion that fundamental particles such as the electron are one or zero dimensional and obey different physical laws than objects comprised of fundamental particles and the even more disturbing view that fundamental particles don't obey physical laws—rather they obey mathematics devoid of physical laws. Perhaps mathematics does not determine physics. It only models physics.

The Schrödinger equation was originally postulated in 1926 as having a solution of the one electron atom. It gives the principal energy levels of the hydrogen atom as eigenvalues of eigenfunction solutions of the Laguerre differential equation. But, as the principal quantum number  $n \gg 1$ , the eigenfunctions become nonsensical since they are sinusoidal over all space; thus, they are nonintegrable, can not be normalized, and are infinite [6]. Despite its wide acceptance, on deeper inspection, the Schrödinger equation solution is plagued with many failings as well as difficulties in terms of a physical interpretation that have caused it to remain controversial since its inception. Only the one electron atom may be solved without approximations, but it fails to predict electron spin and leads to models with nonsensical consequences such as negative energy states of the vacuum, infinities, and negative kinetic energy. In addition to many predictions, which simply do not agree with observations, the Schrödinger equation and succeeding extensions predict noncausality, nonlocality, spooky actions at a distance or quantum telepathy, perpetual motion, and many internal inconsistencies where contradicting statements have to be taken true simultaneously [3-5].

It was reported previously [5] that the behavior of free electrons in superfluid helium has again forced the issue of the meaning of the wavefunction. Electrons form bubbles in superfluid helium which reveal that the electron is real and that a physical interpretation of the wavefunction is necessary. Furthermore, when irradiated with light of energy of about a 0.5 to several electron volts [7], the electrons carry current at different rates as if they exist with different sizes. It has been proposed that the behavior of free electrons in superfluid helium can be explained in terms of the electron breaking into pieces at superfluid helium temperatures [7]. Yet, the electron has proven to be indivisible even under particle accelerator collisions at 90 GeV (LEP II). The nature of the wavefunction needs to be addressed. It is time for the physical rather than the mathematical nature of the wavefunction to be determined.

From the time of its inception, quantum mechanics (QM) has been controversial because its foundations are in conflict with physical laws and are internally inconsistent. Interpretations of quantum mechanics such as hidden variables, multiple worlds, consistency rules, and spontaneous collapse have been put forward in an attempt to base the theory in reality. Unfortunately many theoreticians ignore the requirement that the wave function must be real and physical in order for it to be considered a valid description of reality. For example, regarding this issue Fuchs and Peres believe [8] “Contrary to those desires, quantum theory does *not* describe physical reality. What it does is provide an algorithm for computing *probabilities* for macroscopic events (“detector ticks”) that are the consequences of our experimental interventions. This strict definition of the scope of quantum theory is the only interpretation ever needed, whether by experimenters or theorists.”

With Penning traps, it is possible to measure transitions including those with hyperfine levels of electrons of single ions. This case can be experimentally distinguished from statistics over equivalent transitions in many ions. Whether many or one, the transition energies are always identical within the resonant line width. So, *probabilities* have no place in describing atomic energy levels. Moreover, quantum theory is incompatible with probability theory since it is based on underlying unknown, but determined outcomes as discussed previously [5].

The Copenhagen interpretation provides another meaning of quantum mechanics. It asserts that what we observe is all we can know; any speculation about what an electron, photon, atom, or other atomic-sized entity is really or what it is doing when we are not looking is just that—speculation. The postulate of quantum measurement asserts that the process of measuring an observable forces it into a state of reality. In other words, reality is irrelevant until a measurement is made. In the case of electrons in superfluid helium, the fallacy with this position is that the “ticks” (migration times of electron bubbles) reveal that the electron is real before a measurement is made. Furthermore, experiments on transitions on single ions such as  $Ba^+$  in a Penning trap under continuous observation demonstrate that the postulate of quantum measurement of quantum mechanics is experimentally disproved as discussed previously [5, 9]. These issues and other such flawed philosophies and interpretations of experiments that arise from quantum mechanics were discussed previously [3-5].

QM gives correlations with experimental data. It does not explain the mechanism for the observed data. But, it should not be surprising that it gives good correlations given that the constraints of internal consistency and conformance to physical laws are removed for a wave equation with an infinite number of solutions wherein the solutions may be formulated as an infinite series of eigenfunctions with variable parameters. There are no physical constraints on the parameters. They may even correspond to unobservables such as virtual particles, hyperdimensions, effective nuclear charge, polarization of the vacuum, worm holes, spooky action at a distance, infinities, parallel universes, faster than light travel, etc. If you invoke the constraints of internal consistency and conformance to physical laws, quantum mechanics has never successfully solved a physical problem.

Throughout the history of quantum theory, wherever there was an advance to a new application, it was necessary to repeat a trial-and-error experimentation to find which method of calculation gave the right answers. Often the textbooks present only the successful procedure as if it followed from first principles; and do not mention the actual method by which it was found. In electromagnetic theory based on Maxwell’s equations, one deduces the computational algorithm from the general principles. In quantum theory, the logic is just the opposite. One chooses the principle to fit the empirically successful algorithm. For example, we know that it required a great deal of art and tact over decades of effort to get correct predictions out of

Quantum Electrodynamics (QED). For the right experimental numbers to emerge, one must do the calculation (i.e. subtract off the infinities) in one particular way and not in some other way that appears in principle equally valid. There is a corollary, noted by Kallen: from an inconsistent theory, any result may be derived.

Reanalysis of old experiments and many new experiments including electrons in superfluid helium challenge the Schrödinger equation predictions. Many noted physicists rejected quantum mechanics. Feynman also attempted to use first principles including Maxwell's Equations to discover new physics to replace quantum mechanics [10]. Other great physicists of the 20th century searched. "Einstein [...] insisted [...] that a more detailed, wholly deterministic theory must underlie the vagaries of quantum mechanics" [11]. He felt that scientists were misinterpreting the data. These issues and the results of many experiments such as the wave-particle duality, the Lamb shift, anomalous magnetic moment of the electron, transition and decay lifetimes, experiments invoking interpretations of spooky action at a distance such as the Aspect experiment, entanglement, and double-slit-type experiments are shown to be absolutely predictable and physical in the context of a theory of classical quantum mechanics (CQM) derived from first principles [3-5]. Using the classical wave equation with the constraint of nonradiation based on Maxwell's equations, CQM gives closed form physical solutions for the electron in atoms, the free electron, and the free electron in superfluid helium which match the observations without requiring that the electron is divisible. Moreover, unification of atomic and large scale physics the ultimate objective of natural theory is enabled. CQM holds over a scale of spacetime of 85 orders of magnitude—it correctly predicts the nature of the universe from the scale of the quarks to that of the cosmos.

## **CLASSICAL QUANTUM THEORY OF THE ATOM BASED ON MAXWELL'S EQUATIONS THAT HOLDS OVER ALL SCALES**

In this paper, the old view that the electron is a zero or one-dimensional point in an all-space probability wave function  $\Psi(x)$  is not taken for granted. The theory of classical quantum mechanics (CQM), derived from first principles, must successfully and consistently apply physical laws on all scales [3-5]. Historically, the point at which QM broke with classical laws can be traced to the issue of nonradiation of the one electron atom that was addressed by Bohr with a postulate of stable orbits in defiance of the physics represented by Maxwell's equations [3-5]. Later physics was replaced by "pure mathematics" based on the notion of the inexplicable wave-particle duality nature of electrons which lead to the Schrödinger equation wherein the consequences of radiation predicted by Maxwell's equations was ignored. Ironically, both Bohr and Schrödinger used the electrostatic Coulomb potential of Maxwell's equations, but abandoned the electrodynamic laws. Physical laws may indeed be the root of the observations

thought to be “purely quantum mechanical”, and it may have been a mistake to make the assumption that Maxwell’s electrodynamic equations must be rejected at the atomic level. Thus, in the present approach, the classical wave equation is solved with the constraint that a bound  $n = 1$ -state electron cannot radiate energy.

Thus, herein, derivations consider the electrodynamic effects of moving charges as well as the Coulomb potential, and the search is for a solution representative of the electron wherein there is acceleration of charge motion without radiation. The mathematical formulation for zero radiation based on Maxwell’s equations follows from a derivation by Haus [12]. The function that describes the motion of the electron must not possess spacetime Fourier components that are synchronous with waves traveling at the speed of light. Similarly, nonradiation is demonstrated based on the electron’s electromagnetic fields and the Poynting power vector.

In this paper, a summary of the results of CQM [3, 13-14] is presented. (The details of the derivations are given in Ref. [3].) Specifically, CQM gives closed form solutions for the atom including the stability of the  $n = 1$  state and the instability of the excited states, the equation of the photon and electron in excited states, the equation of the free electron, and photon which predict the wave particle duality behavior of particles and light. The current and charge density functions of the electron may be directly physically interpreted. For example, spin angular momentum results from the motion of negatively charged mass moving systematically, and the equation for angular momentum,  $\mathbf{r} \times \mathbf{p}$ , can be applied directly to the wave function (a current density function) that describes the electron. The magnetic moment of a Bohr magneton, Stern Gerlach experiment, g factor, Lamb shift, , resonant line width and shape, selection rules, correspondence principle, wave particle duality, excited states, reduced mass, rotational energies, and momenta, orbital and spin splitting, spin-orbital coupling (fine structure), Knight shift, and spin-nuclear coupling (hyperfine structure), muonium hyperfine structure interval, ionization energies of two electron atoms, elastic electron scattering from helium atoms, and the nature of the chemical bond are derived in closed form equations based on Maxwell’s equations. The calculations agree with experimental observations.

For any kind of wave advancing with limiting velocity and capable of transmitting signals, the equation of front propagation is the same as the equation for the front of a light wave. By applying this condition to electromagnetic and gravitational fields at particle production, the Schwarzschild metric (SM) is derived from the classical wave equation which modifies general relativity to include conservation of spacetime as a consequence of Eq. (183) (See Ref. [3], Chp. 23 and footnote 7 of Chp. 23), in addition to momentum and matter/energy. The result gives a natural relationship between Maxwell’s equations, special relativity, and general relativity. It gives gravitation from the atom to the cosmos. The universe is time harmonically oscillatory in matter energy and spacetime expansion and contraction with a

minimum radius that is the gravitational radius. In closed form equations with fundamental constants only, CQM gives the deflection of light by stars, the precession of the perihelion of Mercury, the particle masses, the Hubble constant, the age of the universe, the observed acceleration of the expansion, the power of the universe, the power spectrum of the universe, the microwave background temperature, the uniformity of the microwave background radiation at 2.7 K with the microkelvin spatial variation observed by the DASI, the observed violation of the GZK cutoff, the mass density, the large scale structure of the universe, and the identity of dark matter which matches the criteria for the structure of galaxies. In a special case wherein the gravitational potential energy density of a blackhole equals that of the Planck mass, matter converts to energy and spacetime expands with the release of a gamma ray burst. The singularity in the SM is eliminated.

### ONE-ELECTRON ATOMS

One-electron atoms include the hydrogen atom,  $He^+$ ,  $Li^{2+}$ ,  $Be^{3+}$ , and so on. The mass-energy and angular momentum of the electron are constant; this requires that the equation of motion of the electron be temporally and spatially harmonic. Thus, the classical wave equation applies and

$$\left[ \nabla^2 - \frac{1}{v^2} \frac{\partial^2}{\partial t^2} \right] \rho(r, \theta, \phi, t) = 0 \quad (2)$$

where  $\rho(r, \theta, \phi, t)$  is the time dependent charge density function of the electron in time and space. In general, the wave equation has an infinite number of solutions. To arrive at the solution which represents the electron, a suitable boundary condition must be imposed. It is well known from experiments that each single atomic electron of a given isotope radiates to the same stable state. Thus, the physical boundary condition of nonradiation of the bound electron was imposed on the solution of the wave equation for the time dependent charge density function of the electron [3]. The condition for radiation by a moving point charge given by Haus [12] is that its spacetime Fourier transform does possess components that are synchronous with waves traveling at the speed of light. Conversely, it is proposed that the condition for nonradiation by an ensemble of moving point charges that comprises a current density function is

*For non-radiative states, the current-density function must NOT possess spacetime Fourier components that are synchronous with waves traveling at the speed of light.*

The time, radial, and angular solutions of the wave equation are separable. The motion is time harmonic with frequency  $\omega_n$ . A constant angular function is a solution to the wave equation. Solutions of the Schrödinger wave equation comprising a radial function radiate according to

Maxwell's equation as shown previously by application of Haus' condition [3]. In fact, it was found that any function which permitted radial motion gave rise to radiation. A radial function which does satisfy the boundary condition is a radial delta function

$$f(r) = \frac{1}{r^2} \delta(r - r_n) \quad (3)$$

This function defines a constant charge density on a spherical shell where  $r_n = nr_1$  wherein  $n$  is an integer in an excited state as given in the Excited States section, and Eq. (2) becomes the two-dimensional wave equation plus time with separable time and angular functions. Given time harmonic motion and a radial delta function, the relationship between an allowed radius and the electron wavelength is given by

$$2\pi r_n = \lambda_n \quad (4)$$

where the subscript  $n$  is determined during photon absorption as given by Eq. (83). Using the observed de Broglie relationship for the electron mass where the coordinates are spherical,

$$\lambda_n = \frac{h}{p_n} = \frac{h}{m_e v_n} \quad (5)$$

and the magnitude of the velocity for *every* point on the orbitsphere is

$$v_n = \frac{\hbar}{m_e r_n} \quad (6)$$

The sum of the  $|\mathbf{L}_i|$ , the magnitude of the angular momentum of each infinitesimal point of the orbitsphere of mass  $m_i$ , must be constant. The constant is  $\hbar$ .

$$\sum |\mathbf{L}_i| = \sum |\mathbf{r} \times m_i \mathbf{v}| = m_e r_n \frac{\hbar}{m_e r_n} = \hbar \quad (7)$$

Thus, an electron is a spinning, two-dimensional spherical surface (zero thickness <sup>1</sup>), called an *electron orbitsphere*, that can exist in a bound state at only specified distances from the nucleus as shown in Figure 1. The corresponding current function shown in Figure 2 which gives rise to the phenomenon of *spin* is derived in the "Spin Function" section. (See the Appendix of this paper and the Orbitsphere Equation of Motion for  $\ell = 0$  of Ref. [3] at Chp. 1.)

Nonconstant functions are also solutions for the angular functions. To be a harmonic solution of the wave equation in spherical coordinates, these angular functions must be spherical harmonic functions [15]. A zero of the spacetime Fourier transform of the product function of

---

<sup>1</sup> The orbitsphere has zero thickness, but in order that the speed of light is a constant maximum in any frame including that of the gravitational field that propagates out as a light-wave front at particle production, it gives rise to a spacetime dilation equal to  $2\pi$  times the Newtonian gravitational or Schwarzschild radius  $r_g = \frac{2Gm_e}{c^2} = 1.3525 \times 10^{-57} m$  according to Eqs. (178) and (202). This corresponds to a spacetime dilation of  $8.4980 \times 10^{-57} m$  or  $2.8346 \times 10^{-65} s$ . Although the orbitsphere does not occupy space in the third spatial dimension, its mass discontinuity effectively "displaces" spacetime wherein the spacetime dilation can be considered a "thickness" associated with its gravitational field.

two spherical harmonic angular functions, a time harmonic function, and an unknown radial function is sought. The solution for the radial function which satisfies the boundary condition is also a delta function given by Eq. (3). Thus, bound electrons are described by a charge-density (mass-density) function which is the product of a radial delta function, two angular functions (spherical harmonic functions), and a time harmonic function.

$$\rho(r, \theta, \phi, t) = f(r)A(\theta, \phi, t) = \frac{1}{r^2} \delta(r - r_n)A(\theta, \phi, t); \quad A(\theta, \phi, t) = Y(\theta, \phi)k(t) \quad (8)$$

In these cases, the spherical harmonic functions correspond to a traveling charge density wave confined to the spherical shell which gives rise to the phenomenon of orbital angular momentum. The orbital functions which modulate the constant “spin” function shown graphically in Figure 3 are given in the “Angular Functions” section.

### SPIN FUNCTION

The orbitsphere spin function comprises a constant charge (current) density function with moving charge confined to a two-dimensional spherical shell. The current pattern of the orbitsphere spin function comprises an infinite series of correlated orthogonal great circle current loops wherein each point charge (current) density element moves time harmonically with constant angular velocity

$$\omega_n = \frac{\hbar}{m_e r_n^2} \quad (9)$$

The uniform current density function  $Y_0^0(\phi, \theta)$ , the orbitsphere equation of motion of the electron (Eqs. (14-15)), corresponding to the constant charge function of the orbitsphere that gives rise to the spin of the electron is generated from a basis set current-vector field defined as the orbitsphere current-vector field (“orbitsphere-cvf”). This in turn is generated over the surface by two complementary steps of an infinite series of nested rotations of two orthogonal great circle current loops where the coordinate axes rotate with the two orthogonal great circles that serve as a basis set. The algorithm to generate the current density function rotates the great circles and the corresponding x'y'z' coordinates relative to the xyz frame. Each infinitesimal rotation of the infinite series is about the new i'-axis and new j'-axis which results from the preceding such rotation. Each element of the current density function is obtained with each conjugate set of rotations. Due to the symmetry properties of the angular-momentum components and the corresponding current of the orbitsphere-cvf, the uniform current distribution having the same angular momentum components as that of the orbitsphere-cvf is obtained by convolving the orbitsphere-cvf about its resultant angular momentum axis.

For Step One, the current density elements move counter clockwise on the great circle in the y'z'-plane and move clockwise on the great circle in the x'z'-plane. The great circles are

rotated by an infinitesimal angle  $\pm\Delta\alpha_i$  (a positive rotation around the x'-axis or a negative rotation about the z'-axis for Steps One and Two, respectively) and then by  $\pm\Delta\alpha_j$  (a positive rotation around the new y'-axis or a positive rotation about the new x'-axis for Steps One and Two, respectively). The coordinates of each point on each rotated great circle (x',y',z') is expressed in terms of the first (x,y,z) coordinates by the following transforms where clockwise rotations and motions are defined as positive looking along the corresponding axis:

**Step One**

$$\begin{bmatrix} x \\ y \\ z \end{bmatrix} = \begin{bmatrix} \cos(\Delta\alpha_y) & 0 & -\sin(\Delta\alpha_y) \\ 0 & 1 & 0 \\ \sin(\Delta\alpha_y) & 0 & \cos(\Delta\alpha_y) \end{bmatrix} \begin{bmatrix} 1 & 0 & 0 \\ 0 & \cos(\Delta\alpha_x) & \sin(\Delta\alpha_x) \\ 0 & -\sin(\Delta\alpha_x) & \cos(\Delta\alpha_x) \end{bmatrix} \begin{bmatrix} x' \\ y' \\ z' \end{bmatrix}$$

$$\begin{bmatrix} x \\ y \\ z \end{bmatrix} = \begin{bmatrix} \cos(\Delta\alpha_y) & \sin(\Delta\alpha_y)\sin(\Delta\alpha_x) & -\sin(\Delta\alpha_y)\cos(\Delta\alpha_x) \\ 0 & \cos(\Delta\alpha_x) & \sin(\Delta\alpha_x) \\ \sin(\Delta\alpha_y) & -\cos(\Delta\alpha_y)\sin(\Delta\alpha_x) & \cos(\Delta\alpha_y)\cos(\Delta\alpha_x) \end{bmatrix} \begin{bmatrix} x' \\ y' \\ z' \end{bmatrix}$$

(10)

**Step Two**

$$\begin{bmatrix} x \\ y \\ z \end{bmatrix} = \begin{bmatrix} 1 & 0 & 0 \\ 0 & \cos(\Delta\alpha_x) & \sin(\Delta\alpha_x) \\ 0 & -\sin(\Delta\alpha_x) & \cos(\Delta\alpha_x) \end{bmatrix} \begin{bmatrix} \cos(\Delta\alpha_z) & \sin(\Delta\alpha_z) & 0 \\ -\sin(\Delta\alpha_z) & \cos(\Delta\alpha_z) & 0 \\ 0 & 0 & 1 \end{bmatrix} \begin{bmatrix} x' \\ y' \\ z' \end{bmatrix}$$

$$\begin{bmatrix} x \\ y \\ z \end{bmatrix} = \begin{bmatrix} \cos(\Delta\alpha_z) & \sin(\Delta\alpha_z) & 0 \\ -\cos(\Delta\alpha_x)\sin(\Delta\alpha_z) & \cos(\Delta\alpha_x)\cos(\Delta\alpha_z) & \sin(\Delta\alpha_x) \\ \sin(\Delta\alpha_x)\sin(\Delta\alpha_z) & -\sin(\Delta\alpha_x)\cos(\Delta\alpha_z) & \cos(\Delta\alpha_x) \end{bmatrix} \begin{bmatrix} x' \\ y' \\ z' \end{bmatrix}$$

(11)

where the angular sum is  $\lim_{\Delta\alpha \rightarrow 0} \sum_{n=1}^{\frac{\sqrt{2}}{2}\pi} |\Delta\alpha_{i,j}| = \frac{\sqrt{2}}{2}\pi$ .

The orbitsphere is given by  $n$  reiterations of Eqs. (10) and (11) for each point on each of the two orthogonal great circles during each of Steps One and Two. The output given by the non-primed coordinates is the input of the next iteration corresponding to each successive nested rotation by the infinitesimal angle  $\pm\Delta\alpha_i$  or  $\pm\Delta\alpha_j$ , where the magnitude of the angular sum of the  $n$  rotations about each of the  $i$ '-axis and the  $j$ '-axis is  $\frac{\sqrt{2}}{2}\pi$ . Half of the orbitsphere is generated during each of Steps One and Two.

Following Step Two, in order to match the boundary condition that the magnitude of the velocity at any given point on the surface is given by Eq. (6), the output half of the orbitsphere is rotated clockwise by an angle of  $\frac{\pi}{4}$  about the  $z$ -axis. Using Eq. (11) with  $\Delta\alpha_z = \frac{\pi}{4}$  and  $\Delta\alpha_x = 0$  gives the rotation. Then, the one half of the orbitsphere generated from Step One is superimposed with the complementary half obtained from Step Two following its rotation about the  $z$ -axis of  $\frac{\pi}{4}$  to give  $Y_0^0(\phi, \theta)$ , the orbitsphere equation of motion of the electron.

The current pattern of the orbitsphere generated by the nested rotations of the orthogonal great circle current loops is a continuous and total coverage of the spherical surface, but it is shown as a visual representation using 6 degree increments of the infinitesimal angular variable  $\pm\Delta\alpha_i$  and  $\pm\Delta\alpha_j$ , of Eqs. (10) and (11) from the perspective of the  $z$ -axis in Figure 2. In each case, the complete orbitsphere current pattern corresponds all the orthogonal-great-circle

elements which are generated by the rotation of the basis-set according to Eqs. (10) and (11) where  $\pm\Delta\alpha_i$  and  $\pm\Delta\alpha_j$  approach zero and the summation of the infinitesimal angular rotations of  $\pm\Delta\alpha_i$  and  $\pm\Delta\alpha_j$  about the successive i'-axes and j'-axes is  $\frac{\sqrt{2}}{2}\pi$  for each Step. The current pattern gives rise to the phenomenon corresponding to the spin quantum number.

The resultant angular momentum projections of  $\mathbf{L}_{xy} = \frac{\hbar}{4}$  and  $\mathbf{L}_z = \frac{\hbar}{2}$  meet the boundary condition for the unique current having an angular velocity magnitude at each point on the surface given by Eq. (6) and give rise to the Stern Gerlach experiment as shown in Ref. [3]. The angular momentum is constant with respect to rotation of the orbitsphere-cvf about the axis of the resultant angular momentum vector,  $\mathbf{L}_R$ ; thus it is constant about each of the principal axes. Furthermore, the orbitsphere-cvf has the origin as an inversion center ( $C_i$ ) as shown in the previous figures. Due to this symmetry feature of the currents as well as the rotational symmetry of the angular momentum components ( $C_\infty$ ), the convolution of the orbitsphere-cvf with a sphere aligned on the  $\mathbf{L}_R$ -axis over the spherical-coordinate angular span  $\phi = 0$  to  $\phi = 2\pi$  gives rise to the spherically-symmetric current density,  $Y_0^0(\phi, \theta)$ . The details of the derivation of the spin function are given in the Appendix of this paper and Chp. 1 of Ref. [3].

## ANGULAR FUNCTIONS

The time, radial, and angular solutions of the wave equation are separable. Also based on the radial solution, the angular charge and current-density functions of the electron,  $A(\theta, \phi, t)$ , must be a solution of the wave equation in two dimensions (plus time),

$$\left[ \nabla^2 - \frac{1}{v^2} \frac{\partial^2}{\partial t^2} \right] A(\theta, \phi, t) = 0 \quad (12)$$

where  $\rho(r, \theta, \phi, t) = f(r)A(\theta, \phi, t) = \frac{1}{r^2} \delta(r - r_n)A(\theta, \phi, t)$  and  $A(\theta, \phi, t) = Y(\theta, \phi)k(t)$

$$\left[ \frac{1}{r^2 \sin \theta} \frac{\partial}{\partial \theta} \left( \sin \theta \frac{\partial}{\partial \theta} \right)_{r, \phi} + \frac{1}{r^2 \sin^2 \theta} \left( \frac{\partial^2}{\partial \phi^2} \right)_{r, \theta} - \frac{1}{v^2} \frac{\partial^2}{\partial t^2} \right] A(\theta, \phi, t) = 0 \quad (13)$$

where  $v$  is the linear velocity of the electron. The charge-density functions including the time-function factor are

$$\mathfrak{L} = 0$$

$$\rho(r, \theta, \phi, t) = \frac{e}{8\pi r^2} [\delta(r - r_n)] [Y_0^0(\theta, \phi) + Y_\ell^m(\theta, \phi)] \quad (14)$$

$$\mathfrak{L} \neq 0$$

$$\rho(r, \theta, \phi, t) = \frac{e}{4\pi r^2} [\delta(r - r_n)] \left[ Y_0^0(\theta, \phi) + \text{Re} \left\{ Y_\ell^m(\theta, \phi) e^{i\omega_n t} \right\} \right] \quad (15)$$

where  $Y_\ell^m(\theta, \phi)$  are the spherical harmonic functions that spin about the z-axis with angular frequency  $\omega_n$  with  $Y_0^0(\theta, \phi)$  the constant function.  $\text{Re} \left\{ Y_\ell^m(\theta, \phi) e^{i\omega_n t} \right\} = P_\ell^m(\cos\theta) \cos(m\phi + \omega_n' t)$  where to keep the form of the spherical harmonic as a traveling wave about the z-axis,  $\omega_n' = m\omega_n$ .

## ACCELERATION WITHOUT RADIATION

### Special Relativistic Correction to the Electron Radius

The relationship between the electron wavelength and its radius is given by Eq. (4) where  $\lambda$  is the de Broglie wavelength. For each current density element of the spin function, the distance along each great circle in the direction of instantaneous motion undergoes length contraction and time dilation. Using a phase matching condition, the wavelengths of the electron and laboratory inertial frames are equated, and the corrected radius is given by

$$r_n = r_n' \left[ \sqrt{1 - \left(\frac{v}{c}\right)^2} \sin \left[ \frac{\pi}{2} \left(1 - \left(\frac{v}{c}\right)^2\right)^{3/2} \right] + \frac{1}{2\pi} \cos \left[ \frac{\pi}{2} \left(1 - \left(\frac{v}{c}\right)^2\right)^{3/2} \right] \right] \quad (16)$$

where the electron velocity is given by Eq. (6). (See Ref. [3] Chp. 1, Special Relativistic Correction to the Ionization Energies section).  $\frac{e}{m_e}$  of the electron, the electron angular momentum of  $\hbar$ , and  $\mu_B$  are invariant, but the mass and charge densities increase in the laboratory frame due to the relativistically contracted electron radius. As  $v \rightarrow c$ ,  $r/r' \rightarrow \frac{1}{2\pi}$  and  $r = \lambda$  as shown in Figure 4.

### Nonradiation Based on Haus' Condition

The Fourier transform of the electron charge density function given by Eq. (8) is a solution of the three-dimensional wave equation in frequency space ( $\mathbf{k}, \omega$  space) as given in Chp 1, Spacetime Fourier Transform of the Electron Function section, of Ref. [3]. Then the corresponding Fourier transform of the current density function  $K(s, \Theta, \Phi, \omega)$  is given by multiplying by the constant angular frequency.

$$\begin{aligned}
K(s, \Theta, \Phi, \omega) &= 4\pi\omega_n \frac{\sin(2s_n r_n)}{2s_n r_n} \otimes 2\pi \sum_{\nu=1}^{\infty} \frac{(-1)^{\nu-1} (\pi \sin \Theta)^{2(\nu-1)}}{(\nu-1)!(\nu-1)!} \frac{\Gamma\left(\frac{1}{2}\right)\Gamma\left(\nu + \frac{1}{2}\right)}{(\pi \cos \Theta)^{2\nu+1} 2^{\nu+1}} \frac{2\nu!}{(\nu-1)!} s^{-2\nu} \\
&\otimes 2\pi \sum_{\nu=1}^{\infty} \frac{(-1)^{\nu-1} (\pi \sin \Phi)^{2(\nu-1)}}{(\nu-1)!(\nu-1)!} \frac{\Gamma\left(\frac{1}{2}\right)\Gamma\left(\nu + \frac{1}{2}\right)}{(\pi \cos \Phi)^{2\nu+1} 2^{\nu+1}} \frac{2\nu!}{(\nu-1)!} s^{-2\nu} \frac{1}{4\pi} [\delta(\omega - \omega_n) + \delta(\omega + \omega_n)]
\end{aligned} \tag{17}$$

$\mathbf{s}_n \cdot \mathbf{v}_n = \mathbf{s}_n \cdot \mathbf{c} = \omega_n$  implies  $r_n = \lambda_n$  which is given by Eq. (16) in the case that  $k$  is the lightlike  $k^0$ . In this case, Eq. (17) vanishes. Consequently, spacetime harmonics of  $\frac{\omega_n}{c} = k$  or  $\frac{\omega_n}{c} \sqrt{\frac{\epsilon}{\epsilon_0}} = k$  for which the Fourier transform of the current-density function is nonzero do not

exist. Radiation due to charge motion does not occur in any medium when this boundary condition is met. (Nonradiation is also determined from the fields based on Maxwell's equations as given in the Nonradiation Based on the Electromagnetic Fields and the Poynting Power Vector section *infra.* and the same section of Chp 1, Appendix I of Ref. [3].)

### Nonradiation Based on the Electron Electromagnetic Fields and the Poynting Power Vector

A point charge undergoing periodic motion accelerates and as a consequence radiates according to the Larmor formula:

$$P = \frac{1}{4\pi\epsilon_0} \frac{2e^2}{3c^3} a^2 \tag{18}$$

where  $e$  is the charge,  $a$  is its acceleration,  $\epsilon_0$  is the permittivity of free space, and  $c$  is the speed of light. Although an accelerated *point* particle radiates, an *extended distribution* modeled as a superposition of accelerating charges does not have to radiate [12, 16-19]. An ensemble of charges, all oscillating at the same frequency, create a radiation pattern with a number of nodes. The same applies to current patterns in phased array antenna design [20]. It is possible to have an infinite number of charges oscillating in such a way as to cause destructive interference or nodes in all directions. The electromagnetic far field is determined from the current distribution in order to obtain the condition, if it exists, that the electron current distribution given by Eq. (21) must satisfy such that the electron does not radiate.

The charge density functions of the electron orbitsphere in spherical coordinates plus time are given by Eqs. (14-15). For  $\mathfrak{l} = 0$ , the equipotential, uniform or constant charge density function (Eq. (14)) further comprises a current pattern given in the Spin Function section. It also corresponds to the nonradiative  $n=1$ ,  $\ell = 0$  state of atomic hydrogen and to the spin function of the electron. The current density function is given by multiplying Eq. (14) by the

constant angular velocity  $\omega$ . There is acceleration without radiation. In this case, centripetal acceleration. A static charge distribution exists even though each point on the surface is accelerating along a great circle. Haus' condition predicts no radiation for the entire ensemble. The same result is trivially predicted from consideration of the fields and the radiated power. Since the current is not time dependent, the fields are given by

$$\nabla \times \mathbf{H} = \mathbf{J} \quad (19)$$

and

$$\nabla \times \mathbf{E} = 0 \quad (20)$$

which are the electrostatic and magnetostatic cases, respectively, *with no radiation*.

The nonradiation condition given by Eq. (17) may be confirmed by determining the fields and the current distribution condition that is nonradiative based on Maxwell's equations. For  $\mathcal{L} \neq 0$ , the charge-density functions including the time-function factor are given by Eqs. (15). In the cases that  $m \neq 0$ , Eq. (15) is a traveling charge density wave that moves on the surface of the orbitsphere about the z-axis and modulates the orbitsphere corresponding to  $\mathcal{L} = 0$ . Since the charge is moving time harmonically about the z-axis with frequency  $\omega_n$  and the current-density function is given by the time derivative of the charge-density function, the current-density function is given by the normalized product of the constant angular velocity and the charge-density function. The first current term of Eq. (15) is static. Thus, it is trivially nonradiative.

The current due to the time dependent term is

$$\begin{aligned} \mathbf{J} &= \frac{\omega_n}{2\pi} \frac{e}{4\pi r_n^2} N [\delta(r - r_n)] \text{Re} \{ Y_\ell^m(\theta, \phi) \} [\mathbf{u}(t) \times \mathbf{r}] \\ &= \frac{\omega_n}{2\pi} \frac{e}{4\pi r_n^2} N [\delta(r - r_n)] \text{Re} \{ Y_\ell^m(\theta, \phi) e^{i\omega_n t} \} [\mathbf{u} \times \mathbf{r}] \\ &= \frac{\omega_n}{2\pi} \frac{e}{4\pi r_n^2} N [\delta(r - r_n)] \text{Re} \left( P_\ell^m(\cos \theta) e^{im\phi} e^{i\omega_n t} \right) [\mathbf{u} \times \mathbf{r}] \\ &= \frac{\omega_n}{2\pi} \frac{e}{4\pi r_n^2} N [\delta(r - r_n)] \left( P_\ell^m(\cos \theta) \cos(m\phi + \omega_n t) \right) [\mathbf{u} \times \mathbf{r}] \\ &= \frac{\omega_n}{2\pi} \frac{e}{4\pi r_n^2} N [\delta(r - r_n)] \left( P_\ell^m(\cos \theta) \cos(m\phi + \omega_n t) \right) \sin \theta \hat{\phi} \end{aligned} \quad (21)$$

where to keep the form of the spherical harmonic as a traveling wave about the z-axis,  $\dot{\omega}_n = m\omega_n$  and  $N$  and  $N'$  are normalization constants. The vectors are defined as

$$\hat{\phi} = \frac{\hat{\mathbf{u}} \times \hat{\mathbf{r}}}{|\hat{\mathbf{u}} \times \hat{\mathbf{r}}|} = \frac{\hat{\mathbf{u}} \times \hat{\mathbf{r}}}{\sin \theta}; \quad \hat{\mathbf{u}} = \hat{\mathbf{z}} = \textit{orbital axis} \quad (22)$$

$$\hat{\theta} = \hat{\phi} \times \hat{\mathbf{r}} \quad (23)$$

“ $\hat{\phantom{x}}$ ” denotes the unit vectors  $\hat{\mathbf{u}} \equiv \frac{\mathbf{u}}{|\mathbf{u}|}$ , non-unit vectors are designed in bold, and the current function is normalized. For time-varying electromagnetic fields, Jackson [21] gives a

generalized expansion in vector spherical waves that are convenient for electromagnetic boundary-value problems possessing spherical symmetry properties and for analyzing multipole radiation from a localized source distribution. The Green function  $G(\mathbf{x}', \mathbf{x})$  which is appropriate to the equation

$$(\nabla^2 + k^2)G(\mathbf{x}', \mathbf{x}) = -\delta(\mathbf{x}' - \mathbf{x}) \quad (24)$$

in the infinite domain with the spherical wave expansion for the outgoing wave Green function is

$$G(\mathbf{x}', \mathbf{x}) = \frac{e^{-ik|\mathbf{x}-\mathbf{x}'|}}{|\mathbf{x}-\mathbf{x}'|} = ik \sum_{\ell=0}^{\infty} j_{\ell}(kr_{<}) h_{\ell}^{(1)}(kr_{>}) \sum_{m=-\ell}^{\ell} Y_{\ell,m}^*(\theta, \phi) Y_{\ell,m}(\theta, \phi) \quad (25)$$

General coordinates are shown in Figure 5. Jackson [21] further gives the general multipole field solution to Maxwell's equations in a source-free region of empty space with the assumption of a time dependence  $e^{i\omega_n t}$ :

$$\begin{aligned} \mathbf{B} &= \sum_{\ell,m} \left[ a_E(\ell, m) f_{\ell}(kr) \mathbf{X}_{\ell,m} - \frac{i}{k} a_M(\ell, m) \nabla \times g_{\ell}(kr) \mathbf{X}_{\ell,m} \right] \\ \mathbf{E} &= \sum_{\ell,m} \left[ \frac{i}{k} a_E(\ell, m) \nabla \times f_{\ell}(kr) \mathbf{X}_{\ell,m} + a_M(\ell, m) g_{\ell}(kr) \mathbf{X}_{\ell,m} \right] \end{aligned} \quad (26)$$

where the cgs units used by Jackson are retained in this section. The radial functions  $f_{\ell}(kr)$  and  $g_{\ell}(kr)$  are of the form:

$$g_{\ell}(kr) = A_{\ell}^{(1)} h_{\ell}^{(1)} + A_{\ell}^{(2)} h_{\ell}^{(2)} \quad (27)$$

$\mathbf{X}_{\ell,m}$  is the vector spherical harmonic defined by

$$\mathbf{X}_{\ell,m}(\theta, \phi) = \frac{1}{\sqrt{\ell(\ell+1)}} \mathbf{L} Y_{\ell,m}(\theta, \phi) \quad (28)$$

where

$$\mathbf{L} = \frac{1}{i} (\mathbf{r} \times \nabla) \quad (29)$$

The coefficients  $a_E(\ell, m)$  and  $a_M(\ell, m)$  of Eq. (26) specify the amounts of electric  $(\ell, m)$  multipole and magnetic  $(\ell, m)$  multipole fields, and are determined by sources and boundary conditions as are the relative proportions in Eq. (27). Jackson gives the result of the electric and magnetic coefficients from the sources as

$$a_E(\ell, m) = \frac{4\pi k^2}{i\sqrt{\ell(\ell+1)}} \int Y_{\ell}^{m*} \left\{ \rho \frac{\delta}{\delta r} [r j_{\ell}(kr)] + \frac{ik}{c} (\mathbf{r} \cdot \mathbf{J}) j_{\ell}(kr) - ik \nabla \cdot (\mathbf{r} \times \mathbf{M}) j_{\ell}(kr) \right\} d^3 x \quad (30)$$

and

$$a_M(\ell, m) = \frac{-4\pi k^2}{\sqrt{\ell(\ell+1)}} \int j_{\ell}(kr) Y_{\ell}^{m*} \mathbf{L} \cdot \left( \frac{\mathbf{J}}{c} + \nabla \times \mathbf{M} \right) d^3 x \quad (31)$$

respectively, where the distribution of charge  $\rho(\mathbf{x}, t)$ , current  $\mathbf{J}(\mathbf{x}, t)$ , and intrinsic magnetization  $\mathbf{M}(\mathbf{x}, t)$  are harmonically varying sources:  $\rho(\mathbf{x})e^{-\omega_n t}$ ,  $\mathbf{J}(\mathbf{x})e^{-\omega_n t}$ , and  $\mathbf{M}(\mathbf{x})e^{-\omega_n t}$ . From, Eq. (21), the charge and intrinsic magnetization terms are zero. Also, the current  $\mathbf{J}(\mathbf{x}, t)$  is in the  $\hat{\phi}$

direction; thus, the  $a_E(\ell, m)$  coefficient given by Eq. (30) is zero since  $\mathbf{r} \cdot \mathbf{J} = 0$ . Substitution of Eq. (21) into Eq. (31) gives the magnetic multipole coefficient  $a_M(\ell, m)$ :

$$a_M(\ell, m) = \frac{-4\pi k^2}{\sqrt{\ell(\ell+1)}} \int j_\ell(kr) Y_\ell^{m*} \mathbf{L} \cdot \left\{ \frac{\frac{\omega_n}{2\pi} \frac{e}{4\pi r_n^2} N \delta(r-r_n) Y_\ell^m(\theta, \phi) \sin \theta \hat{\phi}}{c} \right\} d^3x \quad (32)$$

Each mass density element of the electron moves about the z-axis along a circular orbit of radius  $r_n \sin \theta$  in such a way that  $\phi$ , changes at a constant rate. That is  $\phi = \omega t$  at time  $t$  where  $\omega_n$  is the constant angular frequency given in Eq. (21), and

$$\mathbf{r}(t) = \mathbf{i} r_n \sin \theta \cos \omega t + \mathbf{j} r_n \sin \theta \sin \omega t \quad (33)$$

is the parametric equation of the circular orbit. Jackson gives the operator in the xy-plane corresponding to the current motion in this plane and the relations for  $Y_\ell^m(\theta, \phi)$  [21].

$$L_+ = L_x + iL_y = e^{i\phi} \left( \frac{\partial}{\partial \theta} + i \cot \theta \frac{\partial}{\partial \phi} \right) \quad (34)$$

$$L_+ Y_\ell^m(\theta, \phi) = \sqrt{(\ell-m)(\ell+m+1)} Y_\ell^{m+1}(\theta, \phi) \quad (35)$$

Using Eq. (34),  $\mathbf{L} \cdot \mathbf{J}$  of Eq. (31) is

$$\begin{aligned} L_+(Y_\ell^m(\theta, \phi) \sin \theta) &= e^{i\phi} \left( \frac{\partial}{\partial \theta} + i \cot \theta \frac{\partial}{\partial \phi} \right) Y_\ell^m(\theta, \phi) \sin \theta \\ &= e^{i\phi} Y_\ell^m(\theta, \phi) \left( \frac{\partial}{\partial \theta} + i \cot \theta \frac{\partial}{\partial \phi} \right) \sin \theta + e^{i\phi} \sin \theta \left( \frac{\partial}{\partial \theta} + i \cot \theta \frac{\partial}{\partial \phi} \right) Y_\ell^m(\theta, \phi) \end{aligned} \quad (36)$$

Using Eq. (35) in Eq. (36) gives

$$L_+(Y_\ell^m(\theta, \phi) \sin \theta) = e^{i\phi} Y_\ell^m(\theta, \phi) \cos \theta + \sin \theta \sqrt{(\ell-m)(\ell+m+1)} Y_\ell^{m+1}(\theta, \phi) \quad (37)$$

The spherical harmonic is given as

$$Y_\ell^m(\theta, \phi) = \sqrt{\frac{2\ell+1}{4\pi} \frac{(\ell-m)!}{(\ell+m)!}} P_\ell^m(\cos \theta) e^{im\phi} = N_{\ell, m} P_\ell^m(\cos \theta) e^{im\phi} \quad (38)$$

Thus, Eq. (37) is given as

$$L_+(Y_\ell^m(\theta, \phi) \sin \theta) = e^{i\phi} N_{\ell, m} P_\ell^m(\cos \theta) e^{im\phi} \cos \theta + \sin \theta \sqrt{(\ell-m)(\ell+m+1)} N_{\ell, m+1} P_\ell^{m+1}(\cos \theta) e^{i(m+1)\phi} \quad (39)$$

Substitution of Eq. (39) into Eq. (32) gives

$$\begin{aligned} a_M(\ell, m) &= \frac{-k^2}{c\sqrt{\ell(\ell+1)}} \frac{\omega_n}{2\pi} \frac{e}{r_n^2} N \\ &\int j_\ell(kr) Y_\ell^{m*}(\theta, \phi) \delta(r-r_n) \left\{ \begin{aligned} &e^{i\phi} N_{\ell, m} P_\ell^m(\cos \theta) e^{im\phi} \cos \theta \\ &+ \sin \theta \sqrt{(\ell-m)(\ell+m+1)} N_{\ell, m+1} P_\ell^{m+1}(\cos \theta) e^{i(m+1)\phi} \end{aligned} \right\} d^3x \end{aligned} \quad (40)$$

Substitution of  $Y_\ell^{-m}(\theta, \phi) = (-1)^m Y_\ell^{m*}(\theta, \phi)$  and Eq. (38) into Eq. (40) and integration with respect to  $dr$  gives

$$a_M(\ell, m) = \frac{-ek^2}{c\sqrt{\ell(\ell+1)}} \frac{\omega_n}{2\pi} Nj_\ell(kr_n) \int_0^{2\pi} \int_0^\pi (-1)^m N_{\ell, -m} P_\ell^{-m}(\cos\theta) e^{-im\phi} \left\{ \begin{array}{l} e^{i\phi} N_{\ell, m} P_\ell^m(\cos\theta) e^{im\phi} \cos\theta \\ + \sin\theta \sqrt{(\ell-m)(\ell+m+1)} N_{\ell, m+1} P_\ell^{m+1}(\cos\theta) e^{i(m+1)\phi} \end{array} \right\} \sin\theta d\theta d\phi \quad (41)$$

The integral in Eq. (41) separated in terms of  $d\theta$  and  $d\phi$  is

$$a_M(\ell, m) = \frac{-ek^2}{c\sqrt{\ell(\ell+1)}} \frac{\omega_n}{2\pi} Nj_\ell(kr_n) \int_0^\pi (-1)^m N_{\ell, -m} P_\ell^{-m}(\cos\theta) \left\{ \begin{array}{l} N_{\ell, m} P_\ell^m(\cos\theta) \cos\theta \\ + \sin\theta \sqrt{(\ell-m)(\ell+m+1)} N_{\ell, m+1} P_\ell^{m+1}(\cos\theta) \end{array} \right\} \sin\theta d\theta \int_0^{2\pi} e^{i\phi} d\phi \quad (42)$$

Consider that the  $d\theta$  integral is finite and designated by  $\Theta$ , then Eq. (42) is given as

$$a_M(\ell, m) = \frac{-ek^2}{c\sqrt{\ell(\ell+1)}} \frac{\omega_n}{2\pi} Nj_\ell(kr_n) \Theta \int_0^{2\pi} e^{i\phi} d\phi \quad (43)$$

From Eq. (26), the far fields are given by

$$\mathbf{B} = -\frac{i}{k} a_M(\ell, m) \nabla \times \mathbf{g}_\ell(kr) \mathbf{X}_{\ell, m} \quad (44)$$

$$\mathbf{E} = a_M(\ell, m) \mathbf{g}_\ell(kr) \mathbf{X}_{\ell, m}$$

where  $a_M(\ell, m)$  is given by Eq. (43).

The power density  $P(t)$  given by the Poynting power vector is

$$P(t) = \mathbf{E} \times \mathbf{H} \quad (45)$$

For a pure multipole of order  $(\ell, m)$ , the time-averaged power radiated per solid angle  $\frac{dP(\ell, m)}{d\Omega}$

given by Jackson [21] is

$$\frac{dP(\ell, m)}{d\Omega} = \frac{c}{8\pi k^2} |a_M(\ell, m)|^2 |\mathbf{X}_{\ell, m}|^2 \quad (46)$$

where  $a_M(\ell, m)$  is given by Eq. (43).

Since the modulation function  $Y_{\ell, m}(\theta, \phi)$  is a traveling charge density wave that moves time harmonically on the surface of the orbitsphere about the z-axis with frequency  $\omega_n$ ,  $\phi$  of the spherical harmonic function is a function of  $t$  as shown in Eq. (33). The time dependence of the source current must also be evaluated in Eq. (43), and it can be written as

$$a_M(\ell, m) = \frac{-ek^2}{c\sqrt{\ell(\ell+1)}} \frac{\omega_n}{2\pi} Nj_\ell(kr_n) \Theta \int_0^{vT_n} \cos(mks(t)) ds \quad (47)$$

where  $s'(t)$  is the angular displacement of the rotating modulation function during one period  $T_n$  and  $v$  is the linear velocity in the  $\hat{\phi}$  direction. Thus,

$$a_M(\ell, m) = \frac{-ek^2}{c\sqrt{\ell(\ell+1)}} \frac{\omega_n}{2\pi} Nj_\ell(kr_n) \Theta \sin(mkvT_n) \quad (48)$$

$$a_M(\ell, m) = \frac{-ek^2}{c\sqrt{\ell(\ell+1)}} \frac{\omega_n}{2\pi} Nj_\ell(kr_n) \Theta \sin(mks) \quad (49)$$

In the case that  $k$  is the lightlike  $k^0$ , then  $k = \omega_n / c$ , and the  $\sin(mks)$  term in Eq. (49) vanishes for

$$R = cT_n \quad (50)$$

$$RT_n^{-1} = c \quad (51)$$

$$Rf = c \quad (52)$$

Thus,

$$s = vT_n = R = r_n = \lambda_n \quad (53)$$

as given by Eq. (16) which is identical to the Haus condition for nonradiation given by Eq. (17). Then, the multipole coefficient  $a_M(\ell, m)$  is zero. For the condition given by Eq. (53), the time-averaged power radiated per solid angle  $\frac{dP(\ell, m)}{d\Omega}$  given by Eqs (46) and (49) is zero. *There is no radiation.*

## MAGNETIC FIELD EQUATIONS OF THE ELECTRON

The orbitsphere is a shell of negative charge current comprising correlated charge motion along great circles. For  $\mathfrak{l} = 0$ , the orbitsphere gives rise to a magnetic moment of 1 Bohr magneton [22]. (The details of the derivation of the magnetic parameters including the electron g factor are given in the Appendix of this paper.)

$$\mu_B = \frac{e\hbar}{2m_e} = 9.274 \times 10^{-24} \text{ JT}^{-1}, \quad (54)$$

The magnetic field of the electron shown in Figure 6 is given by

$$\mathbf{H} = \frac{e\hbar}{m_e r_n^3} (\mathbf{i}_r \cos \theta - \mathbf{i}_\theta \sin \theta) \quad \text{for } r < r_n \quad (55)$$

$$\mathbf{H} = \frac{e\hbar}{2m_e r^3} (\mathbf{i}_r 2 \cos \theta + \mathbf{i}_\theta \sin \theta) \quad \text{for } r > r_n \quad (56)$$

The energy stored in the magnetic field of the electron is

$$E_{mag} = \frac{1}{2} \mu_o \int_0^{2\pi} \int_0^\pi \int_0^\infty H^2 r^2 \sin \theta dr d\theta d\Phi \quad (57)$$

$$E_{mag \text{ total}} = \frac{\pi \mu_o e^2 \hbar^2}{m_e^2 r_1^3} \quad (58)$$

## STERN-GERLACH EXPERIMENT

The Stern-Gerlach experiment implies a magnetic moment of one Bohr magneton and an associated angular momentum quantum number of  $1/2$ . Historically, this quantum number is called the spin quantum number,  $s$  ( $s = \frac{1}{2}$ ;  $m_s = \pm \frac{1}{2}$ ). The superposition of the vector projection of the orbitsphere angular momentum on the z-axis is  $\frac{\hbar}{2}$  with an orthogonal component of  $\frac{\hbar}{4}$ . Excitation of a resonant Larmor precession gives rise to  $\hbar$  on an axis  $\mathbf{S}$  that precesses about the z-axis called the spin axis at the Larmor frequency at an angle of  $\theta = \frac{\pi}{3}$  to give a perpendicular projection of

$$\mathbf{S}_{\perp} = \pm \sqrt{\frac{3}{4}} \hbar \quad (59)$$

and a projection onto the axis of the applied magnetic field of

$$\mathbf{S}_{\parallel} = \pm \frac{\hbar}{2} \quad (60)$$

The superposition of the  $\frac{\hbar}{2}$ , z-axis component of the orbitsphere angular momentum and the  $\frac{\hbar}{2}$ , z-axis component of  $\mathbf{S}$  gives  $\hbar$  corresponding to the observed electron magnetic moment of a Bohr magneton,  $\mu_B$ .

## ELECTRON g FACTOR

Conservation of angular momentum of the orbitsphere permits a discrete change of its “kinetic angular momentum” ( $\mathbf{r} \times m\mathbf{v}$ ) by the applied magnetic field of  $\frac{\hbar}{2}$ , and concomitantly the “potential angular momentum” ( $\mathbf{r} \times e\mathbf{A}$ ) must change by  $-\frac{\hbar}{2}$ .

$$\Delta\mathbf{L} = \frac{\hbar}{2} - \mathbf{r} \times e\mathbf{A} \quad (61)$$

$$= \left[ \frac{\hbar}{2} - \frac{e\phi}{2\pi} \right] \hat{z} \quad (62)$$

In order that the change of angular momentum,  $\Delta\mathbf{L}$ , equals zero,  $\phi$  must be  $\Phi_0 = \frac{h}{2e}$ , the magnetic flux quantum. The magnetic moment of the electron is parallel or antiparallel to the applied field only. During the spin-flip transition, power must be conserved. Power flow is governed by the Poynting power theorem,

$$\nabla \cdot (\mathbf{E} \times \mathbf{H}) = -\frac{\partial}{\partial t} \left[ \frac{1}{2} \mu_o \mathbf{H} \cdot \mathbf{H} \right] - \frac{\partial}{\partial t} \left[ \frac{1}{2} \epsilon_o \mathbf{E} \cdot \mathbf{E} \right] - \mathbf{J} \cdot \mathbf{E} \quad (63)$$

Eq. (64) gives the total energy of the flip transition which is the sum of the energy of reorientation of the magnetic moment (1st term), the magnetic energy (2nd term), the electric

energy (3rd term), and the dissipated energy of a fluxon treading the orbitsphere (4th term), respectively,

$$\Delta E_{mag}^{spin} = 2 \left( 1 + \frac{\alpha}{2\pi} + \frac{2}{3} \alpha^2 \left( \frac{\alpha}{2\pi} \right) - \frac{4}{3} \left( \frac{\alpha}{2\pi} \right)^2 \right) \mu_B B \quad (64)$$

$$\Delta E_{mag}^{spin} = g \mu_B B \quad (65)$$

where the stored magnetic energy corresponding to the  $\frac{\partial}{\partial t} \left[ \frac{1}{2} \mu_o \mathbf{H} \cdot \mathbf{H} \right]$  term increases, the stored electric energy corresponding to the  $\frac{\partial}{\partial t} \left[ \frac{1}{2} \epsilon_o \mathbf{E} \cdot \mathbf{E} \right]$  term increases, and the  $\mathbf{J} \cdot \mathbf{E}$  term is dissipative. The spin-flip transition can be considered as involving a magnetic moment of  $g$  times that of a Bohr magneton. The  $g$  factor is redesignated the fluxon  $g$  factor as opposed to the anomalous  $g$  factor. Using  $\alpha^{-1} = 137.03603(82)$ , the calculated value of  $\frac{g}{2}$  is 1.001 159 652 137. The experimental value [23] of  $\frac{g}{2}$  is 1.001 159 652 188(4). The derivation is given in the Appendix of this paper.

## SPIN AND ORBITAL PARAMETERS

The total function that describes the spinning motion of each electron orbitsphere is composed of two functions. One function, the spin function, is spatially uniform over the orbitsphere, spins with a quantized angular velocity, and gives rise to spin angular momentum. The other function, the modulation function, can be spatially uniform—in which case there is no orbital angular momentum and the magnetic moment of the electron orbitsphere is one Bohr magneton—or not spatially uniform—in which case there is orbital angular momentum. The modulation function also rotates with a quantized angular velocity.

The spin function of the electron corresponds to the nonradiative  $n = 1$ ,  $\ell = 0$  state of atomic hydrogen which is well known as an s state or orbital. (See Figure 1 for the charge function and Figure 2 for the current function.) In cases of orbitals of heavier elements and excited states of one electron atoms and atoms or ions of heavier elements with the  $\ell$  quantum number not equal to zero and which are not constant as given by Eq. (14), the constant spin function is modulated by a time and spherical harmonic function as given by Eq. (15) and shown in Figure 3. The modulation or traveling charge density wave corresponds to an orbital angular momentum in addition to a spin angular momentum. These states are typically referred to as p, d, f, etc. orbitals. Application of Haus's [12] condition also predicts nonradiation for a constant spin function modulated by a time and spherically harmonic orbital function. There is acceleration without radiation as also shown in the Nonradiation Based on the Electron

Electromagnetic Fields and the Poynting Power Vector section. (Also see Abbott and Griffiths, Goedecke, and Daboul and Jensen [16-18]). However, in the case that such a state arises as an excited state by photon absorption, it is radiative due to a radial dipole term in its current density function since it possesses spacetime Fourier Transform components synchronous with waves traveling at the speed of light [12]. (See “Instability of Excited States” section.)

### Moment of Inertia and Spin and Rotational Energies

The moments of inertia and the rotational energies as a function of the  $\mathfrak{l}$  quantum number for the solutions of the time-dependent electron charge density functions (Eqs. (14-15)) given in the Angular Functions section are solved using the rigid rotor equation [15]. The details of the derivations of the results as well as the demonstration that Eqs. (14-15) with the results given *infra.* are solutions of the wave equation are given in Chp 1, Rotational Parameters of the Electron (Angular Momentum, Rotational Energy, Moment of Inertia) section, of Ref. [3].

$$\mathfrak{l} = 0$$

$$I_z = I_{spin} = \frac{m_e r_n^2}{2} \quad (66)$$

$$L_z = I\omega_z = \pm \frac{\hbar}{2} \quad (67)$$

$$E_{rotational} = E_{rotational, spin} = \frac{1}{2} \left[ I_{spin} \left( \frac{\hbar}{m_e r_n^2} \right)^2 \right] = \frac{1}{2} \left[ \frac{m_e r_n^2}{2} \left( \frac{\hbar}{m_e r_n^2} \right)^2 \right] = \frac{1}{4} \left[ \frac{\hbar^2}{2I_{spin}} \right] \quad (68)$$

$$\mathfrak{l} \neq 0$$

$$I_{orbital} = m_e r_n^2 \left[ \frac{\ell(\ell+1)}{\ell^2 + \ell + 1} \right]^{\frac{1}{2}} \quad (69)$$

$$L_z = m\hbar \quad (70)$$

$$L_{z\ total} = L_{z\ spin} + L_{z\ orbital} \quad (71)$$

$$E_{rotational, orbital} = \frac{\hbar^2}{2I} \left[ \frac{\ell(\ell+1)}{\ell^2 + 2\ell + 1} \right] \quad (72)$$

$$T = \frac{\hbar^2}{2m_e r_n^2} \quad (73)$$

$$\langle E_{rotational, orbital} \rangle = 0 \quad (74)$$

From Eq. (74), the time average rotational energy is zero; thus, the principal levels are degenerate except when a magnetic field is applied.

## FORCE BALANCE EQUATION

The radius of the nonradiative ( $n=1$ ) state is solved using the electromagnetic force equations of Maxwell relating the charge and mass density functions wherein the angular momentum of the electron is given by Planck's constant bar. The reduced mass arises naturally from an electrodynamic interaction between the electron and the proton.

$$\frac{m_e}{4\pi r_1^2} \frac{v_1^2}{r_1} = \frac{e}{4\pi r_1^2} \frac{Ze}{4\pi\epsilon_0 r_1^2} - \frac{1}{4\pi r_1^2} \frac{\hbar^2}{mr_n^3} \quad (75)$$

$$r_1 = \frac{a_H}{Z} \quad (76)$$

where  $a_H$  is the radius of the hydrogen atom.

## ENERGY CALCULATIONS

From Maxwell's equations, the potential energy  $V$ , kinetic energy  $T$ , electric energy or binding energy  $E_{ele}$  are

$$V = \frac{-Ze^2}{4\pi\epsilon_0 r_1} = \frac{-Z^2 e^2}{4\pi\epsilon_0 a_H} = -Z^2 X 4.3675 X 10^{-18} J = -Z^2 X 27.2 eV \quad (77)$$

$$T = \frac{Z^2 e^2}{8\pi\epsilon_0 a_H} = Z^2 X 13.59 eV \quad (78)$$

$$T = E_{ele} = -\frac{1}{2} \epsilon_0 \int_{\infty}^{r_1} \mathbf{E}^2 dv \quad \text{where } \mathbf{E} = -\frac{Ze}{4\pi\epsilon_0 r^2} \quad (79)$$

$$E_{ele} = -\frac{Z^2 e^2}{8\pi\epsilon_0 a_H} = -Z^2 X 2.1786 X 10^{-18} J = -Z^2 X 13.598 eV \quad (80)$$

The calculated Rydberg constant is  $10,967,758 m^{-1}$ ; the experimental Rydberg constant is  $10,967,758 m^{-1}$ .

<sup>2</sup> The theories of Bohr, Schrödinger, and presently CQM all give the identical equation for the principal energy levels of the hydrogen atom.

$$E_{ele} = -\frac{Z^2 e^2}{8\pi\epsilon_0 n^2 a_H} = -\frac{Z^2}{n^2} X 2.1786 X 10^{-18} J = -Z^2 X \frac{13.598}{n^2} eV \quad (\text{FN 2.1})$$

In CQM, the two dimensional wave equation is solved for the charge density function of the electron. And, the Fourier transform of the charge density function is a solution of the three dimensional wave equation in frequency ( $k, \omega$ ) space. Whereas, the Schrödinger equation solutions are three dimensional in spacetime. The energy is given by

$$\int_{-\infty}^{\infty} \psi H \psi dv = E \int_{-\infty}^{\infty} \psi^2 dv; \quad (FN2.2)$$

$$\int_{-\infty}^{\infty} \psi^2 dv = 1 \quad (FN 2.3)$$

Thus,

## EXCITED STATES

CQM gives closed form solutions for the resonant photons and excited state electron functions. The angular momentum of the photon given by

$$|\mathbf{m}| = \left| \frac{1}{8\pi} \text{Re}[\mathbf{r} \times (\mathbf{E} \times \mathbf{B}^*)] \right| = \hbar \quad (81)$$

is conserved [21]. The change in angular velocity of the electron is equal to the angular frequency of the resonant photon. The energy is given by Planck's equation. The predicted energies, Lamb shift, hyperfine structure, resonant line shape, line width, selection rules, etc. are in agreement with observation.

The orbitsphere is a dynamic spherical resonator cavity which traps photons of discrete frequencies. The relationship between an allowed radius and the “photon standing wave” wavelength is

$$2\pi r = n\lambda \quad (82)$$

---


$$\int_{-\infty}^{\infty} \psi H \psi dv = E \quad (\text{FN 2.4})$$

In the case that the potential energy of the Hamiltonian,  $H$ , is a constant times the wavenumber, the Schrödinger equation is the well known Bessel equation. Then with one of the solutions for  $\psi$ , Eq. (FN 2.4) is equivalent to an inverse Fourier transform. According to the duality and scale change properties of Fourier transforms, the energy equation of CQM and that of quantum mechanics are identical, the energy of a radial Dirac delta function of radius equal to an integer multiple of the radius of the hydrogen atom (Eq. (FN 2.1)). And, Bohr obtained the same energy formula by postulating nonradiative states with angular momentum

$$L_z = m\hbar \quad (\text{FN 2.5})$$

and solving the energy equation classically.

The mathematics for all three theories converge to Eq. (FN 2.1). However, the physics is quite different. Only CQM is derived from first principles and holds over a scale of spacetime of 85 orders of magnitude. And, the mathematical relationship of CQM and QM is based on the Fourier transform of the radial function. CQM requires that the electron is real and physically confined to a two dimensional surface which corresponds to a solution of the two-dimensional wave equation plus time. The corresponding Fourier transform is a wave over all space which is a solution of the three dimensional wave equation (e.g. the Schrödinger equation). *In essence QM may be considered as a theory dealing with the Fourier transform of an electron rather than the physical electron.* By Parseval's theorem, the energies may be equivalent, but the quantum mechanical case is nonphysical—only mathematical. Thus, it is nonsensical from this perspective. It may mathematically produce numbers which agree with experimental energies, but the mechanisms lack internal consistency and conformity with physical laws. If these are the criteria for a valid solution of physical problems, then quantum mechanics has never successfully solved any problem. The theory of Bohr similarly failed.

Classical revisions may transform Schrödinger's and Heisenberg's quantum theory into what is termed a *classical quantum theory* such that physical descriptions result. For example, in the old quantum theory the spin angular momentum of the electron is called the “intrinsic angular momentum.” This term arises because it is difficult to provide a physical interpretation for the electron's spin angular momentum. Quantum Electrodynamics provides somewhat of a physical interpretation by proposing that the “vacuum” contains fluctuating electric and magnetic fields. In contrast, in CQM, spin angular momentum results from the motion of negatively charged mass moving systematically, and the equation for angular momentum,  $\mathbf{r} \times \mathbf{p}$ , can be applied directly to the wave function (a current density function) that describes the electron. And, quantization is carried by the photon, rather than probability waves of the electron as demonstrated in this paper.

where  $n$  is an integer. The relationship between an allowed radius and the electron wavelength is

$$2\pi(nr_1) = 2\pi r_n = n\lambda_1 = \lambda_n \quad (83)$$

where  $n = 1, 2, 3, 4, \dots$ . The radius of an orbitsphere increases with the absorption of electromagnetic energy. The radii of excited states are solved using the electromagnetic force equations of Maxwell relating the field from the charge of the proton, the electric field of the photon, and charge and mass density functions of the electron wherein the angular momentum of the electron is given by Planck's constant bar (Eq. (75)). The solutions to Maxwell's equations for modes that can be excited in the orbitsphere resonator cavity give rise to four quantum numbers, and the energies of the modes are the experimentally known hydrogen spectrum. The relationship between the electric field equation and the "trapped photon" source charge-density function is given by Maxwell's equation in two dimensions.

$$\mathbf{n} \cdot (\mathbf{E}_1 - \mathbf{E}_2) = \frac{\sigma}{\epsilon_0} \quad (84)$$

The photon standing electromagnetic wave is phase matched with the electron

$$\mathbf{E}_{r_{photon\ n,l,m}} = \frac{e(na_H)^\ell}{4\pi\epsilon_0} \frac{1}{r^{(\ell+2)}} \left[ -Y_0^0(\theta, \phi) + \frac{1}{n} \left[ Y_0^0(\theta, \phi) + \text{Re} \{ Y_\ell^m(\theta, \phi) e^{i\omega_n t} \} \right] \right] \delta(r - r_n) \mathbf{i}_r \quad (85)$$

$$\omega_n = 0 \text{ for } m = 0$$

$$\ell = 1, 2, \dots, n-1$$

$$m = -\ell, -\ell+1, \dots, 0, \dots, +\ell$$

$$\mathbf{E}_{r_{total}} = \frac{e}{4\pi\epsilon_0 r^2} + \frac{e(na_H)^\ell}{4\pi\epsilon_0} \frac{1}{r^{(\ell+2)}} \left[ -Y_0^0(\theta, \phi) + \frac{1}{n} \left[ Y_0^0(\theta, \phi) + \text{Re} \{ Y_\ell^m(\theta, \phi) e^{i\omega_n t} \} \right] \right] \delta(r - r_n) \mathbf{i}_r \quad (86)$$

$$\omega_n = 0 \text{ for } m = 0$$

For  $r = na_H$  and  $m = 0$ , the total radial electric field is

$$\mathbf{E}_{r_{total}} = \frac{1}{n} \frac{e}{4\pi\epsilon_0 (na_H)^2} \mathbf{i}_r \quad (87)$$

The energy of the photon which excites a mode in the electron spherical resonator cavity from radius  $a_H$  to radius  $na_H$  is

$$E_{photon} = \frac{e^2}{8\pi\epsilon_0 a_H} \left[ 1 - \frac{1}{n^2} \right] = h\nu = \hbar\omega \quad (88)$$

The change in angular velocity of the orbitsphere for an excitation from  $n = 1$  to  $n = n$  is

$$\Delta\omega = \frac{\hbar}{m_e(a_H)^2} - \frac{\hbar}{m_e(na_H)^2} = \frac{\hbar}{m_e(a_H)^2} \left[ 1 - \frac{1}{n^2} \right] \quad (89)$$

The kinetic energy change of the transition is

$$\frac{1}{2} m_e (\Delta v)^2 = \frac{e^2}{8\pi\epsilon_0 a_H} \left[ 1 - \frac{1}{n^2} \right] = \hbar\omega \quad (90)$$

The change in angular velocity of the electron orbitsphere is identical to the angular velocity of the photon necessary for the excitation,  $\omega_{photon}$ . The *correspondence principle holds*. It can be demonstrated that the resonance condition between these frequencies is to be satisfied in order to have a net change of the energy field [24].

## ORBITAL AND SPIN SPLITTING

The ratio of the square of the angular momentum,  $M^2$ , to the square of the energy,  $U^2$ , for a pure ( $\ell$ ,  $m$ ) multipole is [25]

$$\frac{M^2}{U^2} = \frac{m^2}{\omega^2} \quad (91)$$

The magnetic moment is defined as

$$\mu = \frac{\text{charge x angular momentum}}{2 \text{ x mass}} \quad (92)$$

The radiation of a multipole of order ( $\ell$ ,  $m$ ) carries  $m\hbar$  units of the z component of angular momentum per photon of energy  $\hbar\omega$ . Thus, the z component of the angular momentum of the corresponding excited state electron orbitsphere is

$$L_z = m\hbar \quad (93)$$

Therefore,

$$\mu_z = \frac{em\hbar}{2m_e} = m\mu_B \quad (94)$$

where  $\mu_B$  is the Bohr magneton. The orbital splitting energy is

$$E_{mag}^{orb} = m\mu_B B \quad (95)$$

The spin and orbital splitting energies superimpose; thus, the principal excited state energy levels of the hydrogen atom are split by the energy  $E_{mag}^{spin/orb}$ .

$$E_{mag}^{spin/orb} = m \frac{e\hbar}{2m_e} B + m_s g \frac{e\hbar}{m_e} B \quad \text{where} \quad (96)$$

$$n = 2, 3, 4, \dots$$

$$\ell = 1, 2, \dots, n-1$$

$$m = -\ell, -\ell+1, \dots, 0, \dots, +\ell$$

$$m_s = \pm \frac{1}{2}$$

For the electric dipole transition, the selection rules are

$$\Delta m = 0, \pm 1 \quad (97)$$

$$\Delta m_s = 0$$

## RESONANT LINE SHAPE AND LAMB SHIFT

The spectroscopic linewidth shown in Figure 7 arises from the classical rise-time band-width relationship, and the Lamb Shift is due to conservation of energy and linear momentum and arises from the radiation reaction force between the electron and the photon. It follows from the Poynting power theorem with spherical radiation that the transition probabilities are given by the ratio of power and the energy of the transition [26]. The transition probability in the case of the electric multipole moment is

$$\frac{1}{\tau} = \frac{\text{power}}{\text{energy}} \quad (98)$$

$$\frac{1}{\tau} = \frac{\left[ \frac{2\pi c}{[(2\ell+1)!]^2} \left(\frac{\ell+1}{\ell}\right) k^{2\ell+1} |Q_{\ell m} + Q_{\ell m}|^2 \right]}{[\hbar\omega]} = 2\pi \left(\frac{e^2}{h}\right) \sqrt{\frac{\mu_0}{\varepsilon_0}} \frac{2\pi}{[(2\ell+1)!]^2} \left(\frac{\ell+1}{\ell}\right) \left(\frac{3}{\ell+3}\right)^2 (kr_n)^{2\ell} \omega \quad (99)$$

$$|\mathbf{E}(\omega)| \propto \int_0^{\infty} e^{-\alpha t} e^{-i\omega t} dt = \frac{1}{\alpha - i\omega} \quad (100)$$

The relationship between the rise-time and the band-width for exponential decay is

$$\tau\Gamma = \frac{1}{\pi} \quad (101)$$

The energy radiated per unit frequency interval is

$$\frac{dI(\omega)}{d\omega} = I_0 \frac{\Gamma}{2\pi} \frac{1}{(\omega - \omega_0 - \Delta\omega)^2 + (\Gamma/2)^2} \quad (102)$$

## LAMB SHIFT

The Lamb Shift of the  ${}^2P_{1/2}$  state of the hydrogen atom is due to conservation of linear momentum of the electron, atom, and photon. The electron component is

$$\Delta f = \frac{\Delta\omega}{2\pi} = \frac{E_{hv}}{h} = \frac{(E_{hv})^2}{2h\mu_e c^2} = 1052.48 \text{ MHz} \quad (103)$$

where  $E_{hv}$  is

$$E_{hv} = 13.5983 \text{ eV} \left(1 - \frac{1}{n^2}\right) \frac{3}{4\pi} \sqrt{\frac{3}{4}} - h\Delta f \quad (104)$$

$$h\Delta f \lll 10 \text{ eV} \quad (105)$$

Therefore,

$$E_{hv} = 13.5983 \text{ eV} \left(1 - \frac{1}{n^2}\right) \frac{3}{4\pi} \sqrt{\frac{3}{4}} \quad (106)$$

The atom component is

$$\Delta f = \frac{\Delta\omega}{2\pi} = \frac{E_{hv}}{h} = \frac{(E_{hv})^2}{2hm_Hc^2} = \frac{\left(13.5983 \text{ eV} \left(1 - \frac{1}{n^2}\right) \left(1 + \frac{1}{2} - \sqrt{\frac{3}{4}}\right)\right)^2}{2hm_Hc^2} = 5.3839 \text{ MHz} \quad (107)$$

The sum of the components is

$$\Delta f = 1052.48 \text{ MHz} + 5.3839 \text{ MHz} = 1057.87 \text{ MHz} \quad (108)$$

The experimental Lamb Shift is

$$\Delta f = 1057.862 \text{ MHz} \quad (109)$$

## SPIN-ORBITAL COUPLING

The electron's motion in the hydrogen atom is always perpendicular to its radius; consequently, as shown by Eq. (7), the electron's angular momentum of  $\hbar$  is invariant. The angular momentum of the photon given in the Photon Equations section is  $|\mathbf{m}| = \left| \frac{1}{8\pi} \text{Re}[\mathbf{r} \times (\mathbf{E} \times \mathbf{B}^*)] \right| = \hbar$ . It is conserved for the solutions for the resonant photons and excited state electron functions given in the Excited States section and the Photon Equations section. Thus, the electrodynamic angular momentum and the inertial angular momentum are matched such that the correspondence principle holds. It follows from the principle of conservation of angular momentum that  $\frac{e}{m_e}$  of Eq. (54) is invariant given in the Special Relativistic Correction to the Electron Radius section and as shown previously [3]. In the case of spin-orbital coupling, the invariant  $\hbar$  of spin angular momentum and orbital angular momentum each give rise to a corresponding invariant magnetic moment of a Bohr magneton, and their corresponding energies superimpose as given in the Orbital and Spin Splitting section. The interaction of the two magnetic moments gives rise to a relativistic spin-orbital coupling energy. The vector orientations of the momenta must be considered as well as the condition that flux must be linked by the electron in units of the magnetic flux quantum in order to conserve the invariant electron angular momentum of  $\hbar$ . The energy may be calculated with the additional conditions of the invariance of the electron's charge and mass to charge ratio  $\frac{e}{m_e}$ .

As shown in the Electron g Factor section (Eqs. (61-65)), flux must be linked by the electron orbitsphere in units of the magnetic flux quantum. The maximum projection of the rotating spin angular momentum of the electron onto an axis given by Eq. (59) is  $\sqrt{\frac{3}{4}}\hbar$ . Then, using the magnetic energy term of Eq. (64), the spin-orbital coupling energy  $E_{s/o}$  is given by

$$E_{s/o} = 2 \frac{\alpha}{2\pi} \left( \frac{e\hbar}{2m_e} \right) \frac{\mu_0 e \hbar}{2(2\pi m_e) \left( \frac{r}{2\pi} \right)^3} \sqrt{\frac{3}{4}} = \frac{\alpha \pi \mu_0 e^2 \hbar^2}{m_e^2 r^3} \sqrt{\frac{3}{4}} \quad (110)$$

In the case that  $n = 2$ , the radius given by Eq. (83) is  $r = 2a_0$ . The predicted energy difference between the  ${}^2P_{3/2}$  and  ${}^2P_{1/2}$  levels of the hydrogen atom,  $E_{s/o}$ , given by Eq. (110) is

$$E_{s/o} = \frac{\alpha\pi\mu_0 e^2 \hbar^2}{8m_e^2 a_0^3} \sqrt{\frac{3}{4}} \quad (111)$$

As in the case of the  ${}^2P_{1/2} \rightarrow {}^2S_{1/2}$  transition, the photon-momentum transfer for the  ${}^2P_{3/2} \rightarrow {}^2P_{1/2}$  transition gives rise to a frequency shift derived after that of the Lamb shift with  $\Delta m_\ell = -1$  included. The energy,  $E_{FS}$ , for the  ${}^2P_{3/2} \rightarrow {}^2P_{1/2}$  transition called the fine structure splitting is given by

$$E_{FS} = \frac{\alpha^5 (2\pi)^2}{8} m_e c^2 \sqrt{\frac{3}{4}} + \left( 13.5983 \text{ eV} \left( 1 - \frac{1}{2^2} \right) \right)^2 \left[ \frac{\left( \frac{3}{4\pi} \left( 1 - \sqrt{\frac{3}{4}} \right) \right)^2}{2h\mu_e c^2} + \frac{\left( 1 + \left( 1 - \sqrt{\frac{3}{4}} \right) \right)^2}{2hm_H c^2} \right] \quad (112)$$

$$= 4.5190 \times 10^{-5} \text{ eV} + 1.75407 \times 10^{-7} \text{ eV}$$

$$= 4.53659 \times 10^{-5} \text{ eV}$$

where the first term corresponds to  $E_{s/o}$  given by Eq. (111) expressed in terms of the mass energy of the electron using Eqs. (184-185) and the second and third terms correspond to the electron recoil and atom recoil, respectively. The energy of  $4.53659 \times 10^{-5} \text{ eV}$  corresponds to a frequency of  $10,969.4 \text{ MHz}$  or a wavelength of  $2.73298 \text{ cm}$ . The experimental value of the  ${}^2P_{3/2} \rightarrow {}^2P_{1/2}$  transition frequency is  $10,969.1 \text{ MHz}$ . The large natural widths of the hydrogen  $2p$  levels limits the experimental accuracy; yet, given this limitation, the agreement between the theoretical and experimental fine structure is excellent.

## INSTABILITY OF EXCITED STATES

For the excited energy states of the hydrogen atom,  $\sigma_{photon}$ , the two dimensional surface charge due to the “trapped photons” at the electron orbitsphere, given by Eq. (84) and Eq. (85) is

$$\sigma_{photon} = \frac{e}{4\pi(r_n)^2} \left[ Y_0^0(\theta, \phi) - \frac{1}{n} \left[ Y_0^0(\theta, \phi) + \text{Re} \{ Y_\ell^m(\theta, \phi) e^{i\omega_n t} \} \right] \right] \delta(r - r_n) \quad (113)$$

where  $n = 2, 3, 4, \dots$ . Whereas,  $\sigma_{electron}$ , the two dimensional surface charge of the electron orbitsphere given by Eq. (15) is

$$\sigma_{electron} = \frac{-e}{4\pi(r_n)^2} \left[ Y_0^0(\theta, \phi) + \text{Re} \{ Y_\ell^m(\theta, \phi) e^{i\omega_n t} \} \right] \delta(r - r_n) \quad (114)$$

The superposition of  $\sigma_{photon}$  (Eq. (113)) and  $\sigma_{electron}$  is equivalent to the sum of a radial electric dipole represented by a doublet function and a radial electric monopole represented by a delta function.

$$\sigma_{photon} + \sigma_{electron} = \frac{e}{4\pi(r_n)^2} \left[ Y_0^0(\theta, \phi) \dot{\delta}(r - r_n) - \frac{1}{n} Y_0^0(\theta, \phi) \delta(r - r_n) - \left( 1 + \frac{1}{n} \right) \left[ \text{Re} \{ Y_\ell^m(\theta, \phi) e^{i\omega_n t} \} \right] \delta(r - r_n) \right]$$

(115)

where  $n = 2, 3, 4, \dots$ . Due to the radial doublet, excited states are radiative since spacetime harmonics of  $\frac{\omega_n}{c} = k$  or  $\frac{\omega_n}{c} \sqrt{\frac{\epsilon}{\epsilon_0}} = k$  do exist for which the spacetime Fourier transform of the current density function is nonzero.

## PHOTON EQUATIONS

The time-averaged angular-momentum density,  $\mathbf{m}$ , of an emitted photon is

$$\mathbf{m} = \int \frac{1}{8\pi c} \text{Re}[\mathbf{r} \times (\mathbf{E} \times \mathbf{B}^*)] dx^4 = \hbar \quad (116)$$

By reiterations of Eqs. (117) and (118), a photon orbitsphere is generated from two orthogonal great circle field lines shown in Figure 8 rather than two great circle current loops as in the case of the electron spin function. The output given by the non-primed coordinates is the input of the next iteration corresponding to each successive nested rotation by the infinitesimal angle  $\Delta\alpha$  where the summation of the rotation about each of the x'-axis and the y'-axis in each case is  $\frac{\sqrt{2}}{2}\pi$ . The right-handed circularly polarized photon orbitsphere shown in Figure 9 corresponds to the case wherein the  $\Delta\alpha$  for the x' and y' rotations are of the same sign, and the mirror image left-handed circularly polarized photon orbitsphere corresponds to the case wherein they are of the opposite sign. A linearly polarized photon orbitsphere is the superposition of the right- and left-handed circularly polarized photon orbitspheres.

## Nested Set of Great Circle Field Lines Generates the Photon Function

**H Field:**

$$\begin{bmatrix} x_1 \\ y_1 \\ z_1 \end{bmatrix} = \begin{bmatrix} \cos(\Delta\alpha) & -\sin^2(\Delta\alpha) & -\sin(\Delta\alpha)\cos(\Delta\alpha) \\ 0 & \cos(\Delta\alpha) & \sin(\Delta\alpha) \\ \sin(\Delta\alpha) & -\cos(\Delta\alpha)\sin(\Delta\alpha) & \cos^2(\Delta\alpha) \end{bmatrix} \begin{bmatrix} x_1' \\ y_1' \\ z_1' \end{bmatrix} \quad (117)$$

**E Field:**

$$\begin{bmatrix} x_1 \\ y_1 \\ z_1 \end{bmatrix} = \begin{bmatrix} \cos(\Delta\alpha) & -\sin^2(\Delta\alpha) & -\sin(\Delta\alpha)\cos(\Delta\alpha) \\ 0 & \cos(\Delta\alpha) & \sin(\Delta\alpha) \\ \sin(\Delta\alpha) & -\cos(\Delta\alpha)\sin(\Delta\alpha) & \cos^2(\Delta\alpha) \end{bmatrix} \begin{bmatrix} x_1' \\ y_1' \\ z_1' \end{bmatrix} \quad (118)$$

where the angular sum is  $\lim_{\Delta\alpha \rightarrow 0} \sum_{n=1}^{\frac{\sqrt{2}}{2}\pi} |\Delta\alpha_{i,j}| = \frac{\sqrt{2}}{2}\pi$ .

The field lines in the lab frame follow from the relativistic invariance of charge as given by Purcell [27]. The relationship between the relativistic velocity and the electric field of a moving charge shown schematically in Figure 10. From Eqs. (117-118) corresponding to the rotations over  $\Delta\alpha$ , the photon equation in the lab frame of a right-handed circularly polarized photon orbitsphere is

$$\mathbf{E} = \mathbf{E}_0 [\mathbf{x} + i\mathbf{y}] e^{-jk_z z} e^{-j\omega t} \quad (119)$$

$$\mathbf{H} = \left( \frac{\mathbf{E}_0}{\eta} \right) [\mathbf{y} - i\mathbf{x}] e^{-jk_z z} e^{-j\omega t} = \mathbf{E}_0 \sqrt{\frac{\epsilon}{\mu}} [\mathbf{y} - i\mathbf{x}] e^{-jk_z z} e^{-j\omega t} \quad (120)$$

with a wavelength of

$$\lambda = 2\pi \frac{c}{\omega} \quad (121)$$

The relationship between the photon orbitsphere radius and wavelength is

$$2\pi r_0 = \lambda_0 \quad (122)$$

The electric field lines of a right-handed circularly polarized photon orbitsphere as seen along the axis of propagation in the lab inertial reference frame as it passes a fixed point is shown in Figure 11.

## Spherical Wave

Photons superimpose, and the amplitude due to  $N$  photons is

$$E_{total} = \sum_{n=1}^N \frac{e^{-ik|\mathbf{r}-\mathbf{r}'|}}{4\pi|\mathbf{r}-\mathbf{r}'|} f(\theta, \phi) \quad (123)$$

In the far field, the emitted wave is a spherical wave

$$E_{total} = E_o \frac{e^{-ikr}}{r} \quad (124)$$

The Green Function is given as the solution of the wave equation. Thus, the superposition of photons gives the classical result. As  $r$  goes to infinity, the spherical wave becomes a plane wave. The double slit interference pattern is predicted. From the equation of a photon, the wave-particle duality arises naturally. The energy is always given by Planck's equation; yet, an interference pattern is observed when photons add over time or space. The results also predict those of the Aspect experiment involving Bell's inequalities [3].

## EQUATIONS OF THE FREE ELECTRON

### Charge Density Function

The radius of an electron orbitsphere increases with the absorption of electromagnetic energy [28]. With the absorption of a photon of energy exactly equal to the ionization energy, the electron becomes ionized and is a plane wave (spherical wave in the limit) with the de Broglie wavelength. The ionized electron traveling at constant velocity is nonradiative and is a two dimensional surface having a total charge of  $e$  and a total mass of  $m_e$ . The solution of the boundary value problem of the free electron is given by the projection of the orbitsphere into a plane that linearly propagates along an axis perpendicular to the plane where the velocity of the plane and the orbitsphere is given by

$$v = \frac{\hbar}{m_e \rho_0} \quad (125)$$

and the radius of the orbitsphere in spherical coordinates is equal to the radius of the free electron in cylindrical coordinates ( $\rho_0 = r_0$ ). The mass density function of a free electron shown in Figure 12 is a two dimensional disk having the mass density distribution in the  $xy(\rho)$ -plane

$$\rho_m(\rho, \phi, z) = \frac{m_e}{\frac{2}{3} \pi \rho_0^3} \pi \left( \frac{\rho}{2\rho_0} \right) \sqrt{\rho_0^2 - \rho^2} \delta(z) \quad (126)$$

and charge-density distribution,  $\rho_e(\rho, \phi, z)$ , in the  $xy$ -plane given by replacing  $m_e$  with  $e$  where the Pi function represents a plane wave. The charge density distribution of the free electron has recently been confirmed experimentally [29-30]. Researchers working at the Japanese National Laboratory for High Energy Physics (KEK) demonstrated that the charge of the free electron increases toward the particle's core and is symmetrical as a function of  $\phi$ . In addition, the

wave-particle duality arises naturally, and the result is consistent with scattering experiments from helium and the double split experiment [3].

### Current Density Function

Consider an electron initially bound as an orbitsphere of radius  $r = r_n = r_o$  ionized from a hydrogen atom with the magnitude of the angular velocity of the orbitsphere is given by

$$\omega = \frac{\hbar}{m_e r^2} \quad (127)$$

The current-density function of the free electron propagating with velocity  $v_z$  along the z-axis in the inertial frame of the proton is given by the vector projection of the current into xy-plane as the radius increases from  $r = r_o$  to  $r = \infty$ . The current-density function of the free electron, is

$$\mathbf{J}(\rho, \phi, z, t) = \left[ \mathcal{P} \left( \frac{\rho}{2\rho_o} \right) \frac{e}{\frac{4}{3} \pi \rho_o^3} \frac{\hbar}{m_e \sqrt{\rho_o^2 - \rho^2}} \mathbf{i}_\phi \right] \quad (128)$$

where  $\rho_o = r_o$ . The angular momentum,  $\mathbf{L}$ , is given by

$$\mathbf{L} \mathbf{i}_z = m_e r^2 \omega \quad (129)$$

Substitution of  $m_e$  for  $e$  in Eq. (128) followed by substitution into Eq. (129) gives the angular momentum density function,  $\mathbf{L}$

$$\mathbf{L} \mathbf{i}_z = \mathcal{P} \left( \frac{\rho}{2\rho_o} \right) \frac{m_e}{\frac{4}{3} \pi \rho_o^3} \frac{\hbar}{m_e \sqrt{\rho_o^2 - \rho^2}} \rho^2 \mathbf{i}_z \quad (130)$$

The total angular momentum of the free electron is given by integration over the two dimensional disk having the angular momentum density given by Eq. (130).

$$\mathbf{L} \mathbf{i}_z = \int_0^{2\pi} \int_0^{\rho_o} \mathcal{P} \left( \frac{\rho}{2\rho_o} \right) \frac{m_e}{\frac{4}{3} \pi \rho_o^3} \frac{\hbar}{m_e \sqrt{\rho_o^2 - \rho^2}} \rho^2 \rho d\rho d\phi = \hbar \mathbf{i}_z \quad (131)$$

The four dimensional spacetime current-density function of the free electron that propagates along the z-axis with velocity given by Eq. (125) corresponding to  $r = r_o = \rho_o$  is given by substitution of Eq. (125) into Eq. (129).

$$\mathbf{J}(\rho, \phi, z, t) = \left[ \mathcal{P} \left( \frac{\rho}{2\rho_o} \right) \frac{e}{\frac{4}{3} \pi \rho_o^3} \frac{\hbar}{m_e \sqrt{\rho_o^2 - \rho^2}} \mathbf{i}_\phi \right] + \frac{e\hbar}{m_e \rho_o} \delta \left( z - \frac{\hbar}{m_e \rho_o} t \right) \mathbf{i}_z \quad (132)$$

The spacetime Fourier Transform of Eq. (132) is

$$\frac{e}{\frac{4}{3} \pi \rho_o^3} \frac{\hbar}{m_e} \text{sinc}(2\pi s \rho_o) + 2\pi e \frac{\hbar}{m_e \rho_o} \delta(\omega - \mathbf{k}_z \cdot \mathbf{v}_z) \quad (133)$$

The boundary condition is that the spacetime harmonics of  $\frac{\omega_n}{c} = k$  or  $\frac{\omega_n}{c} \sqrt{\frac{\epsilon}{\epsilon_o}} = k$  do not exist.

Radiation due to charge motion does not occur in any medium when this boundary condition is met. Thus, no Fourier components that are synchronous with light velocity with the propagation constant  $|\mathbf{k}_z| = \frac{\omega}{c}$  exist, and radiation due to charge motion of the free electron does not occur when this boundary condition is met. It follows from Eq. (125) and the relationship  $2\pi\rho_o = \lambda_o$  that the wavelength of the free electron is the de Broglie wavelength.

$$\lambda_o = \frac{h}{m_e v_z} = 2\pi\rho_o \quad (134)$$

The Stern-Gerlach experiment implies a magnetic moment of one Bohr magneton and an associated angular momentum quantum number of 1/2 ( $s = \frac{1}{2}$ ;  $m_s = \pm \frac{1}{2}$ ). The superposition of the vector projection of the angular momentum of the free electron on to the z-axis is  $\hbar$  corresponding to the observed electron magnetic moment of a Bohr magneton,  $\mu_B$ . Excitation of a resonant Larmor precession causes the free electron to rotate about an  $X_R$ -axis that is in the xy-plane and rotates at the Larmor frequency to reverse the spin direction. In order to conserve angular momentum, a magnetic flux quantum  $\Phi_o = \frac{h}{2e}$  must be linked by the electron during the spin-flip transition, and the electron magnetic moment can only be parallel or antiparallel to an applied field as observed with the Stern-Gerlach experiment. The energy,  $\Delta E_{mag}^{spin}$ , of the spin flip transition corresponding to the  $m_s = \frac{1}{2}$  quantum number is given by Eq. (65).

$$\Delta E_{mag}^{spin} = g\mu_B B \quad (135)$$

(See Chp. 3 of Ref. [3] for details of the derivations.)

## TWO ELECTRON ATOMS

Two electron atoms may be solved from a central force balance equation with the nonradiation condition. The force balance equation using Eq. (6) is

$$\frac{m_e v_2^2}{4\pi r_2^2} = \frac{m_e}{4\pi r_2^2} \frac{\hbar^2}{m_e r_2^3} = \frac{e}{4\pi r_2^2} \frac{(Z-1)e}{4\pi\epsilon_o r_2^2} + \frac{1}{4\pi r_2^2} \frac{\hbar^2}{Zm_e r_2^3} \sqrt{s(s+1)} \quad (136)$$

which gives the radius of both electrons as

$$r_2 = r_1 = a_0 \left( \frac{1}{Z-1} - \frac{\sqrt{s(s+1)}}{Z(Z-1)} \right); \quad s = \frac{1}{2} \quad (137)$$

## Ionization Energies Calculated using the Poynting Power Theorem

For helium, which has no electric field beyond  $r_1$

$$\text{Ionization Energy(He)} = -E(\text{electric}) + E(\text{magnetic}) \quad (138)$$

where,

$$E(\text{electric}) = -\frac{(Z-1)e^2}{8\pi\epsilon_0 r_1} \quad (139)$$

$$E(\text{magnetic}) = \frac{2\pi\mu_0 e^2 \hbar^2}{m_e^2 r_1^3} \quad (140)$$

For  $3 \leq Z$

$$\text{Ionization Energy} = -\text{Electric Energy} - \frac{1}{Z} \text{Magnetic Energy} \quad (141)$$

The energies of several two-electron atoms are given in Table I. The exact solutions for one through twenty-electron atoms are given in Ref. [3].

### ELASTIC ELECTRON SCATTERING FROM HELIUM ATOMS

The aperture distribution function,  $a(\rho, \phi, z)$ , for the elastic scattering of an incident electron plane wave represented by  $\mathcal{T}(z)$  by a helium atom represented by

$$\frac{2}{4\pi(0.567a_o)^2} [\delta(r - 0.567a_o)] \quad (142)$$

is given by the convolution of the plane wave with the helium atom function:

$$a(\rho, \phi, z) = \mathcal{T}(z) \otimes \frac{2}{4\pi(0.567a_o)^2} [\delta(r - 0.567a_o)] \quad (143)$$

The aperture function is

$$a(\rho, \phi, z) = \frac{2}{4\pi(0.567a_o)^2} \sqrt{(0.567a_o)^2 - z^2} \delta(r - \sqrt{(0.567a_o)^2 - z^2}) \quad (144)$$

### Far Field Scattering (circular symmetry)

Applying Huygens' principle to a disturbance caused by the plane wave electron over the helium atom as an aperture gives the amplitude of the far field or Fraunhofer diffraction pattern  $F(s)$  as the Fourier Transform of the aperture distribution. The intensity  $I_1^{ed}$  is the square of the amplitude.

$$F(s) = \frac{2}{4\pi(0.567a_o)^2} 2\pi \int_0^\infty \int_{-\infty}^\infty \sqrt{(0.567a_o)^2 - z^2} \delta(\rho - \sqrt{(0.567a_o)^2 - z^2}) J_0(s\rho) e^{-iws} \rho d\rho dz \quad (145)$$

$$I_1^{ed} = F(s)^2$$

$$= I_e \left\{ \left[ \frac{2\pi}{(z_o w)^2 + (z_o s)^2} \right]^{\frac{1}{2}} \left\{ 2 \left[ \frac{z_o s}{(z_o w)^2 + (z_o s)^2} \right] J_{3/2} \left[ ((z_o w)^2 + (z_o s)^2)^{1/2} \right] - \left[ \frac{z_o s}{(z_o w)^2 + (z_o s)^2} \right]^2 J_{5/2} \left[ ((z_o w)^2 + (z_o s)^2)^{1/2} \right] \right\} \right\}^2 \quad (146)$$

$$s = \frac{4\pi}{\lambda} \sin \frac{\theta}{2}; \quad w = 0 \text{ (units of } \text{\AA}^{-1} \text{)} \quad (147)$$

The experimental results of Bromberg [33], the extrapolated experimental data of Hughes [33], the small angle data of Geiger [34] and the semiexperimental results of Lassettre [33] for the elastic differential cross section for the elastic scattering of electrons by helium atoms is shown graphically in Figure 13. The elastic differential cross section as a function of angle numerically calculated by Khare [33] using the first Born approximation and first-order exchange approximation also appear in Figure 13. These results which are based on a quantum mechanical model are compared with experimentation [33-34]. The closed-form function (Eqs. (146) and (147)) for the elastic differential cross section for the elastic scattering of electrons by helium atoms is shown graphically in Figure 14. The scattering amplitude function,  $F(s)$  (Eq. (145), is shown as an insert. It is apparent from Figure 13 that the quantum mechanical calculations fail completely at predicting the experimental results at small scattering angles; whereas, there is good agreement between Eq. (146) and the experimental results.

## THE NATURE OF THE CHEMICAL BOND OF HYDROGEN

The hydrogen molecule charge and current density functions, bond distance, and energies are solved from the Laplacian in ellipsoidal coordinates with the constraint of nonradiation.

$$(\eta - \zeta)R_\xi \frac{\partial}{\partial \xi} \left( R_\xi \frac{\partial \phi}{\partial \xi} \right) + (\zeta - \xi)R_\eta \frac{\partial}{\partial \eta} \left( R_\eta \frac{\partial \phi}{\partial \eta} \right) + (\xi - \eta)R_\zeta \frac{\partial}{\partial \zeta} \left( R_\zeta \frac{\partial \phi}{\partial \zeta} \right) = 0 \quad (148)$$

The force balance equation for the hydrogen molecule is

$$\frac{\hbar^2}{m_e a^2 b^2} 2ab^2 X = \frac{e^2}{4\pi\epsilon_0} X + \frac{\hbar^2}{2m_e a^2 b^2} 2ab^2 X \quad (149)$$

where

$$X = \frac{1}{\sqrt{\xi + a^2}} \frac{1}{\sqrt{\xi + b^2}} \frac{1}{c} \sqrt{\frac{\xi^2 - 1}{\xi^2 - \eta^2}} \quad (150)$$

Eq. (149) has the parametric solution

$$r(t) = \mathbf{i}a \cos \omega t + \mathbf{j}b \sin \omega t \quad (151)$$

when the semimajor axis,  $a$ , is

$$a = a_0 \quad (152)$$

The internuclear distance,  $2c'$ , which is the distance between the foci is

$$2c' = \sqrt{2}a_0 \quad (153)$$

The experimental internuclear distance is  $\sqrt{2}a_0$ . The semiminor axis is

$$b = \frac{1}{\sqrt{2}} a_0 \quad (154)$$

The eccentricity,  $e$ , is

$$e = \frac{1}{\sqrt{2}} \quad (155)$$

### The Energies of the Hydrogen Molecule

The potential energy of the two electrons in the central field of the protons at the foci is

$$V_e = \frac{-2e^2}{8\pi\epsilon_0\sqrt{a^2 - b^2}} \ln \frac{a + \sqrt{a^2 - b^2}}{a - \sqrt{a^2 - b^2}} = -67.836 \text{ eV} \quad (156)$$

The potential energy of the two protons is

$$V_p = \frac{e^2}{8\pi\epsilon_0\sqrt{a^2 - b^2}} = 19.242 \text{ eV} \quad (157)$$

The kinetic energy of the electrons is

$$T = \frac{\hbar^2}{2m_e a \sqrt{a^2 - b^2}} \ln \frac{a + \sqrt{a^2 - b^2}}{a - \sqrt{a^2 - b^2}} = 33.918 \text{ eV} \quad (158)$$

The energy,  $V_m$ , of the magnetic force between the electrons is

$$V_m = \frac{-\hbar^2}{4m_e a \sqrt{a^2 - b^2}} \ln \frac{a + \sqrt{a^2 - b^2}}{a - \sqrt{a^2 - b^2}} = -16.959 \text{ eV} \quad (159)$$

During bond formation, the electrons undergo a reentrant oscillatory orbit with vibration of the protons. The corresponding energy  $\bar{E}_{osc}$  is the difference between the Doppler and average vibrational kinetic energies:

$$\bar{E}_{osc} = \bar{E}_D + \bar{E}_{Kvib} = (V_e + T + V_m + V_p) \sqrt{\frac{2\bar{E}_K}{Mc^2}} + \frac{1}{2} \hbar \sqrt{\frac{k}{\mu}} \quad (160)$$

The total energy is

$$E_T = V_e + T + V_m + V_p + \bar{E}_{osc} \quad (161)$$

$$E_T = -\frac{e^2}{8\pi\epsilon_0 a_0} \left[ \left( 2\sqrt{2} - \sqrt{2} + \frac{\sqrt{2}}{2} \right) \ln \frac{\sqrt{2} + 1}{\sqrt{2} - 1} - \sqrt{2} \right] \left[ 1 + \sqrt{\frac{2\hbar \sqrt{\frac{e^2}{4\pi\epsilon_0 a_0^3}}}{m_e c^2}} \right] - \frac{1}{2} \hbar \sqrt{\frac{k}{\mu}} = -31.689 \text{ eV}$$

(162)

The energy of two hydrogen atoms is

$$E(2H[a_H]) = -27.21 \text{ eV} \quad (163)$$

The bond dissociation energy,  $E_D$ , is the difference between the total energy of the corresponding hydrogen atoms (Eq. (163)) and  $E_T$  (Eq. (162)).

$$E_D = E(2H[a_H]) - E_T = 4.478 \text{ eV} \quad (164)$$

The experimental energy is  $E_D = 4.478 \text{ eV}$ . The calculated and experimental parameters of  $H_2$ ,  $D_2$ ,  $H_2^+$ , and  $D_2^+$  from Chp. 12 of Ref. [3] are given in Table II.

## COSMOLOGICAL THEORY BASED ON MAXWELL'S EQUATIONS

Maxwell's equations and special relativity are based on the law of propagation of a electromagnetic wave front in the form

$$\frac{1}{c^2} \left( \frac{\partial \omega}{\partial t} \right)^2 - \left[ \left( \frac{\partial \omega}{\partial x} \right)^2 + \left( \frac{\partial \omega}{\partial y} \right)^2 + \left( \frac{\partial \omega}{\partial z} \right)^2 \right] = 0 \quad (165)$$

*For any kind of wave advancing with limiting velocity and capable of transmitting signals, the equation of front propagation is the same as the equation for the front of a light wave.* Thus, the equation

$$\frac{1}{c^2} \left( \frac{\partial \omega}{\partial t} \right)^2 - (\text{grad } \omega)^2 = 0 \quad (166)$$

acquires a general character; it is more general than Maxwell's equations from which Maxwell originally derived it.

A discovery of the present work shown in this section with the results of the previous sections regarding the bound electron is that the classical wave equation governs: (1) the motion of bound electrons, (2) the propagation of any form of energy, (3) measurements between inertial frames of reference such as time, mass, momentum, and length (Minkowski tensor), (4) fundamental particle production and the conversion of matter to energy, (5) a relativistic correction of spacetime due to particle production or annihilation (Schwarzschild metric), (6) the expansion and contraction of the Universe, (7) the basis of the relationship between Maxwell's equations, Planck's equation, the de Broglie equation, Newton's laws, and special, and general relativity.

The relationship between the time interval between ticks  $t$  of a clock in motion with velocity  $v$  relative to an observer and the time interval  $t_0$  between ticks on a clock at rest relative to an observer is [35]

$$(ct)^2 = (ct_0)^2 + (vt)^2 \quad (167)$$

Thus, the time dilation relationship based on the constant maximum speed of light  $c$  in any inertial frame is

$$t = \frac{t_0}{\sqrt{1 - \frac{v^2}{c^2}}} \quad (168)$$

The metric  $g_{\mu\nu}$  for Euclidean space is the Minkowski tensor  $\eta_{\mu\nu}$ . In this case, the separation of proper time between two events  $x^\mu$  and  $x^\mu + dx^\mu$  is  $d\tau^2 = -\eta_{\mu\nu}dx^\mu dx^\nu$ .

## THE EQUIVALENCE OF THE GRAVITATIONAL MASS AND THE INERTIAL MASS

Mass also experimentally causes time dilation (i.e. clocks run slower in the presence of a gravitational field). The equivalence of the gravitational mass and the inertial mass,  $m_g / m_i = \text{universal constant}$ , which is predicted by Newton's law of mechanics and gravitation is experimentally confirmed to less  $1 \times 10^{-11}$  [36]. In physics, the discovery of a universal constant often leads to the development of an entirely new theory. From the universal constancy of the velocity of light,  $c$  the special theory of relativity was derived; and from Planck's constant  $h$ , the quantum theory was deduced. Therefore, the universal constant  $m_g / m_i$  should be the key to the gravitational problem. The energy equation of Newtonian gravitation is

$$E = \frac{1}{2}mv^2 - \frac{GMm}{r} = \frac{1}{2}mv_0^2 - \frac{GMm}{r_0} = \text{constant} \quad (169)$$

Since  $h$ , the angular momentum per unit mass, is

$$h = L/m = |\mathbf{r} \times \mathbf{v}| = r_0 v_0 \sin \phi$$

the eccentricity  $e$  may be written as

$$e = \left[ 1 + \left( v_0^2 - \frac{2GM}{r_0} \right) \frac{r_0^2 v_0^2 \sin^2 \phi}{G^2 M^2} \right]^{1/2} \quad (170)$$

where  $m$  is the inertial mass of a particle,  $v_0$  is the speed of the particle,  $r_0$  is the distance of the particle from a massive object,  $\phi$  is the angle between the direction of motion of the particle and the radius vector from the object, and  $M$  is the total mass of the object (including a particle). The eccentricity  $e$  given by Newton's differential equations of motion in the case of the central field permits the classification of the orbits according to the total energy  $E$  [37] (column 1) and the orbital velocity squared,  $v_0^2$ , relative to the gravitational velocity squared,  $\frac{2GM}{r_0}$  [37]

(column 2):

$E < 0$	$v_0^2 < \frac{2GM}{r_0}$	$e < 1$	ellipse
$E < 0$	$v_0^2 < \frac{2GM}{r_0}$	$e = 0$	circle (special case of ellipse)

$$\begin{array}{llll}
E = 0 & v_0^2 = \frac{2GM}{r_0} & e = 1 & \text{parabolic orbit} \\
E > 0 & v_0^2 > \frac{2GM}{r_0} & e > 1 & \text{hyperbolic orbit} \quad (171)
\end{array}$$

## CONTINUITY CONDITIONS FOR THE PRODUCTION OF A PARTICLE FROM A PHOTON TRAVELING AT LIGHT SPEED

A photon traveling at the speed of light gives rise to a particle with an initial radius equal to its Compton wavelength bar.

$$r = \tilde{\lambda}_c = \frac{\hbar}{mc} = r_\alpha^* \quad (172)$$

The particle must have an orbital velocity equal to Newtonian gravitational escape velocity  $v_g$  of the antiparticle.

$$v_g = \sqrt{\frac{2Gm}{r}} = \sqrt{\frac{2Gm_0}{\tilde{\lambda}_c}} \quad (173)$$

The eccentricity is one. The orbital energy is zero corresponding to conservation of energy. The particle production trajectory is a parabola relative to the center of mass of the antiparticle.

### A Gravitational Field as a Front Equivalent to Light Wave Front

The particle with a finite gravitational mass gives rise to a gravitational field that travels out as a front equivalent to a light wave front. The form of the outgoing gravitational field front traveling at the speed of light is  $f\left(t - \frac{r}{c}\right)$ , and  $d\tau^2$  is given by

$$d\tau^2 = f(r)dt^2 - \frac{1}{c^2} \left[ f(r)^{-1} dr^2 + r^2 d\theta^2 + r^2 \sin^2 \theta d\phi^2 \right] \quad (174)$$

The speed of light as a constant maximum as well as phase matching and continuity conditions of the electromagnetic and gravitational waves require the following form of the squared displacements:

$$(c\tau)^2 + (v_g t)^2 = (ct)^2 \quad (175)$$

$$f(r) = \left( 1 - \left( \frac{v_g}{c} \right)^2 \right) \quad (176)$$

In order that the wave front velocity does not exceed  $c$  in any frame, spacetime must undergo time dilation and length contraction due to the particle production event. *The derivation and result of spacetime time dilation is analogous to the derivation and result of special relativistic time dilation* wherein the relative velocity of two inertial frames replaces the gravitational velocity.

The general form of the metric due to the relativistic effect on spacetime due to mass  $m_0$  with  $v_g$  given by Eq. (173) is

$$d\tau^2 = \left(1 - \left(\frac{v_g}{c}\right)^2\right) dt^2 - \frac{1}{c^2} \left[ \left(1 - \left(\frac{v_g}{c}\right)^2\right)^{-1} dr^2 + r^2 d\theta^2 + r^2 \sin^2 \theta d\phi^2 \right] \quad (177)$$

The gravitational radius,  $r_g$ , of each orbitsphere of the particle production event, each of mass  $m_0$ , and the corresponding general form of the metric are respectively

$$r_g = \frac{2Gm_0}{c^2}, \quad (178)$$

$$d\tau^2 = \left(1 - \frac{r_g}{r}\right) dt^2 - \frac{1}{c^2} \left[ \left(1 - \frac{r_g}{r}\right)^{-1} dr^2 + r^2 d\theta^2 + r^2 \sin^2 \theta d\phi^2 \right] \quad (179)$$

The metric  $g_{\mu\nu}$  for non-Euclidean space due to the relativistic effect on spacetime due to mass  $m_0$  is

$$g_{\mu\nu} = \begin{pmatrix} -\left(1 - \frac{2Gm_0}{c^2 r}\right) & 0 & 0 & 0 \\ 0 & \frac{1}{c^2} \left(1 - \frac{2Gm_0}{c^2 r}\right)^{-1} & 0 & 0 \\ 0 & 0 & \frac{1}{c^2} r^2 & 0 \\ 0 & 0 & 0 & \frac{1}{c^2} r^2 \sin^2 \theta \end{pmatrix} \quad (180)$$

Masses and their effects on spacetime *superimpose*. The separation of proper time between two events  $x^\mu$  and  $x^\mu + dx^\mu$  is

$$d\tau^2 = \left(1 - \frac{2GM}{c^2 r}\right) dt^2 - \frac{1}{c^2} \left[ \left(1 - \frac{2GM}{c^2 r}\right)^{-1} dr^2 + r^2 d\theta^2 + r^2 \sin^2 \theta d\phi^2 \right] \quad (181)$$

The *Schwarzschild metric* (Eq. (181)) gives the relationship whereby matter causes relativistic corrections to spacetime that determines the curvature of spacetime and is the origin of gravity.

### Particle Production Continuity Conditions from Maxwell's Equations, and the Schwarzschild Metric

The photon to particle event requires a transition state that is continuous wherein the velocity of a transition state orbitsphere is the speed of light. The radius,  $r$ , is the Compton wavelength bar,  $\tilde{\lambda}_c$ , given by Eq. (172). At production, the Planck equation energy, the electric potential energy, and the magnetic energy are equal to  $m_0 c^2$ .

The *Schwarzschild metric* gives the relationship whereby matter causes relativistic corrections to spacetime that determines the masses of fundamental particles. Substitution of  $r = \tilde{\lambda}_c$ ;  $dr = 0$ ;  $d\theta = 0$ ;  $\sin^2 \theta = 1$  into the Schwarzschild metric gives

$$d\tau = dt \left( 1 - \frac{2Gm_0}{c^2 r_\alpha^*} - \frac{v^2}{c^2} \right)^{\frac{1}{2}} \quad (182)$$

with  $v^2 = c^2$ , the relationship between the proper time and the coordinate time is

$$\tau = ti \sqrt{\frac{2GM}{c^2 r_\alpha^*}} = ti \sqrt{\frac{2GM}{c^2 \tilde{\lambda}_c}} = ti \frac{v_g}{c} \quad (183)$$

When the orbitsphere velocity is the speed of light, continuity conditions based on the constant maximum speed of light given by Maxwell's equations are mass energy = Planck equation energy = electric potential energy = magnetic energy = mass/spacetime metric energy.

Therefore,

$$m_o c^2 = \hbar \omega^* = V = E_{mag} = E_{spacetime} \quad (184)$$

$$m_o c^2 = \hbar \omega^* = \frac{\hbar^2}{m_o \tilde{\lambda}_c^2} = \alpha^{-1} \frac{e^2}{4\pi \epsilon_0 \tilde{\lambda}_c} = \alpha^{-1} \frac{\pi \mu_0 e^2 \hbar^2}{(2\pi m_o)^2 \tilde{\lambda}_c^3} = \frac{\alpha \hbar}{1 \text{ sec}} \sqrt{\frac{\tilde{\lambda}_c c^2}{2Gm}} \quad (185)$$

The continuity conditions based on the constant maximum speed of light given by the Schwarzschild metric are:

$$\frac{\text{proper time}}{\text{coordinate time}} = \frac{\text{gravitational wave condition}}{\text{electromagnetic wave condition}} = \frac{\text{gravitational mass phase matching}}{\text{charge/inertial mass phase matching}}$$

$$\frac{\text{proper time}}{\text{coordinate time}} = i \frac{\sqrt{\frac{2Gm}{c^2 \tilde{\lambda}_c}}}{\alpha} = i \frac{v_g}{\alpha c} \quad (186)$$

## MASSES OF FUNDAMENTAL PARTICLES

Each of the Planck equation energy, electric energy, and magnetic energy corresponds to a particle given by the relationship between the proper time and the coordinate time [3]. The electron and down-down-up neutron correspond to the Planck equation energy. The muon and strange-strange-charmed neutron correspond to the electric energy. The tau and bottom-bottom-top neutron correspond to the magnetic energy. The particle must possess the escape velocity  $v_g$  relative to the antiparticle where  $v_g < c$ . According to Newton's law of gravitation, the eccentricity is one and the particle production trajectory is a parabola relative to the center of mass of the antiparticle.

### Electron and Muon Production

A clock is defined in terms of a self consistent system of units used to measure the particle mass<sup>3</sup>. The proper time of the particle is equated with the coordinate time according to the Schwarzschild metric corresponding to light speed. The special relativistic condition corresponding to the Planck energy (Eq. (185)) gives the mass of the electron [3].

$$2\pi \frac{\hbar}{mc^2} = \sec \sqrt{\frac{2Gm^2}{c\alpha^2\hbar}} \quad (187)$$

$$m_e = \left( \frac{h\alpha}{\sec c^2} \right)^{\frac{1}{2}} \left( \frac{c\hbar}{2G} \right)^{\frac{1}{4}} = 9.0998 \times 10^{-31} \text{ kg} \quad (188)$$

where  $m_{e \text{ experimental}} = 9.10945455 \times 10^{-31} \text{ kg}$ .

The special relativistic condition corresponding to the electric energy (Eq. (185)) gives the mass of the muon [3].

$$m_\mu = \frac{\hbar}{c} \left( \frac{1}{2Gm_e(\alpha \sec)^2} \right)^{\frac{1}{3}} = 1.8874 \times 10^{-28} \text{ kg} \quad (189)$$

where  $m_{\mu \text{ experimental}} = 1.88355 \times 10^{-28} \text{ kg}$ . The difference between the calculated and experimental values of the electron and muon masses are due to the slight difference between the present MKS second and the definition of the corresponding time unit defined by Eq. (187). The relation between the muon and electron masses which is independent of the definition of the imaginary time ruler  $ti$  given by Eq. (187) including the contribution of the neutrinos given in Chp. 27, the Leptons section, of Ref. [3] is

$$\frac{m_\mu}{m_e} = \left( \frac{\alpha^{-2}}{2\pi} \right)^{\frac{2}{3}} \frac{\left( 1 + 2\pi \frac{\alpha^2}{2} \right)}{\left( 1 + \frac{\alpha}{2} \right)} = 206.76828 \quad (206.76827) \quad (190)$$

The experimental lepton mass ratios according to the 1998 CODATA and the Particle Data Group are given in parentheses [38-39].

### Down-Down-Up Neutron (DDU)

The corresponding equations for production of the members of the neutron family are derived from the corresponding energies also [3]. For example, the mass of the neutron comprised of down-down-up quarks given by the Planck energy is

---

<sup>3</sup> Presently the second is defined as the time required for 9,192,631,770 vibrations within the cesium-133 atom. The “sec” as defined in Eq. (187) is a fundamental constant, namely, the metric of spacetime (it is almost identically equal to the present value for reasons explained in Ref. [3]). A unified theory can only provide the relationships between all measurable observables in terms of a clock defined in terms of fundamental constants according to those observables and used to measure them. The so defined “clock” measures “clicks” on an observable in one aspect, and in another, it is the ruler of spacetime of the universe with the implicit dependence of spacetime on matter-energy conversion as shown in the Relationship of Matter to Energy and Spacetime Expansion section.

$$2\pi \frac{2\pi\hbar}{\frac{m_N}{3} \left[ \frac{1}{2\pi} - \frac{\alpha}{2\pi} \right] c^2} = \sec \sqrt{\frac{2G \left[ \frac{m_N}{3} \left[ \frac{1}{2\pi} - \frac{\alpha}{2\pi} \right] \right]^2}{3c(2\pi)^2 \hbar}} \quad (191)$$

$$m_{N \text{ calculated}} = (3)(2\pi) \left( \frac{1}{1-\alpha} \right) \left( \frac{2\pi\hbar}{\sec c^2} \right)^{\frac{1}{2}} \left( \frac{2\pi(3)ch}{2G} \right)^{\frac{1}{4}} = 1.6726 \times 10^{-27} \text{ kg} \quad (192)$$

where  $m_{N \text{ experimental}} = 1.6749 \times 10^{-27} \text{ kg}$ . The relation between the neutron and electron masses which is independent of the definition of the imaginary time ruler  $ti$  given by Eq. (187) including the contribution of the neutrinos given in Chp. 30, the Quarks section, of Ref. [3] is

$$\frac{m_N}{m_e} = \frac{12\pi^2}{1-\alpha} \sqrt{\frac{\sqrt{3}}{\alpha}} \frac{\left( 1 + 2\pi \frac{\alpha^2}{2} \right)}{\left( 1 - 2\pi \frac{\alpha^2}{2} \right)} = 1838.67 \quad (1838.68) \quad (193)$$

The parameters of the nucleons and the beta decay energy of the neutron are given in the Weak Nuclear Force: Beta Decay of the Neutron section and the Proton and Neutron section and of Ref. [3], respectively.

## GRAVITATIONAL POTENTIAL ENERGY

Three families of quarks are given by Eq. (191) with the corresponding energies given by Eq. (185) [3]. The gravitational potential energy gives the possibility of a fourth family. The gravitational radius,  $\alpha_G$  or  $r_G$ , of an orbitsphere of mass  $m_0$  is defined as

$$\alpha_G = r_G = \frac{Gm_0}{c^2} \quad (194)$$

When  $r_G = r_\alpha^* = \tilde{\lambda}_c$ , the gravitational potential energy equals  $m_0 c^2$

$$r_G = \frac{Gm_0}{c^2} = \tilde{\lambda}_c = \frac{\hbar}{m_0 c}, \quad (195)$$

$$E_{\text{grav}} = \frac{Gm_0^2}{r} = \frac{Gm_0^2}{\tilde{\lambda}_c} = \frac{Gm_0^2}{r_\alpha^*} = \hbar\omega^* = m_0 c^2 \quad (196)$$

The mass  $m_0$  is the Planck mass,  $m_u$ ,

$$m_u = m_0 = \sqrt{\frac{\hbar c}{G}} \quad (197)$$

The corresponding gravitational velocity,  $v_G$ , is defined as

$$v_G = \sqrt{\frac{Gm_0}{r}} = \sqrt{\frac{Gm_0}{\tilde{\lambda}_c}} = \sqrt{\frac{Gm_u}{\tilde{\lambda}_c}} \quad (198)$$

## Relationship of the Equivalent Planck Mass Particle Production Energies

For the Planck mass particle, the relationships corresponding to Eq. (185) are: (mass energy = Planck equation energy = electric potential energy = magnetic energy = gravitational potential energy = mass/spacetime metric energy)

$$m_o c^2 = \hbar \omega^* = V = E_{mag} = E_{grav} = E_{spacetime} \quad (199)$$

$$m_o c^2 = \hbar \omega^* = \frac{\hbar^2}{m_o \lambda_c^2} = \alpha^{-1} \frac{e^2}{4\pi\epsilon_0 \lambda_c} = \alpha^{-1} \frac{\pi\mu_0 e^2 \hbar^2}{(2\pi m_o)^2 \lambda_c^3} = \alpha^{-1} \frac{\mu_0 e^2 c^2}{2h} \sqrt{\frac{Gm_o}{\lambda_c}} \sqrt{\frac{\hbar c}{G}} = \frac{\alpha \hbar}{1 \text{ sec}} \sqrt{\frac{\lambda_c c^2}{2Gm}}$$

(200)

These equivalent energies give the particle masses in terms of the gravitational velocity,  $v_G$  and the Planck mass,  $m_u$

$$m_o = \alpha^{-1} \frac{\mu_0 e^2 c}{2h} \sqrt{\frac{Gm_o}{\lambda_c}} m_u = \alpha^{-1} \frac{\mu_0 e^2 c}{2h} \sqrt{\frac{Gm_o}{c^2 \lambda_c}} m_u = \alpha^{-1} \frac{\mu_0 e^2 c}{2h} \frac{v_G}{c} m_u = \frac{v_G}{c} m_u \quad (201)$$

### Planck Mass Particles

A pair of particles each of the Planck mass corresponding to the gravitational potential energy is not observed since the velocity of each transition state orbitsphere is the gravitational velocity  $v_G$  that in this case is the speed of light; whereas, the Newtonian gravitational escape velocity  $v_g$  is  $\sqrt{2}$  the speed of light. In this case, an electromagnetic wave of mass energy equivalent to the Planck mass travels in a circular orbit about the center of mass of another electromagnetic wave of mass energy equivalent to the Planck mass wherein the eccentricity is equal to zero and the escape velocity can never be reached. The Planck mass is a “measuring stick.” The extraordinarily high Planck mass ( $\sqrt{\frac{\hbar c}{G}} = 2.18 \times 10^{-8} \text{ kg}$ ) is the unobtainable mass bound imposed by the angular momentum and speed of the photon relative to the gravitational constant. It is analogous to the unattainable bound of the speed of light for a particle possessing finite rest mass imposed by the Minkowski tensor.

### Astrophysical Implications of Planck Mass Particles

The limiting speed of light eliminates the singularity problem of Einstein’s equation that arises as the radius of a blackhole equals the Schwarzschild radius. General relativity with the singularity eliminated resolves the paradox of the infinite propagation velocity required for the gravitational force in order to explain why the angular momentum of objects orbiting a gravitating body does not increase due to the finite propagation delay of the gravitational force according to special relativity [40]. When the gravitational potential energy density of a massive body such as a blackhole equals that of a particle having the Planck mass, the matter may

transition to photons of the Planck mass. Even light from a blackhole will escape when the decay rate of the trapped matter with the concomitant spacetime expansion is greater than the effects of gravity which oppose this expansion. Gamma-ray bursts are the most energetic phenomenon known that can release an explosion of gamma rays packing 100 times more energy than a supernova explosion [41]. The annihilation of a blackhole may be the source of  $\gamma$ -ray bursts. The source may be due to conversion of matter to photons of the Planck mass/energy which may also give rise to cosmic rays which are the most energetic particles known, and their origin is also a mystery [42]. According to the GZK cutoff, the cosmic spectrum cannot extend beyond  $5 \times 10^{19} \text{ eV}$ , but AGASA, the world's largest air shower array, has shown that the spectrum is extending beyond  $10^{20} \text{ eV}$  without any clear sign of cutoff [43]. Photons, each of the Planck mass, may be the source of these inexplicably energetic cosmic rays.

### RELATIONSHIP OF MATTER TO ENERGY AND SPACETIME EXPANSION

The Schwarzschild metric gives the relationship whereby matter causes relativistic corrections to spacetime. The limiting velocity  $c$  results in the contraction of spacetime due to particle production, which is given by  $2\pi r_g$  where  $r_g$  is the gravitational radius of the particle. This has implications for the expansion of spacetime when matter converts to energy.  $Q$  the mass/energy to expansion/contraction quotient of spacetime is given by the ratio of the mass of a particle at production divided by  $T$ , the period of production.

$$Q = \frac{m_0}{T} = \frac{m_0}{\frac{2\pi r_g}{c}} = \frac{m_0}{2\pi \frac{2Gm_0}{c^2}} = \frac{c^3}{4\pi G} = 3.22 \times 10^{34} \frac{\text{kg}}{\text{sec}} \quad (202)$$

The gravitational equations with the equivalence of the particle production energies (Eq. (185)) permit the conservation of mass/energy ( $E = mc^2$ ) and spacetime ( $\frac{c^3}{4\pi G} = 3.22 \times 10^{34} \frac{\text{kg}}{\text{sec}}$ ). With the conversion of  $3.22 \times 10^{34} \text{ kg}$  of matter to energy, spacetime expands by 1 sec. The photon has inertial mass and angular momentum, but due to Maxwell's equations and the implicit special relativity it does not have a gravitational mass. The observed gravitational deflection of light is predicted [3].

### Cosmological Consequences

*The Universe is closed* (it is finite but with no boundary). It is a 3-sphere Universe-Riemannian three dimensional hyperspace plus time of constant positive curvature at each r-sphere. *The Universe is oscillatory in matter/energy and spacetime* with a finite minimum radius, the gravitational radius. Spacetime expands as mass is released as energy which provides the basis of the atomic, thermodynamic, and cosmological arrows of time. Different regions of

space are isothermal even though they are separated by greater distances than that over which light could travel during the time of the expansion of the Universe [44]. Presently, stars and large scale structures exist which are older than the elapsed time of the present expansion as stellar, galaxy, and supercluster evolution occurred during the contraction phase [45–51]. The maximum power radiated by the Universe which occurs at the beginning of the expansion phase is  $P_U = \frac{c^5}{4\pi G} = 2.89 \times 10^{51} W$ . Observations beyond the beginning of the expansion phase are not possible since the Universe was entirely matter filled.

### The Period of Oscillation of the Universe Based on Closed Propagation of Light

Mass/energy is conserved during harmonic expansion and contraction. The gravitational potential energy  $E_{grav}$  given by Eq. (196) with  $m_0 = m_U$  is equal to  $m_U c^2$  when the radius of the Universe  $r$  is the gravitational radius  $r_G$ . The gravitational velocity  $v_G$  (Eq. (198) with  $r = r_G$  and  $m_0 = m_U$ ) is the speed of light in a circular orbit wherein the eccentricity is equal to zero and the escape velocity from the Universe can never be reached. The period of the oscillation of the Universe and the period for light to transverse the Universe corresponding to the gravitational radius  $r_G$  must be equal. The harmonic oscillation period,  $T$ , is

$$T = \frac{2\pi r_G}{c} = \frac{2\pi G m_U}{c^3} = \frac{2\pi G (2 \times 10^{54} \text{ kg})}{c^3} = 3.10 \times 10^{19} \text{ sec} = 9.83 \times 10^{11} \text{ years} \quad (203)$$

where the mass of the Universe,  $m_U$ , is approximately  $2 \times 10^{54} \text{ kg}$ . (The initial mass of the Universe of  $2 \times 10^{54} \text{ kg}$  is based on internal consistency with the size, age, Hubble constant, temperature, density of matter, and power spectrum.) Thus, the observed Universe will expand as mass is released as photons for  $4.92 \times 10^{11} \text{ years}$ . At this point in its world line, the Universe will obtain its maximum size and begin to contract.

### THE DIFFERENTIAL EQUATION OF THE RADIUS OF THE UNIVERSE

Based on conservation of mass/energy ( $E = mc^2$ ) and spacetime ( $\frac{c^3}{4\pi G} = 3.22 \times 10^{34} \frac{\text{kg}}{\text{sec}}$ ). The Universe behaves as a simple harmonic oscillator having a restoring force,  $F$ , which is proportional to the radius. The proportionality constant,  $k$ , is given in terms of the potential energy,  $E$ , gained as the radius decreases from the maximum expansion to the minimum contraction.

$$\frac{E}{R^2} = k \quad (204)$$

Since the gravitational potential energy  $E_{grav}$  is equal to  $m_U c^2$  when the radius of the Universe  $r$  is the gravitational radius  $r_G$

$$F = -k\aleph = -\frac{m_U c^2}{r_G^2} \aleph = -\frac{m_U c^2}{\left(\frac{Gm_U}{c^2}\right)^2} \aleph \quad (205)$$

And, considering the oscillation, the differential equation of the radius of the Universe, is

$$m_U \ddot{\aleph} + \frac{m_U c^2}{r_G^2} \aleph = m_U \ddot{\aleph} + \frac{m_U c^2}{\left(\frac{Gm_U}{c^2}\right)^2} \aleph = 0 \quad (206)$$

The *maximum radius of the Universe*, the amplitude,  $r_0$ , of the time harmonic variation in the radius of the Universe, is given by the quotient of the total mass of the Universe and  $Q$  (Eq. (202)), the mass/energy to expansion/contraction quotient.

$$r_0 = \frac{m_U}{Q} = \frac{m_U}{\frac{c^3}{4\pi G}} = \frac{2 \times 10^{54} \text{ kg}}{\frac{c^3}{4\pi G}} = 1.97 \times 10^{12} \text{ light years} \quad (207)$$

The *minimum radius* which corresponds to the gravitational radius,  $r_g$ , given by Eq. (178) with  $m_0 = m_U$  is

$$r_g = \frac{2Gm_U}{c^2} = 2.96 \times 10^{27} \text{ m} = 3.12 \times 10^{11} \text{ light years} \quad (208)$$

When the radius of the Universe is the gravitational radius,  $r_g$ , the proper time is equal to the coordinate time by Eq. (183), and the gravitational escape velocity  $v_g$  of the Universe is the speed of light. The radius of the Universe as a function of time as shown in Figure 15 is

$$\aleph = \left( r_g + \frac{cm_U}{Q} \right) - \frac{cm_U}{Q} \cos \left( \frac{2\pi t}{\frac{2\pi r_G}{c}} \right) = \left( \frac{2Gm_U}{c^2} + \frac{cm_U}{\frac{c^3}{4\pi G}} \right) - \frac{cm_U}{\frac{c^3}{4\pi G}} \cos \left( \frac{2\pi t}{\frac{2\pi Gm_U}{c^3}} \right) \quad (209)$$

The expansion/contraction rate,  $\dot{\aleph}$ , as shown in Figure 16 is given by time derivative of Eq. (209)

$$\dot{\aleph} = 4\pi c \times 10^{-3} \sin \left( \frac{2\pi t}{\frac{2\pi Gm_U}{c^3}} \right) \frac{\text{km}}{\text{sec}} \quad (210)$$

## THE HUBBLE CONSTANT

The *Hubble constant* is given by the ratio of the expansion rate given in units of  $\frac{\text{km}}{\text{sec}}$  divided by the radius of the expansion in  $Mpc$ . The radius of expansion is equivalent to the radius of the light sphere with an origin at the time point when the Universe stopped contracting and started to expand.

$$H = \frac{\dot{\delta}}{t \text{ Mpc}} = \frac{4\pi \times 10^{-3} \sin\left(\frac{2\pi}{\frac{2\pi G m_U}{c^3}}\right) \frac{\text{km}}{\text{sec}}}{t \text{ Mpc}} \quad (211)$$

For  $t = 10^{10}$  light years  $= 3.069 \times 10^3 \text{ Mpc}$ , the Hubble constant,  $H_0$ , is

$$H_0 = 78.6 \frac{\text{km}}{\text{sec} \cdot \text{Mpc}} \quad (212)$$

The experimental value [52] as shown in Figure 17 is

$$H_0 = 80 \pm 17 \frac{\text{km}}{\text{sec} \cdot \text{Mpc}} \quad (213)$$

### THE DENSITY OF THE UNIVERSE AS A FUNCTION OF TIME

The density of the Universe as a function of time  $\rho_U(t)$  given by the ratio of the mass as a function of time and the volume as a function of time as shown in Figure 18 is

$$\rho_U(t) = \frac{m_U(t)}{V(t)} = \frac{m_U(t)}{\frac{4}{3}\pi \delta(t)^3} = \frac{\frac{m_U}{2} \left( 1 + \cos\left(\frac{2\pi}{\frac{2\pi G m_U}{c^3}}\right) \right)}{\frac{4}{3}\pi \left( \left( \frac{2Gm_U}{c^2} + \frac{cm_U}{c^3} \right) - \frac{cm_U}{4\pi G} \cos\left(\frac{2\pi}{\frac{2\pi G m_U}{c^3}}\right) \right)^3}, \quad (214)$$

For  $t = 10^{10}$  light years,  $\rho_U = 1.7 \times 10^{-32} \text{ g/cm}^3$ . The density of luminous matter of stars and gas of galaxies is about  $\rho_U = 2 \times 10^{-31} \text{ g/cm}^3$  [53–54].

### THE POWER OF THE UNIVERSE AS A FUNCTION OF TIME, $P_U(t)$

From  $E = mc^2$  and Eq. (202),

$$P_U(t) = \frac{c^5}{8\pi G} \left( 1 + \cos\left(\frac{2\pi t}{\frac{2\pi r_G}{c}}\right) \right) \quad (215)$$

For  $t = 10^{10}$  light years,  $P_U(t) = 2.88 \times 10^{51} \text{ W}$ . The observed power is consistent with that predicted. The power of the Universe as a function of time is shown in Figure 19.

### THE TEMPERATURE OF THE UNIVERSE AS A FUNCTION OF TIME

The temperature of the Universe as a function of time,  $T_U(t)$ , as shown in Figure 20, follows from the Stefan-Boltzmann law.

$$T_U(t) = \left( \frac{1}{1 + \frac{Gm_U(t)}{c^2 \mathcal{N}(t)}} \right) \left[ \frac{R_U(t)}{e\sigma} \right]^{\frac{1}{4}} = \left( \frac{1}{1 + \frac{Gm_U(t)}{c^2 \mathcal{N}(t)}} \right) \left[ \frac{\frac{P_U(t)}{4\pi \mathcal{N}(t)^2}}{e\sigma} \right]^{\frac{1}{4}} \quad (216)$$

The calculated uniform temperature is about 2.7 K which is in agreement with the observed microwave background temperature [44].

## POWER SPECTRUM OF THE COSMOS

The power spectrum of the cosmos, as measured by the Las Campanas survey, generally follows the prediction of cold dark matter on the scales of 200 million to 600 million light-years. However, the power increases dramatically on scales of 600 million to 900 million light-years [51]. This discrepancy means that the universe is much more structured on those scales than current theories can explain.

The universe is oscillatory in matter/energy and spacetime with a finite minimum radius. The *minimum radius* which corresponds to the gravitational radius,  $r_g$ , given by Eq. (208) is  $3.12 \times 10^{11}$  light years. The minimum radius is larger than that provided by the current expansion, approximately 10 billion light years [52]. The universe is a four dimensional hyperspace of constant positive curvature at each r-sphere. The coordinates are spherical, and the space can be described as a series of spheres each of constant radius  $r$  whose centers coincide at the origin. The existence of the mass  $m_U$  causes the area of the spheres to be less than  $4\pi r^2$  and causes the clock of each r-sphere to run so that it is no longer observed from other r-spheres to be at the same rate. The Schwarzschild metric given by Eq. (181) is the general form of the metric which allows for these effects. Consider the present observable universe that has undergone expansion for 10 billion years. The radius of the universe as a function of time from the coordinate r-sphere is of the same form as Eq. (209). The average size of the universe,  $r_U$ , is given as the sum of the gravitational radius,  $r_g$ , and the observed radius, 10 billion light years.

$$r_U = r_g + 10^{10} \text{ light yrs} = 3.12 \times 10^{11} \text{ light yrs} + 10^{10} \text{ light years} = 3.22 \times 10^{11} \text{ light yrs} \quad (217)$$

The frequency of Eq. (209) is one half the amplitude of spacetime expansion from the conversion of the mass of universe into energy according to Eq. (202). Thus, keeping the same relationships, the frequency of the current expansion function is the reciprocal of one half the current age. Substitution of the average size of the universe, the frequency of expansion, and the amplitude of expansion, 10 billion light years, into Eq. (209) gives *the radius of the universe as a function of time for the coordinate r-sphere*.

$$\aleph = 3.22 \times 10^{11} - 1 \times 10^{10} \cos\left(\frac{2\pi t}{5 \times 10^9 \text{ light years}}\right) \text{ light years} \quad (218)$$

The Schwarzschild metric gives the relationship between the proper time and the coordinate time. The infinitesimal temporal displacement,  $d\tau^2$ , is given by Eq. (181). In the case that  $dr^2 = d\theta^2 = d\phi^2 = 0$ , the relationship between the proper time and the coordinate time is

$$d\tau^2 = \left(1 - \frac{2Gm_U}{c^2 r}\right) dt^2 \quad (219)$$

$$\tau = t \sqrt{1 - \frac{r_g}{r}} \quad (220)$$

The maximum power radiated by the universe is given by Eqs. (215) which occurs when the proper radius, the coordinate radius, and the gravitational radius  $r_g$  are equal. For the present universe, the coordinate radius is given by Eq. (217). The gravitational radius is given by Eq. (208). The maximum of the power spectrum of a trigonometric function occurs at its frequency [55]. Thus, the coordinate maximum power according to Eq. (218) occurs at  $5 \times 10^9 \text{ light years}$ . The maximum power corresponding to the proper time is given by the substitution of the coordinate radius, the gravitational radius  $r_g$ , and the coordinate power maximum into Eq. (220).

The power maximum in the proper frame occurs at

$$\tau = 5 \times 10^9 \text{ light years} \sqrt{1 - \frac{3.12 \times 10^{11} \text{ light years}}{3.22 \times 10^{11} \text{ light years}}} \quad (221)$$

$$\tau = 880 \times 10^6 \text{ light years}$$

The power maximum of the current observable universe is predicted to occur on the scale of  $880 \times 10^6 \text{ light years}$ . There is excellent agreement between the predicted value and the experimental value of  $600 - 900 \times 10^6 \text{ light years}$  [51].

## THE EXPANSION/CONTRACTION ACCELERATION, $\ddot{\aleph}$

The expansion/contraction acceleration rate,  $\ddot{\aleph}$ , as shown in Figure 21, is given by the time derivative of Eq. (210).

$$\ddot{\aleph} = 2\pi \frac{c^4}{Gm_U} \cos\left(\frac{2\pi t}{\frac{2\pi Gm_U}{c^3} \text{ sec}}\right) = H_o = 78.7 \cos\left(\frac{2\pi}{3.01 \times 10^5 \text{ Mpc}}\right) \frac{\text{km}}{\text{sec} \cdot \text{Mpc}} \quad (222)$$

The differential in the radius of the Universe,  $\Delta\aleph$ , due to its acceleration is given by  $\Delta\aleph = 1/2\ddot{\aleph}t^2$ . The differential in expanded radius for the elapsed time of expansion,  $t = 10^{10} \text{ light years}$  corresponds to a decrease in brightness of a supernovae standard candle of about an order of magnitude of that expected where the distance is taken as  $\Delta\aleph$ . This result

based on the predicted rate of acceleration of the expansion is consistent with the experimental observation [56–58].

Furthermore, the microwave background radiation image obtained by the Boomerang telescope [59] is consistent with a Universe of nearly flat geometry since the commencement of its expansion. The data is consistent with a large offset radius of the Universe with a fractional increase in size since the commencement of expansion about 10 billion years ago. More details on these results are given in the Differential Equation of the Radius of the Universe section of Ref. [3].

### POWER SPECTRUM OF THE COSMIC MICROWAVE BACKGROUND

When the universe reaches the maximum radius corresponding to the maximum contribution of the amplitude,  $r_o$ , of the time harmonic variation in the radius of the universe, (Eq. (207)), it is entirely radiation filled. Since the photon has no gravitational mass, the radiation is uniform. As energy converts into matter the power of the universe may be considered negative for the first quarter cycle starting from the point of maximum expansion as given by Eq. (228), and spacetime contracts according to Eq. (202). The gravitational field from particle production travels as a light wave front. As the universe contracts to a minimum radius, the gravitational radius given by Eq. (208), constructive interference of the gravitational fields occurs for distances which are integers of the amplitude,  $r_o$ , of the time harmonic variation in the radius of the universe for the times when the power is negative according to Eq. (228). The resulting slight variations in the density of matter are observed from our present r-sphere. The observed radius of expansion is equivalent to the radius of the light sphere with an origin at the time point when the universe stopped contracting and started to expand. The spherical harmonic parameter  $\ell$  is given by the ratio of the amplitude,  $r_o$ , of the time harmonic variation in the radius of the universe, (Eq. (207)) divided by the present radius of the light sphere where the universe is a 3-sphere universe—Riemannian three dimensional hyperspace plus time of constant positive curvature at each r-sphere. For  $t = 10^{10} \text{ light years} = 3.069 \times 10^3 \text{ Mpc}$ , the fundamental  $\ell$  is given by

$$\ell = \frac{r_o}{t} = \frac{\frac{2 \times 10^{54} \text{ kg}}{c^3}}{t} = \frac{1.97 \times 10^{12} \text{ light years}}{10^{10} \text{ light years}} = 197 \quad (223)$$

The number of constructive interferences is given by the maximum integer of the ratio of the amplitude,  $r_o$ , of the time harmonic variation in the radius of the universe, (Eq. (207)) divided by the minimum radius, the gravitational radius (Eq. (208)). The number of peaks are

$$\frac{r_0}{r_g} = \frac{\frac{2 \times 10^{54} \text{ kg}}{c^3}}{\frac{2Gm_U}{c^2}} = \frac{1.97 \times 10^{12} \text{ light years}}{3.12 \times 10^{11} \text{ light years}} = 6.3 \rightarrow 6 \quad (224)$$

The peaks are predicted to occur at the fundamental plus harmonics of the fundamental—integer multiples,  $n = 2, 3, 4, 5$ , and  $6$ , of the fundamental  $\ell = 197$ .

$$\begin{aligned} \ell &= 197 \text{ (fundamental)} \\ \ell &= 197 + n197 \quad n = 2, 3, 4, 5, \text{ and } 6 \text{ (harmonics)} \end{aligned} \quad (225)$$

From Eq. (225), the predicted harmonic parameters  $\ell$  are given in Table III.

The harmonic peaks correspond to the condition that the amplitude of the harmonic term of the radius of the universe  $r_0(n)$  is a reciprocal integer that of the maximum amplitude  $r_o$ . Thus,  $r_0(n)$  is given by

$$r_0(n) = \frac{r_o}{n} = \frac{\frac{2 \times 10^{54} \text{ kg}}{c^3}}{n} = \frac{1.97 \times 10^{12} \text{ light years}}{n} \quad (226)$$

The power flow of radiant energy into mass decreases as the radius contracts, and the relative intensities of the peaks follow from the power flow. The relative intensities are given by the normalized power as a function of  $t(n)$ , the time at which the magnitude of the amplitude of the harmonic term of the radius of the universe  $r_0(n)$  is given by Eq. (226) corresponding to each contracted radius at which constructive interference occurs. Starting the clock at the point of the maximum expansion wherein the universe is entirely radiation filled and the CMB is uniform, the time at which the magnitude of the amplitude of the harmonic term of the radius of the universe  $r_0(n)$  is given by Eq. (226) follows from Eq. (209).

$$\begin{aligned} r_0(n) &= \frac{r_o}{n} = \frac{1.97 \times 10^{12}}{n} = 1.97 \times 10^{12} \cos\left(\frac{2\pi t(n)}{9.83 \times 10^{11} \text{ yrs}}\right) \text{ light years} \\ t(n) &= \frac{9.83 \times 10^{11}}{2\pi} \cos^{-1}\left(\frac{1}{n}\right) \text{ yrs} = 1.564 \times 10^{11} \cos^{-1}\left(\frac{1}{n}\right) \text{ yrs} \end{aligned} \quad (227)$$

The power of the universe as a function of time is given by Eq. (215) and is shown in Figure 19. To express the negative power flow relative to the radiant energy of the universe corresponding to the conversion of energy into matter, the power of the universe as a function of time may be expressed as

$$\begin{aligned} P_U(t) &= -\frac{c^5}{4\pi G} \cos\left(\frac{2\pi t}{9.83 \times 10^{11} \text{ yrs}}\right) W \\ P_U(t) &= -2.9 \times 10^{51} \cos\left(\frac{2\pi t}{9.83 \times 10^{11} \text{ yrs}}\right) W \end{aligned} \quad (228)$$

where  $t = 0$  corresponds to the time when the universe reaches the maximum radius corresponding to the maximum contribution of the amplitude,  $r_o$ , of the time harmonic variation in the radius of the universe, (Eq. (207)). At  $t = 0$  as defined, the universe is entirely radiation filled, and the power into particle production is a maximum. At  $t = \frac{\frac{\pi}{2}}{\frac{2\pi}{9.83 \times 10^{11} \text{ yrs}}}$  according to

Eq. (228), particle production is in balance with matter to energy conversion, and the latter dominates for the following half cycle.

The relative intensities are given by substitution of Eq. (227) into Eq. (228) that is normalized by the magnitude of the maximum power which occurs at the maximum radius. Thus, the relative intensities are given by

$$I(n) = \cos \left[ \frac{2\pi \left( 1.564 \times 10^{11} \cos^{-1} \left( \frac{1}{n} \right) \text{ yrs} \right)}{9.83 \times 10^{11} \text{ yrs}} \right] = \frac{1}{n} \quad (229)$$

The relative intensities  $I(n)$  as a function of peak  $n$  are given in Table III.

The cosmic microwave background radiation is an average temperature of 2.7 K, with deviations of 30 or so  $\mu K$  in different parts of the sky representing slight variations in the density of matter. The measurements of the anisotropy in the Cosmic Microwave Background (CMB) have been measured with the Degree Angular Scale Interferometer (DASI) [60]. The angular power spectrum was measured in the range  $100 < \ell < 900$ , and peaks in the power spectrum from the temperature fluctuations of the cosmic microwave background radiation appear at certain values of  $\ell$  of spherical harmonics. Peaks were observed at  $\ell \approx 200$ ,  $\ell \approx 550$ , and  $\ell \approx 800$  with relative intensities of 1, 0.5, and 0.3, respectively (Figure 1 of Ref. [60]). There is excellent agreement between the predicted parameters given in Table III and the observed peaks.

## THE PERIODS OF SPACETIME EXPANSION/CONTRACTION AND PARTICLE DECAY/PRODUCTION FOR THE UNIVERSE ARE EQUAL

The period of the expansion/contraction cycle of the radius of the Universe,  $T$ , is given by Eq. (203). It follows from the Poynting power theorem with spherical radiation that the transition lifetimes are given by the ratio of energy and the power of the transition (Eqs. (98-99)). Exponential decay applies to electromagnetic energy decay

$$h(t) = e^{-\alpha t} u(t) = e^{-\frac{2\pi}{T} t} u(t) \quad (230)$$

The coordinate time is imaginary because energy transitions are spacelike due spacetime expansion from matter to energy conversion. For example, the mass of the electron (a fundamental particle) is given by

$$\frac{2\pi\lambda_c}{\sqrt{\frac{2Gm_e}{\lambda_c}}} = \frac{2\pi\lambda_c}{v_g} = i\alpha^{-1} \text{ sec} \quad (231)$$

where  $v_g$  is Newtonian gravitational velocity (Eq. (173)). When the gravitational radius  $r_g$  is the radius of the Universe, the proper time is equal to the coordinate time by Eq. (183), and the gravitational escape velocity  $v_g$  of the Universe is the speed of light. Replacement of the coordinate time,  $t$ , by the spacelike time,  $it$ , gives

$$h(t) = \text{Re} \left[ e^{-i\frac{2\pi}{T}t} \right] = \cos \frac{2\pi}{T}t \quad (232)$$

where the period is  $T$  (Eq. (203)). The continuity conditions based on the constant maximum speed of light (Maxwell's equations) are given by Eqs. (184-185). The continuity conditions based on the constant maximum speed of light (Schwarzschild metric) are given by Eq. (186). The periods of spacetime expansion/contraction and particle decay/production for the Universe are equal because only the particles which satisfy Maxwell's equations and the relationship between proper time and coordinate time imposed by the Schwarzschild metric may exist.

## WAVE EQUATION

The general form of the light front wave equation is given by Eq. (165). The equation of the radius of the Universe,  $\aleph$ , may be written as

$$\aleph = \left( \frac{2Gm_U}{c^2} + \frac{cm_U}{4\pi G} \right) - \frac{cm_U}{4\pi G} \cos \left( \frac{2\pi}{\frac{2\pi Gm_U}{c^3}} \left( t - \frac{\aleph}{c} \right) \right), \quad (233)$$

which is a solution of the wave equation for a light wave front.

## CONCLUSION

Maxwell's equations, Planck's equation, the de Broglie equation, Newton's laws, and special, and general relativity are unified. Classical physical laws apply on all scales.

## APPENDIX: DERIVATION OF THE SPIN FUNCTION—THE ORBITS PHERE EQUATION OF MOTION FOR $\ell = 0$

### Stern-Gerlach-Experiment Boundary Condition

It is known from the Stern-Gerlach experiment that a beam of silver atoms is split into two components when passed through an inhomogeneous magnetic field. This implies that the electron is a spin 1/2 particle with an intrinsic angular momentum in the direction of the applied field (spin axis) of  $\pm \frac{\hbar}{2}$ , and the magnitude of the angular momentum vector which precesses about the spin axis is  $\sqrt{\frac{3}{4}}\hbar$ . Furthermore, the magnitude of the splitting implies a magnetic moment of  $\mu_B$ , a full Bohr magneton, given by Eq. (54) corresponding to  $\hbar$  of total angular momentum on the axis of the applied field.

The algorithm to generate the  $Y_0^0(\phi, \theta)$  orbitsphere equation of motion of the electron (Eqs. (14-15)) is developed in this section. It was shown in the Angular Functions section that the integral of the magnitude of the angular momentum over the orbitsphere must be constant. The constant is  $\hbar$  as given by Eq. (7). It is shown in this section that the projection of the intrinsic orbitsphere angular momentum onto the spin axis is  $\pm \frac{\hbar}{2}$ , and the projection onto  $\mathbf{S}$ , the axis which precesses about the spin axis, is  $\hbar$  with a precessing component in the perpendicular plane of  $\sqrt{\frac{3}{4}}\hbar$  and a component on the spin axis of  $\pm \frac{\hbar}{2}$ . Thus, the mystery of an intrinsic angular momentum of  $\pm \frac{\hbar}{2}$  and a total angular momentum in a resonant RF experiment of  $\mathbf{L}_z = \hbar$  is resolved since the sum of the intrinsic and spin-axis projection of the precessing component is  $\hbar$ . The Stern-Gerlach experiment implies a magnetic moment of one Bohr magneton and an associated angular momentum quantum number of 1/2. Historically, this quantum number is called the spin quantum number,  $s$  ( $s = \frac{1}{2}$ ;  $m_s = \pm \frac{1}{2}$ ), and that designation is maintained.

The electron has a measured magnetic field and corresponding magnetic moment of a Bohr magneton and behaves as a spin 1/2 particle or fermion. For any magnetic field, the solution for the corresponding current from Maxwell's equations is unique. Thus, the electron field requires a unique current according to Maxwell's equations. Several boundary conditions must be satisfied, and the orbitsphere equation of motion for  $\mathfrak{L} = 0$  is solved as a boundary value problem. The boundary conditions are:

(1) each infinitesimal point (position) on the orbitsphere comprising a charge (mass)-density element must have the same angular and linear velocity given by Eqs. (6) and (9), respectively;

(2) according to condition 1, every such infinitesimal point must move along a great circle and the current-density distribution must be uniform;

(3) the electron magnetic moment must align completely parallel or antiparallel with an applied magnetic field in agreement with the Stern-Gerlach experiment;

(4) according to condition 3, the projection of the intrinsic angular momentum of the orbitsphere onto the z-axis must be  $\pm \frac{\hbar}{2}$ , and the projection into the transverse plane must be  $\pm \frac{\hbar}{4}$  to achieve the spin 1/2 aspect;

(5) the Larmor excitation of the electron in the applied magnetic field must give rise to a component of electron spin angular momentum that precess about the applied magnetic field such that the contribution along the z-axis is  $\pm \frac{\hbar}{2}$  and the projection onto the orthogonal axis which precesses about the z-axis must be  $\pm \sqrt{\frac{3}{4}}\hbar$ ;

(6) due to conditions 4 and 5, the angular momentum components corresponding to the current of the orbitsphere and that due to the Larmor precession must rise to a total angular momentum on the applied-field axis of  $\pm \hbar$ ;

(7) due to condition 6, the precessing electron has a magnetic moment of a Bohr magneton, and

(8) the energy of the transition of the alignment of the magnetic moment with an applied magnetic field must be given by Eqs. (64-65) corresponding to the extended electron having a total angular momentum on the applied-field axis of  $\pm \hbar$ .

Consider the derivation of Eqs. (1.58) and (1.59) of Ref. [3]. The moment of inertia of a point particle is  $mr^2$ , and that of a globe spinning about some axis is  $I = \frac{2}{3}mr^2$ . For  $\mathfrak{L} = 0$ , the electron mass and charge are uniformly distributed over the orbitsphere, a two-dimensional, spherical shell, but the orbitsphere is *not* analogous to a globe. The velocity of a point mass on a spinning globe is a function of  $\theta$ , but the magnitude of the velocity at each point of the orbitsphere is not a function of  $\theta$ . To picture the distinction, it is a useful concept to consider that the orbitsphere is comprised of an infinite number of point elements that move on the spherical surface. Then, each point on the sphere with mass  $m_i$  has the same angular velocity

( $\omega_n$ ), the same magnitude of linear velocity ( $v_n$ ), and the same moment of inertia ( $m_n r_n^2$ ). The motion of each point of the orbitsphere is along a great circle, and the motion along each great circle is correlated with the motion on all other great circles such that the sum of all the contributions of the corresponding angular momenta is different from that of a point or globe. The orbitsphere angular momentum is uniquely directed disproportionately along two orthogonal axes.

The current-density function of the orbitsphere is generated from a basis set current-vector field defined as the orbitsphere current-vector field (“orbitsphere-cvf”). This in turn is generated from orthogonal great circle current loops that serve as basis elements. Due to the symmetry properties of the angular-momentum components and the corresponding current of the orbitsphere-cvf, a uniform current distribution having the same angular momentum components as that of the orbitsphere-cvf is obtained by convolving the orbitsphere-cvf about its resultant angular momentum axis. This uniform current density function comprises  $Y_0^0(\phi, \theta)$ , the orbitsphere equation of motion of the electron (Eqs. (14-15)). Then, the uniform, equipotential charge-density function of the orbitsphere having only a radial discontinuous field at the surface according to Eq. (1) of footnote 8 of Ref. [3] is constant in time due to the motion of the current along great circles. The current flowing into any given point of the orbitsphere equals the current flowing out to satisfy the current continuity condition,  $\nabla \cdot J = 0$ .

The current-vector field pattern of the orbitsphere-cvf is not spatially uniform. There is no coincidence or nonuniqueness of elements of the current-vector field. But, there are many crossings among elements at single points on the two dimensional surface of the electron, and the density of the crossings is nonuniform over the surface. *Thus, each element of the basis set to generate the current pattern, a great circle current loop, must be one dimensional so that the crossings are zero dimensional with no element interaction at their crossing.* (This is a logical and necessary geometric progression for the construction of a fundamental particle which is two-dimensional.) In the limit, the basis set generates a continuous two-dimensional current density with a constant charge (mass) density wherein the crossings have no effect on the vector fields. Each one-dimensional element is independent of the others, and its contribution to the angular momentum and magnetic field independently superimposes with that of the others.

This unique aspect of a fundamental particle has the same properties of the superposition properties of the electric and magnetic fields of a photon. As shown in the Excited States of the One-Electron Atom (Quantization), the Creation of Matter from Energy, Pair Production, and the Leptons sections of Ref. [3], the angular momentum in the electric and magnetic fields is conserved in excited states and in the creation of an electron from a photon in agreement with Maxwell’s equations. It is useful to regard an electron as a photon frozen in time. The particle-production conditions are given in the latter sections.

The equation of motion for each charge-density element (and correspondingly for each mass-density element) which gives the current pattern of the orbitsphere-cvf is generated in two steps as follows:

Here a procedure is used to generate the current pattern of the orbitsphere-cvf from which the physical properties are derived in the Spin Angular Momentum of the Orbitsphere with  $\mathfrak{L} = 0$  section and are shown to match the boundary conditions.

The current-density of the orbitsphere-cvf is *continuous*, but it may be modeled as a current pattern comprising a superposition of an infinite series of correlated orthogonal great circle current loops. The *time-independent* current pattern is obtained by defining a basis set for generating the current distribution over the surface of a spherical shell of zero thickness. As such a basis set, consider that the electron current is first evenly distributed within two orthogonally linked great-circle current loops. These loops will be further divided into two sets of linked orthogonal pairs wherein each pair undergoes independent transformations over the surface wherein the electron current is correspondingly divided by the number of basis loops, four, and then by the angular span of the transformations to form a normalized current density in each case. The *continuous* uniform electron current density function  $Y_0^0(\phi, \theta)$  (Eqs. (14-15)) is then generated from this orbitsphere-cvf as a basis element wherein the superposition of the orbitsphere-cvf elements must be normalized to give the electron current.

The stationary or laboratory Cartesian coordinate system for the first step, Step One, of the algorithm to generate the orbitsphere-cvf is shown in Figure 22 as the xyz-system. It is also designated the orbitsphere-cvf reference frame. The primed coordinate system is the stationary frame for the basis elements wherein a first current loop always lies in the y'z'-plane, and a second current loop always lies in the x'z'-plane. The primed coordinates are only coincident with the corresponding xyz-coordinates for the initial positions as shown in Figure 22 since the current density pattern is generated by a series of transformations of the primed coordinates relative to the unprimed coordinates. Each successive transformation of the primed system defines an orientation of the basis set in the x'y'z'-frame relative to the xyz-frame that comprises a current element of the current density pattern.

Rotations and reflections are the transformations on the surface of a sphere that may be used to generate the orbitsphere-cvf. The orbitsphere-cvf is simply generated by two steps, each comprising an infinite series of nested rotations of the two orthogonal great circle current loops each by an infinitesimal angle  $\pm\Delta\alpha_i$  and  $\pm\Delta\alpha_j$ , about the new i'-axis and new j'-axis, respectively, which results from the preceding such rotation. Each orientation following the conjugate i' and j' rotation of the two orthogonal great circle current loops wherein the first

current loop lies in the j'k'-plane, and the second current loop lies in the i'k'-plane is an element of the infinite series wherein for Step One i'=x', j'=y', k'=z' and for Step Two i'=z', j'=x', k'=y'.

For Step One, the first such pair of orthogonal great circle current loops is shown in Figure 22. The second element of the series is generated by rotation of the first element by an infinitesimal angle  $\pm\Delta\alpha_x$  about the first x'-axis followed by a rotation by the infinitesimal angle  $\pm\Delta\alpha_y$  about the new (second) y'-axis to form a second x'-axis. The third element of the series is generated by the rotation of the second element by the same infinitesimal angle  $\pm\Delta\alpha_x$  about the second x'-axis followed by the rotation by the same infinitesimal angle  $\pm\Delta\alpha_y$  about the new (third) y'-axis. In general, the (n + 1)th element of the series is generated by the rotation of the nth basis coordinate system by the infinitesimal angle  $\pm\Delta\alpha_x$  about the nth x'-axis followed by the rotation of the nth orbitsphere-cvf coordinate system by the infinitesimal angle  $\pm\Delta\alpha_y$  about the (n + 1)th new y'-axis.

The sign of the corresponding angle is maintained throughout the rotations, and the summation of the reiterative rotations about each of the i'-axis and the j'-axis is

$$\lim_{\Delta\alpha \rightarrow 0} \sum_{n=1}^{\frac{\sqrt{2}}{2}\pi} |\Delta\alpha_{i',j'}| = \frac{\sqrt{2}}{2}\pi$$
 when the k'-axis rotates from the k-axis to the -k-axis. (The total angle,  $\frac{\sqrt{2}}{2}\pi$ , is the hypotenuse of the triangle having the sides of  $\frac{\pi}{2}$  radians corresponding to i'-axis rotations and  $\frac{\pi}{2}$  radians corresponding to j'-axis rotations.) Step One and Step Two comprise the use of  $\Delta\alpha_x$  and  $\Delta\alpha_y$  as given in Table IV.

Next, consider two infinitesimal charge (mass)-density elements at two separate positions or points, one and two, of the two orthogonal great circle current loops that serve as the basis set as shown in Figures 22 and 23. The vector projection of the corresponding angular momentum at each point of each current element is integrated over the entire orbitsphere-cvf surface to give the electron angular momentum. The correct current pattern is confirmed by achieving the condition that the magnitude of the velocity at any point on the surface is given by Eq. (6) and by obtaining the required angular momentum projections of  $\frac{\hbar}{2}$  and  $\frac{\hbar}{4}$  along and the z-axis and along an axis in the xy-plane, respectively, as given in the Spin Angular Momentum of the Orbitsphere with  $\ell = 0$  section.

Thus, the orbitsphere-cvf is generated from two orthogonal great circle current loops which are rotated about the nth i'-axis and then about the (n + 1)th j'-axis in Two Steps. For Step One, consider two charge (mass)-density elements, point one and two, in the basis-set reference frame at time zero. Element one is at  $x' = 0$ ,  $y' = 0$ , and  $z' = r_n$  and element two is at  $x' = r_n$ ,  $y' = 0$ , and  $z' = 0$ . Let element one move on a great circle counter clockwise toward the -y'-axis,

as shown in Figure 22, and let element two move clockwise on a great circle toward the z'-axis, as shown in Figure 22. The equations of motion, in the sub-basis-set reference frame are given by

point one:

$$\dot{x}'_1 = 0 \quad \dot{y}'_1 = -r_n \sin(\omega_n t) \quad \dot{z}'_1 = r_n \cos(\omega_n t) \quad (234a)$$

point two:

$$\dot{x}'_2 = r_n \cos(\omega_n t) \quad \dot{y}'_2 = 0 \quad \dot{z}'_2 = r_n \sin(\omega_n t) \quad (234b)$$

For Step Two, consider two charge (mass)-density elements, point one and two, in the basis-set reference frame at time zero. Element one is at  $x' = 0$ ,  $y' = r_n$ , and  $z' = 0$  and element two is at  $x' = r_n$ ,  $y' = 0$ , and  $z' = 0$ . Let element one move clockwise on a great circle toward the -z'-axis as shown in Figure 23, and let element two move counter clockwise on a great circle toward the y'-axis as shown in Figure 23. The equations of motion, in the basis-set reference frame are given by

point one:

$$\dot{x}'_1 = 0 \quad \dot{y}'_1 = r_n \cos(\omega_n t) \quad \dot{z}'_1 = -r_n \sin(\omega_n t) \quad (235a)$$

point two:

$$\dot{x}'_2 = r_n \cos(\omega_n t) \quad \dot{y}'_2 = r_n \sin(\omega_n t) \quad \dot{z}'_2 = 0 \quad (235b)$$

The great circles are rotated by an infinitesimal angle  $\pm\Delta\alpha_i$  (a rotation around the x'-axis or z'-axis for Steps One and Two, respectively) and then by  $\pm\Delta\alpha_j$  (a rotation around the new y'-axis or x'-axis for Steps One and Two, respectively) where the positive directions are shown in Figures 22 and 23, respectively. The coordinates of each point on each rotated great circle ( $x',y',z'$ ) is expressed in terms of the first (x,y,z) coordinates by the following transforms where clockwise rotations are defined as positive:

**Step One**

$$\begin{bmatrix} x \\ y \\ z \end{bmatrix} = \begin{bmatrix} \cos(\Delta\alpha_y) & 0 & -\sin(\Delta\alpha_y) \\ 0 & 1 & 0 \\ \sin(\Delta\alpha_y) & 0 & \cos(\Delta\alpha_y) \end{bmatrix} \begin{bmatrix} 1 & 0 & 0 \\ 0 & \cos(\Delta\alpha_x) & \sin(\Delta\alpha_x) \\ 0 & -\sin(\Delta\alpha_x) & \cos(\Delta\alpha_x) \end{bmatrix} \begin{bmatrix} x' \\ y' \\ z' \end{bmatrix}$$

$$\begin{bmatrix} x \\ y \\ z \end{bmatrix} = \begin{bmatrix} \cos(\Delta\alpha_y) & \sin(\Delta\alpha_y)\sin(\Delta\alpha_x) & -\sin(\Delta\alpha_y)\cos(\Delta\alpha_x) \\ 0 & \cos(\Delta\alpha_x) & \sin(\Delta\alpha_x) \\ \sin(\Delta\alpha_y) & -\cos(\Delta\alpha_y)\sin(\Delta\alpha_x) & \cos(\Delta\alpha_y)\cos(\Delta\alpha_x) \end{bmatrix} \begin{bmatrix} x' \\ y' \\ z' \end{bmatrix}$$

(236a)

**Step Two**

$$\begin{bmatrix} x \\ y \\ z \end{bmatrix} = \begin{bmatrix} 1 & 0 & 0 \\ 0 & \cos(\Delta\alpha_x) & \sin(\Delta\alpha_x) \\ 0 & -\sin(\Delta\alpha_x) & \cos(\Delta\alpha_x) \end{bmatrix} \begin{bmatrix} \cos(\Delta\alpha_z) & \sin(\Delta\alpha_z) & 0 \\ -\sin(\Delta\alpha_z) & \cos(\Delta\alpha_z) & 0 \\ 0 & 0 & 1 \end{bmatrix} \begin{bmatrix} x' \\ y' \\ z' \end{bmatrix}$$

$$\begin{bmatrix} x \\ y \\ z \end{bmatrix} = \begin{bmatrix} \cos(\Delta\alpha_z) & \sin(\Delta\alpha_z) & 0 \\ -\cos(\Delta\alpha_x)\sin(\Delta\alpha_z) & \cos(\Delta\alpha_x)\cos(\Delta\alpha_z) & \sin(\Delta\alpha_x) \\ \sin(\Delta\alpha_x)\sin(\Delta\alpha_z) & -\sin(\Delta\alpha_x)\cos(\Delta\alpha_z) & \cos(\Delta\alpha_x) \end{bmatrix} \begin{bmatrix} x' \\ y' \\ z' \end{bmatrix}$$

(236b)

where the angular sum is  $\lim_{\Delta\alpha \rightarrow 0} \sum_{n=1}^{\frac{\sqrt{2}}{2}\pi} |\Delta\alpha_{i,j}| = \frac{\sqrt{2}}{2} \pi$ .

The orbitsphere-cvf is given by  $n$  reiterations of Eqs. (236a) and (236b) for each point on each of the two orthogonal great circles during each of Steps One and Two where the sign of  $\pm\Delta\alpha_i$  and  $\pm\Delta\alpha_j$  for each Step are given in Table IV. The output given by the non-primed

coordinates is the input of the next iteration corresponding to each successive nested rotation by the infinitesimal angle  $\pm\Delta\alpha_i$  or  $\pm\Delta\alpha_j$ , where the magnitude of the angular sum of the  $n$  rotations about each of the  $i$ '-axis and the  $j$ '-axis is  $\frac{\sqrt{2}}{2}\pi$ . Half of the orbitsphere-cvf is generated during each of Steps One and Two.

Thus, in the limit as the number of nested conjugate rotations  $n$  goes to infinity and the incremental rotation angles  $\pm\Delta\alpha_i$  and  $\pm\Delta\alpha_j$ , each go to zero, the orbitsphere-cvf is generated from two orthogonal great circle current loops which are rotated about the  $n$ th  $i$ '-axis and then about the  $(n+1)$ th  $j$ '-axis until the  $k$ '-axis coincides with the  $-k$ -axis in two separate implementations of the algorithm comprising the Two Steps. Each Step involves a unique combination of the initial direction of the angular momentum vectors and orientation of the incremental rotation angles as summarized in Table IV. In the case of the  $n$ th element of Step One, the intersection of the two orthogonal great circle current loops occurs at the  $n$ th  $z$ '-axis which is along a great circle in a half-plane that is parallel with the  $z$ -axis and bisects the  $-x+y$ -quadrant of Figure 22. The nested rotations is also equivalent to rotating the orthogonal-great-circle basis set about the axis  $(\mathbf{i}_x, \mathbf{i}_y, 0\mathbf{i}_z)$  by an angle  $\pi$ . In the case of the  $n$ th element of Step Two, the intersection of the two orthogonal great circle current loops occurs at the  $n$ th  $y$ '-axis which is along a great circle in a half-plane that is parallel with the  $y$ -axis and bisects the  $-x-z$ -quadrant of Figure 23. The nested rotations is also equivalent to rotating the orthogonal-great-circle basis set about the axis  $(-\mathbf{i}_x, 0\mathbf{i}_y, \mathbf{i}_z)$  by an angle  $-\pi$ .

Following Step Two, in order to match the boundary condition that the magnitude of the velocity at any given point on the surface is given by Eq. (6), the output half of the orbitsphere-cvf is rotated clockwise by an angle of  $\frac{\pi}{4}$  about the  $z$ -axis. Using Eq. (236b) with  $\Delta\alpha_z = \frac{\pi}{4}$  and  $\Delta\alpha_x = 0$  gives the rotation. Then, the one half of the orbitsphere-cvf generated from Step One is superimposed with the complementary half obtained from Step Two following its rotation about the  $z$ -axis of  $\frac{\pi}{4}$  to give the orbitsphere-cvf.

The current pattern of the orbitsphere-cvf generated by the nested rotations of the orthogonal great circle current loops is a continuous and total coverage of the spherical surface, but it is shown as a visual representation using 6 degree increments of the infinitesimal angular variable  $\pm\Delta\alpha_i$  and  $\pm\Delta\alpha_j$ , of Eqs. (236a) and (236b) from the  $z$ -axis perspective in Figure 2. The complete orbitsphere-cvf current pattern corresponds to all the correlated points, points one and two, of the orthogonal great circles shown in Figures 22 and 23 which are rotated according to Eqs. (236a) and (236b) where  $\pm\Delta\alpha_i$  and  $\pm\Delta\alpha_j$ , approach zero and the summation of the infinitesimal angular rotations of  $\pm\Delta\alpha_i$  and  $\pm\Delta\alpha_j$ , about the successive  $i$ '-axes and  $j$ '-axes is

$\frac{\sqrt{2}}{2}\pi$  for each Step. The pattern also represents the momentum-vector field which is not equivalent to the mass (charge) density which for  $Y_0^0(\phi, \theta)$  is uniform. Thus, the patterns represent the directions of the nonuniform flow of the uniform and constant mass and charge distribution of  $Y_0^0(\phi, \theta)$ . The resultant angular momentum vector of the  $\mathbf{L}_{xy}$  and  $\mathbf{L}_z$  components of the orbitsphere-cvf,  $\mathbf{L}_R$ , is aligned along the z-axis, and the orbitsphere-cvf serves as a basis element to generate  $Y_0^0(\phi, \theta)$  by its convolution about the z-axis axis as visually represented in Figure 1.

### SPIN ANGULAR MOMENTUM OF THE ORBITSPHERE WITH $\mathfrak{L} = 0$

As demonstrated in Figures 2, 22 and 23, the orbitsphere-cvf is generated from two orthogonal great circle current loops which are rotated about the  $n$ th  $i'$ -axis and then about the  $(n+1)$ th  $j'$ -axis in Two Steps of the series of  $n$  nested conjugate rotations. Next, consider two infinitesimal charge (mass)-density elements at two separate positions or points, one and two, of the two orthogonal great circle current loops that serve as the sub-basis set as shown in each of Figures 22 and 23. The vector projection of the corresponding angular momentum at each point of each current element is integrated over the entire orbitsphere-cvf surface to give the corresponding electron angular momentum. The correct current pattern is confirmed by achieving the condition that the magnitude of the velocity at any point on the surface is given by Eq. (6) and by obtaining the required angular momentum projections of  $\frac{\hbar}{2}$  and  $\frac{\hbar}{4}$  along the z-axis and along an axis in the xy-plane, respectively, to satisfy the Stern-Gerlach-experimental boundary condition.

The mass density,  $\frac{m_e}{4\pi r_1^2}$ , of the orbitsphere of radius  $r_1$  is uniform; however, the projections of the angular momenta of the great circle current loops of the orbitsphere onto the z-axis and onto the xy-plane are not. The resultant vectors can be derived by considering the contributions of the momenta corresponding to the two orthogonal great circle current loops of Figures 22 and 23 as each basis set generates the current pattern of the orbitsphere-cvf in the Two Steps. The electron current, and thus, the momentum is first evenly distributed within the two orthogonally linked great-circle current loops each with a mass of  $\frac{m_e}{2}$ . The total sum of the magnitude of the angular momentum from the contributions from all of the infinitesimal points on the orbitsphere is  $\hbar$  (Eq. (7)). Thus, the angular momentum of each great circle at this point is  $\frac{\hbar}{2}$ . The planes of the great circles are oriented at an angle of  $\frac{\pi}{2}$  with respect to each other, and the resultant angular momentum is  $\frac{\hbar}{\sqrt{2}}$  in the plane transverse to the axis on which they

intersect. These loops are further divided into two sets of linked orthogonal pairs that undergo the independent transformations over the surface during Steps One and Two where the electron momentum and mass is correspondingly divided again by two. Thus, the angular momentum of each great circle of each algorithmic Step is  $\frac{\hbar}{4}$  and the resultant angular momentum is  $\frac{\hbar}{2\sqrt{2}}$  in the transverse plane. In cases where the angular momentum vectors are rotated relative to the xyz-coordinate system during the algorithm, the angular momenta are then divided by the angular span of the rotation to form normalized momentum densities corresponding to the normalized current densities. Half of the angular momentum is distributed over the orbitsphere-cvf in Step One and the other half is distributed in Step Two.

Consider the vector current directions shown in Figure 22. During Step One,  $\Delta\alpha_x$  and  $\Delta\alpha_y$  are both positive, and the resultant angular momentum vector of magnitude  $\frac{\hbar}{2\sqrt{2}}$  moves along a half a great circle in the plane that is parallel to the z-axis and bisects the +x-y-quadrant and the -x+y-quadrant. The trajectory of the resultant angular momentum vector from the xy-plane to the z-axis and back to the xy-plane is shown in Figure 24 where the angle  $\theta$  of the resultant angular momentum vector from the initial xy-plane position varies from  $\theta = 0$  to  $\theta = \pi$ . Here it can be appreciated that the vector projections onto the z-axis all add positively and the vector projections into the xy-plane sum to zero. With the initial direction defined as positive, the projection in the xy-plane varies from a maximum of  $\frac{\hbar}{2\sqrt{2}}$  to zero to  $\frac{\hbar}{2\sqrt{2}}$ . The projection onto the z-axis varies from zero to a maximum of  $\frac{\hbar}{2\sqrt{2}}$  to zero again. In each case, the projection of the angular momentum is periodic over the angular range of  $\theta$ . The total of each projection,  $\mathbf{L}_{xy}$  and  $\mathbf{L}_z$ , is the integral as a function of  $\theta$  of the magnitude of the resultant vector of the two orthogonal angular momentum component vectors corresponding to the two orthogonal great circles. For Step One, the vector projection of the angular momentum onto the xy-plane is given by sum of the vector contributions from each great circle:

$$\begin{aligned} \mathbf{L}_{xy} &= \sqrt{\frac{2}{\pi} \int_0^{\frac{\pi}{2}} \left[ \frac{\hbar}{4} \cos\theta \right]^2 + \left[ \frac{\hbar}{4} \cos\theta \right]^2 d\theta} - \sqrt{\frac{2}{\pi} \int_{\frac{\pi}{2}}^{\pi} \left[ \frac{\hbar}{4} \cos\theta \right]^2 + \left[ \frac{\hbar}{4} \cos\theta \right]^2 d\theta} \\ &= \frac{\hbar}{2\sqrt{2}} \frac{1}{\sqrt{2}} - \frac{\hbar}{2\sqrt{2}} \frac{1}{\sqrt{2}} = 0 \end{aligned} \quad (237a)$$

where each angular integral is normalized by,  $\frac{\pi}{2}$ , the angular range of  $\theta$ . Similarly, the vector projection of the angular momentum onto the z-axis as shown in Figure 24 is

$$\mathbf{L}_z = \sqrt{\frac{1}{\pi} \int_0^\pi \left[ \frac{\hbar}{4} \sin\theta \right]^2 + \left[ \frac{\hbar}{4} \sin\theta \right]^2} d\theta = \frac{\hbar}{2\sqrt{2}} \frac{1}{\sqrt{2}} = \frac{\hbar}{4} \quad (237b)$$

where each angular integral is normalized by,  $\pi$ , the angular range of  $\theta$ .

Consider the vector current directions shown in Figure 23. During Step Two,  $\Delta\alpha_z$  is negative,  $\Delta\alpha_x$  is positive, and the nested rotations causes the orthogonal great-circle basis set to rotate about the vector  $\left(-\frac{\hbar}{4}\mathbf{i}_x, 0\mathbf{i}_y, \frac{\hbar}{4}\mathbf{i}_z\right)$ . Thus, the resultant angular momentum vector of magnitude  $\frac{\hbar}{2\sqrt{2}}$  is stationary throughout the nested rotations that transform the axes as given in Table IV. Then, the  $\frac{\pi}{4}$  rotation of about the z-axis following Step Two only rotates  $\mathbf{L}_x$  by the same angle in the xy-plane such that the component is oriented along the bisector of the -x+y-quadrant as shown in Figure 23. Thus, the resultant angular momentum component of Step Two that is transverse to the z-axis,  $\mathbf{L}_{xy}$ , is in the direction of  $(-\mathbf{i}_x, \mathbf{i}_y, 0\mathbf{i}_z)$  which is also the direction of the trajectory of the angular momentum component vectors of Step One as shown in Figure 24. The resultant angular momentum projections are as given in Figure 23:

$$\mathbf{L}_{xy} = \frac{\hbar}{4} \quad (238a)$$

$$\mathbf{L}_z = \frac{\hbar}{4} \quad (238b)$$

The total vector projection of the angular momentum onto the xy-plane given by the sum of Eqs. (237a) and (238a) is

$$\mathbf{L}_{xy} = 0 + \frac{\hbar}{4} = \frac{\hbar}{4} \quad (239a)$$

The total vector projection of the angular momentum into the z-axis given by the sum of Eqs. (237b) and (238b) is

$$\mathbf{L}_z = \frac{\hbar}{4} + \frac{\hbar}{4} = \frac{\hbar}{2} \quad (239b)$$

The trajectories of the angular momenta and the resultant projections,  $\mathbf{L}_{xy}$  and  $\mathbf{L}_z$ , given in Table IV have been confirmed by computer simulations [61]. These results meet the boundary condition for the unique current having an angular velocity magnitude at each point on the surface given by Eq. (6) and give rise to the Stern Gerlach experiment as shown *infra.*, in the Magnetic Parameters of the Electron (Bohr Magneton) section, and in the Electron g Factor section. The further constraint that the current density is uniform such that the charge density is uniform, corresponding to an equipotential, minimum energy surface, is satisfied by the using orbisphere-cvf as a basis element to generate  $Y_0^0(\phi, \theta)$ .

The angular momentum is constant with respect to rotation of the orbisphere-cvf about the axis of the resultant angular momentum vector,  $\mathbf{L}_R$ . In this case, the corresponding

component angular momentum  $\mathbf{L}_{xy}$  is rotationally constant about the xy-axis; thus, the corresponding  $\mathbf{L}_x$  and  $\mathbf{L}_y$  components are rotationally constant about the x-and y-axes, respectively. The component  $\mathbf{L}_z$  is further rotationally constant about the z-axis. The constancy of the angular momentum with respect to rotation about each of the principal axes determines that the corresponding rotational symmetry of each axes is  $C_\infty$ . Since (1) the angular momentum density is distributed uniformly over the great circles that serve as basis elements to generate the orbitsphere-cvf, (2) the current is perpendicular to the corresponding angular momentum component, (3) only xy-components of angular momentum canceled during Step One, and (4) the xy-components that canceled in Step One did so symmetrically along  $\mathbf{L}_{xy}$ , an operator exists that transforms the orbitsphere-cvf into a spatially uniform distribution while maintaining the resultant angular momentum vector,  $\mathbf{L}_R$ . Thus, the orbitsphere-cvf serves a basis element to generate  $Y_0^0(\phi, \theta)$ , the orbitsphere equation of motion of the electron (Eqs. (14-15)) to give rise to electron spin.

Since the angular momentum is generated using rotations of great circle current loops that are mutually orthogonal to the angular momentum components and to each other, and the nested rotations gives a continuous and total coverage of the spherical surface, the orbitsphere-cvf has the origin as an inversion center ( $C_i$ ) as shown in Figure 2. Due to this symmetry feature of the currents as well as the rotational symmetry of the angular momentum components ( $C_\infty$ ), the convolution of the orbitsphere-cvf with a sphere aligned on the  $\mathbf{L}_R$ -axis over the spherical-coordinate angular span  $\phi=0$  to  $\phi=2\pi$  gives rise to a current density having a rotational symmetry of  $C_\infty$  about each of the x, y, and z axes. The inversion center insures that there exists a plane of symmetry of  $\sigma_H$  for each  $C_\infty$ . Thus, there are  $\infty C_\infty$  axes perpendicular to each  $C_\infty$ . A current distribution with this symmetry must belong to the spherically-symmetric point group. The same result can be obtained from considerations of the symmetry point group of the orbitsphere-cvf with respect to  $\mathbf{L}_R$  and the result of a continuous superposition over a  $2\pi$  rotation of the orbitsphere-cvf about  $\mathbf{L}_R$ .

The convolution of the orbitsphere-cvf (defined by the symbol  $O(r_1, \theta, \phi)$ ) about  $\mathbf{L}_R$  with the a constant sphere at the origin is given by the

$$Y_0^0(\phi, \theta) = \frac{1}{2\pi r_1} O(r_1, \theta, \phi) \otimes \delta(\phi - \phi) \quad (239c)$$

$$Y_0^0(\phi, \theta) = \frac{1}{2\pi r_1} O(r_1, \theta, \phi) \int_0^{2\pi} \delta(\phi - \phi) d\phi$$

The current pattern generated by the convolution of the orbitsphere-cvf with a sphere is a continuous, uniform, and total coverage of the spherical surface, but a visual representation is achieved by using the orbitsphere-cvf as a basis set and superimposing the orbitsphere-cvf elements formed by infinitesimal angular rotations about  $\mathbf{L}_R$  such that the angular sum is  $2\pi$ .

From Eqs. (239a) and (239b), the resultant angular momentum vector  $\mathbf{L}_R$  has magnitude  $\frac{\sqrt{5}\hbar}{4}$  along the direction of the spherical-coordinate angles  $\theta = 0.4636 \text{ rad}$ ,  $\phi = \frac{3\pi}{4} \text{ rad}$ . To perform the rotation about  $\mathbf{L}_R$ , the orbitsphere-cvf is first rotated counter clockwise about the vector  $(\mathbf{i}_x, \mathbf{i}_y, 0\mathbf{i}_z)$  by an angle  $-0.4636 \text{ rad}$  using Eq. (236a) wherein  $\Delta\alpha_x$  and  $\Delta\alpha_y$  are each  $-\sqrt{2}(0.4636) \text{ rad}$  to align  $\mathbf{L}_R$  with the z-axis. Next, a series of  $n$  rotations are performed about the z-axis using Eq. (236b) wherein  $\Delta\alpha_z = +q\frac{2\pi}{n}$  ( $q = 0, 1, 2, 3, 4..n$ ) and  $\Delta\alpha_x = 0$  to form  $n + 1$  orbitsphere-cvf elements. The superposition of the elements is normalized by  $n + 1$  and the final uniform orbitsphere designated  $Y_0^0(\phi, \theta)$  is rotated clockwise about the vector  $(\mathbf{i}_x, \mathbf{i}_y, 0\mathbf{i}_z)$  by an angle  $0.4636 \text{ rad}$  using Eq. (236a) wherein  $\Delta\alpha_x$  and  $\Delta\alpha_y$  are each  $+\sqrt{2}(0.4636) \text{ rad}$ . Then, the electron current,  $Y_0^0(\phi, \theta)$ , is a continuous uniform superposition of an infinite number of the orbitsphere-cvf basis element onto and over a two-dimensional surface wherein each orbitsphere-cvf is aligned on the  $\mathbf{L}_R$ -axis and the orbitsphere-cvf is a two-dimensional vector field comprised of an infinite number of one-dimensional great circles having zero-dimensional crossings.

The Stern Gerlach experiment described below demonstrates that the magnetic moment of the electron can only be parallel or antiparallel to an applied magnetic field. In spherical coordinates, this implies a spin quantum number of  $1/2$  corresponding to an angular momentum on the z-axis of  $\frac{\hbar}{2}$ . However, the Zeeman splitting energy corresponds to a magnetic moment of  $\mu_B$  and implies an electron angular momentum on the z-axis of  $\hbar$ —twice that given by Eq. (234-239). Consider the case of a magnetic field applied to the orbitsphere. The magnetic moment corresponding to the angular momentum along the z-axis results in the alignment of the z-axis of the orbitsphere with the magnetic field while the  $\frac{\hbar}{4}$  resultant vector in the xy-plane causes precession about the applied field. The precession frequency is the Larmor frequency given by the product of the gyromagnetic ratio of the electron,  $\frac{e}{2m}$ , and the magnetic flux  $\mathbf{B}$  [62]. The precessing electron can interact with a resonant photon that gives rise to Zeeman splitting—energy levels corresponding to parallel or antiparallel alignment of the electron magnetic moment with the magnetic field. The energy of the transition between these states is that of the resonant photon. The angular momentum of the precessing orbitsphere comprises the initial  $\frac{\hbar}{2}$  projection on the z-axis and the initial  $\frac{\hbar}{4}$  vector component in the xy-plane that then precesses about the z-axis. As shown in the Excited States of the One-Electron Atom (Quantization) section of Ref. [3], conservation of the angular momentum of the photon of  $\hbar$  gives rise to  $\hbar$  of

electron angular momentum. The parameters of the photon standing wave for the Zeeman effect are given in the Magnetic Parameters of the Electron (Bohr Magnetron) section and the Boundary Conditions of the Electron in a Magnetic Field are Met section.

The angular momentum of the orbitsphere in a magnetic field comprises the static  $\frac{\hbar}{2}$  projection on the z-axis (Eq. (239b)) and the  $\frac{\hbar}{4}$  vector component in the xy-plane (Eq. (239a)) that precess about the z-axis at the Larmor frequency. A resonant excitation of the Larmor precession frequency gives rise to a trapped photon with  $\hbar$  of angular momentum along a precessing  $\mathbf{S}$ -axis. In the coordinate system rotating at the Larmor frequency (denoted by the axes labeled  $X_R$ ,  $Y_R$ , and  $Z_R$  in Figure 25), the  $X_R$ -component of magnitude  $\frac{\hbar}{4}$  and  $\mathbf{S}$  of magnitude  $\hbar$  are stationary. The  $\frac{\hbar}{4}$  angular momentum along  $X_R$  with a corresponding magnetic moment of  $\frac{\mu_B}{4}$  (Eq. (295)) causes  $\mathbf{S}$  to rotate in the  $Y_R Z_R$ -plane to an angle of  $\theta = \frac{\pi}{3}$  such that the torques due to the  $Z_R$ -component of  $\frac{\hbar}{2}$  and the orthogonal  $X_R$ -component of  $\frac{\hbar}{4}$  are balanced. Then the  $Z_R$ -component due to  $\mathbf{S}$  is  $\pm \hbar \cos \frac{\pi}{3} = \pm \frac{\hbar}{2}$ . The reduction of the magnitude of  $\mathbf{S}$  along  $Z_R$  from  $\hbar$  to  $\frac{\hbar}{2}$  corresponds to the ratio of the  $X_R$ -component and the static  $Z_R$ -component of  $\frac{4}{\hbar} = \frac{1}{2}$ <sup>4</sup>. Since the  $X_R$ -component is  $\frac{\hbar}{4}$ , the  $Z_R$ -component of  $\mathbf{S}$  is  $\frac{\hbar}{2}$  which adds to the initial  $\frac{\hbar}{2}$  component to give a total  $Z_R$ -component of  $\hbar$ .

---

<sup>4</sup> The torque balance can be appreciated by considering that  $\mathbf{S}$  is aligned with  $Z_R$  if the  $X_R$ -component is zero, and the three vectors are mutually orthogonal if the  $X_R$ -component is  $\frac{\hbar}{2}$ . The balance can be shown by considering the magnetic energies resulting from the corresponding torques when they are balanced. Using Eqs. (290) and (292), the potential energy  $E_V$  due to the projection of  $\mathbf{S}$ 's angular momentum of  $\hbar$  along  $Z_R$  having  $\frac{\hbar}{2}$  of angular momentum is

$$E_V = \mu_B B \cos \theta = \mu_B \frac{1}{2} B_{\mu_B} \cos \theta = \frac{1}{2} \hbar \omega_{\mu_B} \cos \theta \quad (\text{FN 4.1})$$

where  $B_{\mu_B}$  is the flux due to a magnetic moment of a Bohr magneton and  $\omega_{\mu_B}$  is the corresponding gyromagnetic frequency. The application of a magnetic moment along the  $X_R$ -axis causes  $\mathbf{S}$  to precess about the  $Z_R$  and  $X_R$ -axes. In the  $X_R Y_R Z_R$ -frame rotating at  $\omega_{\mu_B}$ ,  $\mathbf{S}$  precesses about the  $X_R$ -axis. The corresponding precession energy  $E_{X_R}$  of  $\mathbf{S}$  about the  $X_R$ -component of  $\frac{\hbar}{4}$  is the corresponding Larmor energy

In summary, since the vector  $\mathbf{S}$  that precesses about the z-axis at an angle of  $\theta = \frac{\pi}{3}$  and an angle of  $\phi = \frac{\pi}{2}$  with respect to  $\mathbf{L}_{xy}$  given by Eq. (239a) and has a magnitude of  $\hbar$ , the  $\mathbf{S}$  projections in the  $X_R Y_R$ -plane and along the  $Z_R$ -axis are

$$\mathbf{S}_{\perp} = \hbar \sin \frac{\pi}{3} = \pm \sqrt{\frac{3}{4}} \hbar \mathbf{i}_{Y_R} \quad (240a)$$

$$\mathbf{S}_{\parallel} = \pm \hbar \cos \frac{\pi}{3} = \pm \frac{\hbar}{2} \mathbf{i}_{Z_R} \quad (240b)$$

The plus or minus sign of Eqs. (240a) and (240b) corresponds to the two possible vector orientations which are observed with the Stern-Gerlach experiment described below. The sum of the torques in the external magnetic field is balanced unless an RF field is applied to cause a Stern-Gerlach transition as discussed in the Boundary Conditions of the Electron in a Magnetic Field are Met section.

As shown in Figure 26,  $\mathbf{S}$  forms a cone in time in the nonrotating laboratory frame with an angular momentum of  $\hbar$  that is the source of the known magnetic moment of a Bohr magneton (Eq. (295)) as shown in the Magnetic Parameters of the Electron (Bohr Magnetron) section. The projection of this angular momentum onto the z-axis of  $\frac{\hbar}{2}$  adds to the z-axis component before the magnetic field was applied to give a total of  $\hbar$ . Thus, in the absence of a resonant precession, the z-component of the angular momentum is  $\frac{\hbar}{2}$ , but the excitation of the precessing  $\mathbf{S}$  component gives  $\hbar$ —twice the angular momentum on the z-axis. In addition, rather than a continuum of orientations with corresponding energies, the orientation of the

---


$$E_{X_R} = -\frac{1}{4} \hbar \omega_{\mu_B} \quad (\text{FN 4.2})$$

The energy  $E_{Z_R}$  of the magnetic moment corresponding to  $\mathbf{S}$  rotating about  $Z_R$  having  $\frac{\hbar}{2}$  of angular momentum is the corresponding Larmor energy:

$$E_{Z_R} = \frac{1}{2} \hbar \omega_{\mu_B} \quad (\text{FN 4.3})$$

At torque balance, the potential energy is equal to the sum of the Larmor energies:

$$E_{Z_R} + E_{X_R} = \hbar \left( \frac{1}{2} - \frac{1}{4} \right) \omega_{\mu_B} = \frac{\hbar}{2} \left( 1 - \frac{1}{2} \right) \omega_{\mu_B} = \frac{1}{2} \hbar \omega_{\mu_B} \cos \theta \quad (\text{FN 4.4})$$

Balance occurs when  $\theta = \frac{\pi}{3}$ . Thus, the intrinsic torques are balanced. Furthermore, energy is conserved relative to the external field as well as the intrinsic,  $Z_R$  and  $X_R$ -components of the orbitsphere, and the Larmor relationships for both the gyromagnetic ratio and the potential energy of the resultant magnetic moment are satisfied as shown in the Boundary Conditions of the Electron in a Magnetic Field are Met section.

magnetic moment must be only parallel or antiparallel to the magnetic field. This arises from conservation of angular momentum between the “static” and “dynamic” z-axis projections of the angular momentum with the additional constraint that the angular momentum has a “kinetic” as well as a “potential” or vector potential component. To conserve angular momentum, flux linkage by the electron is quantized in units of the magnetic flux quantum,  $\Phi_0 = \frac{h}{2e}$ , as shown in the Boundary Conditions of the Electron in a Magnetic Field are Met section and in the Electron g Factor section. Thus, the spin quantum number is  $s = \frac{1}{2}$ ;  $m_s = \pm \frac{1}{2}$ , but the observed Zeeman splitting corresponds to a full Bohr magneton due to  $\hbar$  of angular momentum. This aspect was historically felt to be inexplicable in terms of classical physics and merely postulated in the past.

The demonstration that the boundary conditions of the electron in a magnetic field are met appears in the Boundary Conditions of the Electron in a Magnetic Field are Met section. The observed electron parameters are explained physically. Classical laws give 1.) a gyromagnetic ratio of  $\frac{e}{2m}$ , 2.) a Larmor precession frequency of  $\frac{e\mathbf{B}}{2m}$ , 3.) the Stern-Gerlach experimental result of quantization of the angular momentum that implies a spin quantum number of 1/2 corresponding to an angular momentum of  $\frac{\hbar}{2}$  on the z-axis, and 4.) the observed Zeeman splitting due to a magnetic moment of a Bohr magneton  $\mu_B = \frac{e\hbar}{2m_e}$  corresponding to an angular momentum of  $\hbar$  on the z-axis. Furthermore, the solution is relativistically invariant as shown in the Special Relativistic Correction to the Ionization Energies section of Ref. [3]. Dirac originally attempted to solve the bound electron physically with stability with respect to radiation according to Maxwell’s equations with the further constraints that it was relativistically invariant and gave rise to electron spin [19]. He was unsuccessful and resorted to the current mathematical-probability-wave model that has many problems as discussed previously [5, 63] and in Chp. 1, Appendix II of Ref. [3].

## MAGNETIC PARAMETERS OF THE ELECTRON (BOHR MAGNETON)

### The Magnetic Field of an Orbitsphere from Spin

The orbitsphere with  $\ell = 0$  is a shell of negative charge current comprising correlated charge motion along great circles. The superposition of the vector projection of the orbitsphere angular momentum on the z-axis is  $\frac{\hbar}{2}$  with an orthogonal component of  $\frac{\hbar}{4}$ . As shown in the Orbitsphere Equation of Motion for  $\ell = 0$  section, the application of a magnetic field to the orbitsphere gives rise to a precessing angular momentum vector  $\mathbf{S}$  directed from the origin of the

orbitsphere at an angle of  $\theta = \frac{\pi}{3}$  relative to the applied magnetic field. The precession of  $\mathbf{S}$  with an angular momentum of  $\hbar$  forms a cone in the nonrotating laboratory frame to give a perpendicular projection of  $\mathbf{S}_\perp = \pm\sqrt{\frac{3}{4}}\hbar$  (Eq. (240a)) and a projection onto the axis of the applied magnetic field of  $\mathbf{S}_\parallel = \pm\frac{\hbar}{2}$  (Eq. (240b)). The superposition of the  $\frac{\hbar}{2}$  z-axis component of the orbitsphere angular momentum and the  $\frac{\hbar}{2}$  z-axis component of  $\mathbf{S}$  gives  $\hbar$  corresponding to the observed magnetostatic electron magnetic moment of a Bohr magneton. The  $\hbar$  of angular momentum along  $\mathbf{S}$  has a corresponding precessing magnetic moment of 1 Bohr magneton [64]:

$$\mu_B = \frac{e\hbar}{2m_e} = 9.274 \times 10^{-24} \text{ JT}^{-1} \quad (241)$$

The rotating magnetic field of  $\mathbf{S}$  is discussed in the Boundary Conditions of the Electron in a Magnetic Field are Met section. The magnetostatic magnetic field corresponding to  $\mu_B$  derived below is given by

$$\mathbf{H} = \frac{e\hbar}{m_e r_n^3} (\mathbf{i}_r \cos \theta - \mathbf{i}_\theta \sin \theta) \quad \text{for } r < r_n \quad (242)$$

$$\mathbf{H} = \frac{e\hbar}{2m_e r^3} (\mathbf{i}_r 2 \cos \theta + \mathbf{i}_\theta \sin \theta) \quad \text{for } r > r_n \quad (243)$$

It follows from Eq. (241), the relationship for the Bohr magneton, and relationship between the magnetic dipole field and the magnetic moment  $\mathbf{m}$  [65] that Eqs. (242) and (243) are the equations for the magnetic field due to a magnetic moment of a Bohr magneton,  $\mathbf{m} = \mu_B \mathbf{i}_z$  where  $\mathbf{i}_z = \mathbf{i}_r \cos \theta - \mathbf{i}_\theta \sin \theta$ . Note that the magnetic field is a constant for  $r < r_n$ . See Figure 6. It is shown in the Magnetic Parameters of the Electron (Bohr Magnetron) section that the energy stored in the magnetic field of the electron orbitsphere is

$$E_{mag, total} = \frac{\pi \mu_o e^2 \hbar^2}{m_e^2 r_1^3} \quad (244)$$

### Derivation of the Magnetic Field

For convenience the angular momentum vector with a magnitude in the stationary frame of  $\hbar$  will be defined as the z-axis as shown in Figure 6<sup>5</sup>. The magnetic field must satisfy the following relationships:

---

<sup>5</sup> As shown in the Boundary Conditions of the Electron in a Magnetic Field are Met section, the angular momentum of  $\hbar$  on the  $\mathbf{S}$ -axis is due to a photon standing wave that is phase-matched to a spherical harmonic source current, a spherical harmonic dipole  $Y_\ell^m(\theta, \phi) = \sin \theta$  with respect to the  $\mathbf{S}$ -axis. The dipole spins about the  $\mathbf{S}$ -axis at the angular velocity given by Eq. (9). Since the field is magnetostatic in the RF rotating frame, the

$$\nabla \cdot \mathbf{H} = 0 \text{ in free space} \quad (245)$$

$$\mathbf{n} \times (\mathbf{H}_a - \mathbf{H}_b) = \mathbf{K} \quad (246)$$

$$\mathbf{n} \cdot (\mathbf{H}_a - \mathbf{H}_b) = 0 \quad (247)$$

$$\mathbf{H} = -\nabla \psi \quad (248)$$

Since the field is magnetostatic, the current is equivalent to current loops along the z-axis. Then, the z-component of the current,  $|i|$ , for a current loop of total charge,  $e$ , oriented at an angle  $\theta$  with respect to the z-axis is given by the product of the charge, the angular velocity given by Eq. (9), and  $\sin \theta$  where the projection of the current of the orbitsphere perpendicular to the z-axis which carries the incremental current,  $\mathbf{i}i_\phi$ , is a function of  $\sin \theta$ .

$$|i| = \frac{e\hbar}{m_e r_n^2} \sin \theta \quad (249)$$

The angular function of the current-density of the orbitsphere is normalized by the geometrical factor  $N$  [66] given by

$$N = \frac{4\pi r_n^3}{2\pi \int_{-r_n}^{r_n} (r_n^2 - z^2) dz} = \frac{3}{2} \quad (250)$$

corresponding to the angular momentum of  $\hbar$ . (Eq. (250) can also be expressed in spherical coordinates for the density of a uniform shell divided by the integral in  $\theta$  and  $\phi$  of that of a spherical dipole squared [67]. The integration gives  $\frac{8\pi}{3}$  which normalized by the uniform mass density factor of  $4\pi$  gives the geometrical factor of  $\left(\frac{2}{3}\right)^{-1}$ ) The current-density  $\mathbf{K}i_\phi$  along the z-

axis having a vector orientation perpendicular to the angular momentum vector is given by dividing the magnitude of  $\mathbf{i}i_\phi$  (Eq. (249)) by the length  $r_n$ . The current-density of the orbitsphere in the incremental length  $dz$  is

$$\mathbf{K}(\rho, \phi, z) = \mathbf{i}_\phi N \frac{e\hbar}{m_e r_n^3} = \mathbf{i}_\phi \frac{3}{2} \frac{e\hbar}{m_e r_n^3} \quad (251)$$

Because

$$z = r \cos \theta \quad (252)$$

the differential length is given by

$$dz = -\sin \theta r_n d\theta \quad (253)$$

---

current is equivalent to current loops along the  $\mathbf{S}$ -axis. Thus, the derivation of the corresponding magnetic field is the same as that of the stationary field given in this section.

and so the current-density in the differential length  $r_n d\theta$  as measured along the periphery of the orbitsphere is a function of  $\sin \theta$  as given in Eq. (249). From Eq. (251), the surface current-density function of the orbitsphere about the z-axis (**S**-axis) is given by

$$\mathbf{K}(r, \theta, \varphi) = \mathbf{i}_\phi \frac{3}{2} \frac{e\hbar}{m_e r_n^3} \sin \theta \quad (254)$$

Substitution of Eq. (254) into Eq. (246) gives

$$H_\theta^a - H_\theta^b = \frac{3}{2} \frac{e\hbar}{m_e r_n^3} \sin \theta \quad (255)$$

To obtain  $H_\theta$ , the derivative of  $Y$  with respect to  $\theta$  must be taken, and this suggests that the  $\theta$  dependence of  $Y$  be taken as  $\cos \theta$ . The field is finite at the origin and is zero at infinity; so, solutions of Laplace's equation in spherical coordinates are selected because they are consistent with these conditions [68].

$$\Psi = C \left[ \frac{r}{r_n} \right] \cos \theta ; \quad r < r_n \quad (256)$$

$$\Psi = A \left[ \frac{r_n}{r} \right]^2 \cos \theta ; \quad r > r_n \quad (257)$$

The negative gradients of these potentials are

$$\mathbf{H} = \frac{-C}{r_n} (\mathbf{i}_r \cos \theta - \mathbf{i}_\theta \sin \theta) \quad \text{for } r < r_n \quad (258)$$

$$\mathbf{H} = \frac{A}{r_n} \left[ \frac{r_n}{r} \right]^3 (\mathbf{i}_r 2 \cos \theta + \mathbf{i}_\theta \sin \theta) \quad \text{for } r > r_n \quad (259)$$

The continuity conditions of Eqs. (246), (247), (254), and (255) are applied to obtain the following relationships among the variables

$$\frac{-C}{r_n} = \frac{2A}{r_n} \quad (260)$$

$$\frac{A}{r_n} - \frac{C}{r_n} = \frac{3}{2} \frac{e\hbar}{m_e r_n^3} \quad (261)$$

Solving the variables algebraically gives the magnetic fields of an electron:

$$\mathbf{H} = \frac{e\hbar}{m_e r_n^3} (\mathbf{i}_r \cos \theta - \mathbf{i}_\theta \sin \theta) \quad \text{for } r < r_n \quad (262)$$

$$\mathbf{H} = \frac{e\hbar}{2m_e r^3} (\mathbf{i}_r 2 \cos \theta + \mathbf{i}_\theta \sin \theta) \quad \text{for } r > r_n \quad (263)$$

The field is that of a Bohr magneton which matches the observed boundary conditions given in the Orbitosphere Equation of Motion for  $\ell = 0$  section including the required spherical symmetry. The demonstration that the boundary conditions of the electron in a magnetic field are met appears in the Boundary Conditions of the Electron in a Magnetic Field are Met section.

### Derivation of the Energy

The energy stored in the magnetic field of the electron is

$$E_{mag} = \frac{1}{2} \mu_o \int_0^\infty \int_0^{2\pi} \int_0^\pi H^2 r^2 \sin \theta dr d\theta d\Phi \quad (264)$$

$$E_{mag \text{ total}} = E_{mag \text{ external}} + E_{mag \text{ internal}} \quad (265)$$

$$E_{mag \text{ internal}} = \frac{1}{2} \mu_o \int_0^{r_1} \int_0^{2\pi} \int_0^\pi \left[ \frac{e\hbar}{m_e r_1^3} \right]^2 (\cos^2 \theta + \sin^2 \theta) r^2 \sin \theta dr d\theta d\Phi \quad (266)$$

$$= \frac{2 \pi \mu_o e^2 \hbar^2}{3 m_e^2 r_1^3} \quad (267)$$

$$E_{mag \text{ external}} = \frac{1}{2} \mu_o \int_0^{r_1} \int_0^{2\pi} \int_0^\pi \left[ \frac{e\hbar}{2 m_e r_1^3} \right]^2 (4 \cos^2 \theta + \sin^2 \theta) r^2 \sin \theta dr d\theta d\Phi \quad (268)$$

$$= \frac{\pi \mu_o e^2 \hbar^2}{3 m_e^2 r_1^3} \quad (269)$$

$$E_{mag \text{ total}} = \frac{2 \pi \mu_o e^2 \hbar^2}{3 m_e^2 r_1^3} + \frac{\pi \mu_o e^2 \hbar^2}{3 m_e^2 r_1^3} \quad (270)$$

$$E_{mag \text{ total}} = \frac{\pi \mu_o e^2 \hbar^2}{m_e^2 r_1^3} = \frac{4 \pi \mu_o \mu_B^2}{r_1^3} \quad (271)$$

### BOUNDARY CONDITIONS OF THE ELECTRON IN A MAGNETIC FIELD ARE MET

As shown in the Electron g Factor section, when a magnetic field with flux  $\mathbf{B}$  is applied to an electron in a central field which comprises current loops, the orbital radius of each does not change due to the Lorentzian force provided by  $\mathbf{B}$ , but the velocity changes as follows [69]:

$$\Delta v = \frac{erB}{2m_e} \quad (272)$$

corresponding to precession frequency of

$$\omega = \frac{\Delta v}{r} = \frac{eB}{2m_e} = \gamma_e B \quad (273)$$

where  $\gamma_e$  is the electron gyromagnetic ratio and  $\omega$  is the Larmor frequency. Eq. (272) applies to the current perpendicular to the magnetic flux. In this case, the moment of inertia  $I$  of the orbitsphere due which is independent of and superimposes the spin moment of inertia is

$$I = \frac{2}{3} m_e r_1^2 \quad (274)$$

since the charge (mass) is uniformly distributed on a spherical surface [66]. From Eqs. (273) and (274), the corresponding angular momentum  $L$  and rotational energy  $E_{rot}$  are

$$L = I\omega = \frac{2}{3} m_e r_1^2 \gamma_e B \quad (275)$$

and

$$E_{rot} = \frac{1}{2} I\omega^2 = \frac{1}{3} m_e r_1^2 (\gamma_e B)^2 \quad (276)$$

respectively. The change in the magnetic moment corresponding to Eq. (272) is [69]:

$$\Delta \mathbf{m} = -\frac{e^2 r_1^2}{4m_e} \mathbf{B} \quad (277)$$

Using Eqs. (273-277), in the case of a very strong magnetic flux of 10 T applied to atomic hydrogen:

$$\omega = 8.794 \times 10^{11} \text{ rad} \cdot \text{sec}^{-1} \quad (278)$$

$$I = 1.701 \times 10^{-51} \text{ kg} \cdot \text{m}^2 \quad (279)$$

$$L = 1.496 \times 10^{-39} \text{ J} \cdot \text{s} \quad (280)$$

$$E_{rot} = 6.576 \times 10^{-28} \text{ J} = 4.104 \times 10^{-9} \text{ eV} \quad (281)$$

and

$$\Delta m = 1.315 \times 10^{-28} \text{ J} \cdot \text{T}^{-1} \quad (282)$$

where the radius is given by Eq. (76) and  $2/3$ , the geometrical factor of a uniformly charged sphere [66], was used in the case of Eq. (282). Thus, these effects of the magnetic field are very small when they are compared to the intrinsic angular momentum of the electron of

$$L = \hbar = 1.055 \times 10^{-34} \text{ J} \cdot \text{s} \quad (283)$$

The electronic angular frequency of hydrogen given by Eqs. (9) and (76)

$$\omega_1 = \frac{\hbar}{m_e r_1^2} = 4.134 \times 10^{16} \text{ rad} \cdot \text{sec}^{-1} \quad (284)$$

the total kinetic energy given by Eq. (78)

$$T = 13.606 \text{ eV} \quad (285)$$

and the magnetic moment of a Bohr magneton given by Eq. (241)

$$\mu_B = \frac{e\hbar}{2m_e} = 9.274 \times 10^{-24} \text{ JT}^{-1} \quad (286)$$

$E_{rot}$  is the energy that arises due to the application of the external flux  $\mathbf{B}$ . Thus, the external work required to apply the field is also given by Eq. (281). Since the orbitsphere is uniformly charged and is superconducting, this energy is conserved when the field is removed. It is also independent of the direction of the magnetic moment due to the intrinsic angular momentum of the orbitsphere of  $\hbar$ . The corresponding magnetic moment given by Eq. (277) does not change when the intrinsic magnetic moment of the electron changes orientation. Thus, it does not contribute to the energy of a spin-flip transition observed by the Stern Gerlach experiment. It always opposes the applied field and gives rise to the phenomenon of the diamagnetic susceptibility of materials which Eq. (277) predicts with very good agreement with observations [69]. Eq. (277) also predicts the absolute chemical shifts of hydride ions that match experimental observations as shown in the Hydrino Hydride Ion Nuclear Magnetic Resonance Shift section of Ref. [3].

As shown in the Spin Angular Momentum of the Orbitsphere with  $\ell = 0$  section, the angular momentum of the orbitsphere in a magnetic field comprises the initial  $\frac{\hbar}{2}$  projection on the z-axis and the initial  $\frac{\hbar}{4}$  vector component in the xy-plane that precesses about the z-axis. A resonant excitation of the Larmor precession frequency gives rise to an additional component of angular momentum which is consistent with Maxwell's equations. As shown in the Excited States of the One-Electron Atom (Quantization) section of Ref. [3], conservation of the  $\hbar$  of angular momentum of a trapped photon can give rise to  $\hbar$  of electron angular momentum along the  $\mathbf{S}$ -axis. The photon standing waves of excited states are spherical harmonic functions which satisfy Laplace's equation in spherical coordinates and provide the force balance for the corresponding charge (mass) density waves. Consider the photon in the case of the precessing electron with a Bohr magneton of magnetic moment along the  $\mathbf{S}$ -axis. The radius of the orbitsphere is unchanged, and the photon gives rise to current on the surface that satisfies the condition

$$\nabla \cdot \mathbf{J} = 0 \quad (287)$$

corresponding to a rotating spherical harmonic dipole [70] that phase-matches the current (mass) density of Eq. (254). Thus, the electrostatic energy is constant, and only the magnetic energy need be considered as given by Eqs. (290-292). The corresponding central field at the orbitsphere surface given by the superposition of the central field of the proton and that of the photon follows from Eqs. (2.10-2.17) of Ref [3]:

$$\mathbf{E} = \frac{e}{4\pi\epsilon_0 r^2} \left[ Y_0^0(\theta, \phi) \mathbf{i}_r + \text{Re} \left\{ Y_\ell^m(\theta, \phi) e^{i\omega_n t} \right\} \mathbf{i}_y \delta(r - r_1) \right] \quad (288)$$

where the spherical harmonic dipole  $Y_\ell^m(\theta, \phi) = \sin \theta$  is with respect to the  $\mathbf{S}$ -axis. The dipole spins about the  $\mathbf{S}$ -axis at the angular velocity given by Eq. (9). The resulting current is nonradiative as shown by Eq. (17) and in Chp. 1, Appendix I of Ref. [3]. Thus, the field in the RF rotating frame is magnetostatic as shown in Figure 6 but directed along the  $\mathbf{S}$ -axis. However, the precessing dipole results in magnetic dipole radiation or absorption during a Stern-Gerlach transition. The application of a magnetic field causes alignment of the intrinsic electron magnetic moment of atoms of a material such that the population of electrons parallel versus antiparallel is a Boltzmann distribution which depends on the temperature of the material. Following the removal of the field, the original random-orientation distribution is restored as is the original temperature. The distribution may be altered by the application of an RF pulse at the Larmor frequency.

The application of a magnetic field with a resonant Larmor excitation gives rise to a precessing angular momentum vector  $\mathbf{S}$  of magnitude  $\hbar$  directed from the origin of the orbitsphere at an angle of  $\theta = \frac{\pi}{3}$  relative to the applied magnetic field.  $\mathbf{S}$  rotates about the axis of the applied field at the Larmor frequency. The magnitude of the components of  $\mathbf{S}$  that are parallel and orthogonal to the applied field (Eqs (240a-240b)) are  $\frac{\hbar}{2}$  and  $\sqrt{\frac{3}{4}}\hbar$ , respectively. Since both the RF field and the orthogonal components shown in Figure 25 rotate at the Larmor frequency, the RF field that causes a Stern Gerlach transition produces a stationary magnetic field with respect to these component as described by Patz [71].

The component of Eq. (240b) adds to the initial  $\frac{\hbar}{2}$  parallel component to give a total of  $\hbar$  in the stationary frame corresponding to a Bohr magneton,  $\mu_B$ , of magnetic moment. Eqs. (273) and (277) also hold in the case of the Stern Gerlach experiment. Superposition holds for Maxwell's equations, and only the angular momentum given by Eqs. (234-239) and the source current corresponding to Eq. (288) need be considered. Since it does not change, the diamagnetic component given from Eq. (272) does not contribute to the spin-flip transition as discussed *supra*. The potential energy of a magnetic moment  $\mathbf{m}$  in the presence of flux  $\mathbf{B}$  [64] is

$$E = \mathbf{m} \cdot \mathbf{B} \quad (289)$$

The angular momentum of the electron gives rise to a magnetic moment of  $\mu_B$ . Thus, the energy  $\Delta E_{mag}^{spin}$  to switch from parallel to antiparallel to the field is given by Eq. (308)

$$\Delta E_{mag}^{spin} = 2 \mu_B \mathbf{i}_z \cdot \mathbf{B} = 2 \mu_B B \cos \theta = 2 \mu_B B \quad (290)$$

In the case of an applied flux of 10 T, Eq. (290) gives

$$\Delta E_{mag}^{spin} = 1.855 \times 10^{-22} J = 1.158 \times 10^{-3} eV \quad (291)$$

$\Delta E_{mag}^{spin}$  is also given by Planck's equation. It can be shown from conservation of angular momentum considerations (Eqs. (293-299)) that the Zeeman splitting is given by Planck's equation and the Larmor frequency based on the gyromagnetic ratio (Eq. (273)). The electron's magnetic moment may only be parallel or antiparallel to the magnetic field rather than at a continuum of angles including perpendicular according to Eq. (289). No continuum of energies predicted by Eq. (289) for a pure magnetic dipole are possible. The energy difference for the magnetic moment to flip from parallel to antiparallel to the applied field is

$$\Delta E_{mag}^{spin} = 2\hbar\omega = 1.855 \times 10^{-22} J = 1.158 \times 10^{-3} eV \quad (292)$$

corresponding to magnetic dipole radiation.

As demonstrated in the Orbitsphere Equation of Motion for  $\ell = 0$  section,  $\frac{\hbar}{2}$  of the orbitsphere angular momentum designated the static component is initially parallel to the field. An additional  $\frac{\hbar}{2}$  parallel component designated the dynamic component comes from the  $\hbar$  of angular momentum along  $\mathbf{S}$ . The angular momentum in the presence of an applied magnetic field is [72]

$$\mathbf{L} = \mathbf{r} \times (m_e \mathbf{v} + e\mathbf{A}) \quad (293)$$

where  $\mathbf{A}$  is the vector potential evaluated at the location of the orbitsphere. The circular integral of  $\mathbf{A}$  is the flux linked by the electron. During a Stern-Gerlach transition a resonant RF photon is absorbed or emitted, and the  $\hbar$  component along  $\mathbf{S}$  reverses direction. It is shown by Eqs. (296-299) that the dynamic parallel component of angular momentum corresponding to the vector potential due to the lightlike transition is equal to the "kinetic angular momentum" ( $\mathbf{r} \times m\mathbf{v}$ ) of  $\frac{\hbar}{2}$ . Conservation of angular momentum of the orbitsphere requires that the static angular momentum component concomitantly flips. The static component of angular momentum undergoes a spin flip, and concomitantly the "potential angular momentum" ( $\mathbf{r} \times e\mathbf{A}$ ) of the dynamic component must change by  $-\frac{\hbar}{2}$  due to the linkage of flux by the electron such that the total angular momentum is conserved.

In spherical coordinates, the relationship between the vector potential  $\mathbf{A}$  and the flux  $\mathbf{B}$  is

$$2\pi r A = \pi^2 B \quad (294)$$

Eq. (294) can be substituted into Eq. (293) since the magnetic moment  $m$  is given [64] as

$$m = \frac{\text{charge} \cdot \text{angular momentum}}{2 \cdot \text{mass}} \quad (295)$$

and the corresponding energy is consistent with Eqs. (290) and (292) in this case as follows:

$$\Delta \mathbf{m} = -\frac{e(\mathbf{r} \times e\mathbf{A})}{2m_e} = \frac{e\hbar}{2m_e} = \frac{\mu_B}{2} \quad (296)$$

The boundary condition that the angular momentum is conserved is shown by Eqs. (305-307). It can be shown that Eq. (296) is also consistent with the vector potential along the axis of the applied field [72] given by

$$\mathbf{A} = \cos\frac{\pi}{3} \mu_0 \frac{e\hbar}{2m_e r^2} \sin\theta \hat{\mathbf{a}}_\phi = \mu_0 \frac{1}{2} \frac{e\hbar}{2m_e r^2} \sin\theta \hat{\mathbf{a}}_\phi \quad (297)$$

Substitution of Eq. (297) into Eq. (296) gives

$$\Delta \mathbf{m} = -\frac{e(\mathbf{r} \times e\mu_0 \frac{1}{2} \frac{e\hbar}{2m_e r^2} \sin\theta \hat{\mathbf{a}}_\phi)}{2m_e} = -\frac{1}{2} \left[ \frac{\mu_0 e^2}{2m_e r} \right] \frac{e\hbar}{2m_e} \quad (298)$$

with the geometrical factor of 2/3 [66] and the current given by Eq. (254). Since  $k$  is the lightlike  $k^0$ , then  $k = \omega_n / c$  corresponding to the RF photon field. The relativistic corrections of Eq. (298) are given by Eqs. (1.218) and (1.219) of Ref. [3] and the relativistic radius  $r = \tilde{\lambda}_c$  given by Eq. (1.217) of Ref. [3]. The relativistically corrected Eq. (298) is

$$\Delta \mathbf{m} = -\frac{1}{2} (2\pi\alpha)^{-1} \left[ \frac{\mu_0 e^2}{2m_e \alpha a_0} \right] \frac{e\hbar}{2m_e} = \frac{\mu_B}{2} \quad (299)$$

The magnetic flux of the electron is given by

$$\nabla \times \mathbf{A} = \mathbf{B} \quad (300)$$

Substitution of Eq. (297) into Eq. (300) gives 1/2 the flux of Eq. (263).

From Eq. (295), the  $\frac{\hbar}{2}$  of angular momentum before and after the field is applied corresponds to an initial magnetic moment on the applied-field-axis of  $\frac{\mu_B}{2}$ . After the field is applied, the contribution of  $\frac{\mu_B}{2}$  from Eq. (296) with Eq. (294) gives a total magnetic moment along the applied-field-axis of  $\mu_B$ , a Bohr magneton, wherein the additional contribution (Eq. (295)) arises from the angular momentum of  $\hbar$  on the S-axis. Thus, even though the magnitude of the vector projection of the angular momentum of the electron in the direction of the magnetic field is  $\frac{\hbar}{2}$ , the magnetic moment corresponds to  $\hbar$  due to the  $\frac{\hbar}{2}$  contribution from the dynamic component, and the quantized transition is due to the requirement of angular momentum conservation as given by Eq. (295).

Eq. (289) implies a continuum of energies; whereas, Eq. (296) shows that the static-kinetic and dynamic vector potential components of the angular momentum are quantized at  $\frac{\hbar}{2}$ .

Consequently, as shown in the Electron g Factor section, the flux linked during a spin transition is quantized as the magnetic flux quantum:

$$\Phi_0 = \frac{h}{2e} \quad (301)$$

Only the states corresponding to

$$m_s = \pm \frac{1}{2} \quad (302)$$

are possible due to conservation of angular momentum. It is further shown using the Poynting Power vector with the requirement that flux is linked in units of the magnetic flux quantum, that the factor 2 of Eqs. (290) and (292) is replaced by the electron g factor.

### ELECTRON g FACTOR

As demonstrated by Purcell [62], when a magnetic field is applied to an electron in a central field which comprises a current loop, the orbital radius does not change, but the velocity changes as follows:

$$\Delta v = \frac{erB}{2m_e} \quad (303)$$

This corresponds to diamagnetism and gives rise to precession with a corresponding resonance as shown in the Boundary Conditions of the Electron in a Magnetic Field are Met section. The angular momentum in the presence of an applied magnetic field is [62]

$$\mathbf{L} = \mathbf{r} \times (m_e \mathbf{v} + e\mathbf{A}) \quad (304)$$

where  $\mathbf{A}$  is the vector potential evaluated at the location of the orbitsphere. Conservation of angular momentum of the orbitsphere permits a discrete change of its “kinetic angular momentum” ( $\mathbf{r} \times m\mathbf{v}$ ) with respect to the field of  $\frac{\hbar}{2}$ , and concomitantly the “potential angular momentum” ( $\mathbf{r} \times e\mathbf{A}$ ) must change by  $-\frac{\hbar}{2}$ . The flux change,  $\phi$ , of the orbitsphere for  $r < r_n$  is determined as follows [62]:

$$\Delta \mathbf{L} = \frac{\hbar}{2} - \mathbf{r} \times e\mathbf{A} \quad (305)$$

$$= \left[ \frac{\hbar}{2} - \frac{e2\pi r A}{2\pi} \right] \hat{z} \quad (306)$$

$$= \left[ \frac{\hbar}{2} - \frac{e\phi}{2\pi} \right] \hat{z} \quad (307)$$

In order that the change in angular momentum,  $\Delta \mathbf{L}$ , equals zero,  $\phi$  must be  $\Phi_0 = \frac{h}{2e}$ , the magnetic flux quantum. Thus, to conserve angular momentum in the presence of an applied magnetic field, the orbitsphere magnetic moment can be parallel or antiparallel to an applied field as observed with the Stern-Gerlach experiment, and the flip between orientations is accompanied by the “capture” of the magnetic flux quantum by the orbitsphere “coils”

comprising infinitesimal loops of charge moving along geodesics (great circles). A superconducting loop with a weak link also demonstrates this effect [73].

The energy to flip the orientation of the orbitsphere due to its magnetic moment of a Bohr magneton,  $\mu_B$ , is

$$\Delta E_{mag}^{spin} = 2\mu_B B \quad (308)$$

where

$$\mu_B = \frac{e\hbar}{2m_e} \quad (309)$$

During the spin-flip transition, power must be conserved. Power flow is governed by the Poynting power theorem,

$$\nabla \cdot (\mathbf{E} \times \mathbf{H}) = -\frac{\partial}{\partial t} \left[ \frac{1}{2} \mu_o \mathbf{H} \cdot \mathbf{H} \right] - \frac{\partial}{\partial t} \left[ \frac{1}{2} \epsilon_o \mathbf{E} \cdot \mathbf{E} \right] - \mathbf{J} \cdot \mathbf{E} \quad (310)$$

### Stored Magnetic Energy

Energy superimposes; thus, the calculation of the spin-flip energy is determined as a sum of contributions. The energy change corresponding to the “capture” of the magnetic flux quantum is derived below. From Eq. (271) for one electron,

$$\frac{1}{2} \mu_o \mathbf{H} \cdot \mathbf{H} = E_{mag}^{fluxon} = \frac{\pi \mu_o e^2 \hbar^2}{(m_e)^2 r_n^3} \quad (311)$$

is the energy stored in the magnetic field of the electron. The orbitsphere is equivalent to a Josephson junction which can trap integer numbers of fluxons where the quantum of magnetic flux is  $\Phi_0 = \frac{h}{2e}$ . Consider Eq. (311). During the flip transition a fluxon treads the orbitsphere at the speed of light; therefore, the radius of the orbitsphere in the lab frame is  $2\pi$  times the relativistic radius in the fluxon frame as shown in the Special Relativistic Correction to the Ionization Energies section of Ref. [3]. Thus, the energy of the transition corresponding to the “capture” of a fluxon by the orbitsphere,  $E_{mag}^{fluxon}$ , is

$$E_{mag}^{fluxon} = \frac{\pi \mu_o e^2 \hbar^2}{(m_e)^2 (2\pi r_n)^3} \quad (312)$$

$$= \frac{\mu_o e^2}{4\pi^2 m_e r_n} \left( \frac{e\hbar}{2m_e} \right) \left( \frac{h}{2e\pi r_n^2} \right) \quad (313)$$

$$= \frac{\mu_o e^2}{4\pi^2 m_e r_n} \mu_B \left( \frac{\Phi_0}{A} \right) \quad (314)$$

where  $A$  is the area and  $\Phi_0$  is the magnetic flux quantum.

$$E_{mag}^{fluxon} = 2 \left[ \frac{e^2 \mu_o}{2m_e r_n} \right] \frac{1}{4\pi^2} \mu_B B \quad (315)$$

where the nth fluxon treading through the area of the orbitsphere is equivalent to the applied magnetic flux. Furthermore, the term in brackets can be expressed in terms of the fine structure constant,  $\alpha$ , as follows:

$$\frac{e^2 \mu_o}{2m_e r_n} = \frac{e^2 \mu_o c v}{2m_e v r_n c} \quad (316)$$

Substitution of Eq. (6) gives

$$\frac{e^2 \mu_o}{2m_e r_n} = \frac{e^2 \mu_o c v}{2\hbar c} \quad (317)$$

Substitution of

$$c = \sqrt{\frac{1}{\epsilon_o \mu_o}} \quad (318)$$

and

$$\alpha = \frac{\mu_o e^2 c}{2\hbar} \quad (319)$$

gives

$$\frac{e^2 \mu_o c v}{2\hbar c} = 2\pi\alpha \frac{v}{c} \quad (320)$$

The fluxon treads the orbitsphere at  $v = c$  ( $k$  is the lightlike  $k^0$ , then  $k = \omega_n / c$ ). Thus,

$$E_{mag}^{fluxon} = 2 \frac{\alpha}{2\pi} \mu_B B \quad (321)$$

### Stored Electric Energy

The superposition of the vector projection of the orbitsphere angular momentum on the z-axis is  $\frac{\hbar}{2}$  with an orthogonal component of  $\frac{\hbar}{4}$ . Excitation of a resonant Larmor precession gives rise to  $\hbar$  on an axis  $\mathbf{S}$  that precesses about the spin axis at an angle of  $\theta = \frac{\pi}{3}$ .  $\mathbf{S}$  rotates about the z-axis at the Larmor frequency.  $\mathbf{S}_\perp$ , the transverse projection, is  $\pm\sqrt{\frac{3}{4}}\hbar$  (Eq. (240a)), and  $\mathbf{S}_\parallel$ , the projection onto the axis of the applied magnetic field, is  $\pm\frac{\hbar}{2}$  (Eq. (240b)). As shown in the Spin Angular Momentum of the Orbitsphere with  $\ell = 0$  section, the superposition of the  $\frac{\hbar}{2}$  z-axis component of the orbitsphere angular momentum and the  $\frac{\hbar}{2}$  z-axis component of  $\mathbf{S}$  gives  $\hbar$  corresponding to the observed electron magnetic moment of a Bohr magneton,  $\mu_B$ . The reorientation of  $\mathbf{S}$  and the orbitsphere angular momentum from parallel to antiparallel to the magnetic field applied along the z-axis gives rise to a current. The current is acted on by the flux corresponding to  $\Phi_0$ , the magnetic flux quantum, linked by the electron during the transition

which gives rise to a Hall voltage. The electric field corresponding to the Hall voltage corresponds to the electric power term,  $\frac{\delta}{\delta t} \left[ \frac{1}{2} \epsilon_0 \mathbf{E} \cdot \mathbf{E} \right]$ , of the Poynting power theorem (Eq. (310)).

Consider a conductor in a uniform magnetic field and assume that it carries a current driven by an electric field perpendicular to the magnetic field. The current in this case is not parallel to the electric field, but is deflected at an angle to it by the magnetic field. This is the Hall Effect, and it occurs in most conductors.

A spin-flip transition is analogous to Quantum Hall Effect given in the corresponding section of Ref. [3] wherein the applied magnetic field quantizes the Hall conductance. The current is then precisely perpendicular to the magnetic field, so that no dissipation (that is no ohmic loss) occurs. This is seen in two-dimensional systems, at cryogenic temperatures, in quite high magnetic fields. Furthermore, the ratio of the total electric potential drop to the total current, the Hall resistance,  $R_H$ , is precisely equal to

$$R_H = \frac{h}{ne^2} \quad (322)$$

The factor  $n$  is an integer in the case of the Integral Quantum Hall Effect, and  $n$  is a small rational fraction in the case of the Fractional Quantum Hall Effect. In an experimental plot [74] as the function of the magnetic field, the Hall resistance exhibits flat steps precisely at these quantized resistance values; whereas, the regular resistance vanishes (or is very small) at these Hall steps. Thus, the quantized Hall resistance steps occur for a transverse superconducting state.

Consider the case that an external magnetic field is applied along the x-axis to a two dimensional superconductor in the yz-plane which exhibits the Integral Quantum Hall Effect. (See Figure 27.) Conduction electrons align with the applied field in the x direction as the field permeates the material. The normal current carrying electrons experience a Lorentzian force,  $\mathbf{F}_L$ , due to the magnetic flux. The y-directed Lorentzian force on an electron having a velocity  $\mathbf{v}$  in the z direction by an x-directed applied flux,  $\mathbf{B}$ , is

$$\mathbf{F}_L = e\mathbf{v} \times \mathbf{B} \quad (323)$$

The electron motion is a cycloid where the center of mass experiences an  $\mathbf{E} \times \mathbf{B}$  drift [75]. Consequently, the normal Hall Effect occurs. Conduction electron energy states are altered by the applied field and by the electric field corresponding to the Hall Effect. The electric force,  $\mathbf{F}_H$ , due to the Hall electric field,  $\mathbf{E}_y$ , is

$$\mathbf{F}_H = e\mathbf{E}_y \quad (324)$$

When these two forces are equal and opposite, conduction electrons propagate in the z direction alone. For this special case, it is demonstrated in Jackson [75] that the ratio of the corresponding Hall electric field  $E_H$  and the applied magnetic flux is

$$E_H/B = v \quad (325)$$

where  $v$  is the electron velocity. And, it is demonstrated in the Integral Quantum Hall Effect section of Ref. [3] that the Hall resistance,  $R_H$ , in the superconducting state is given by

$$R_H = \frac{h}{ne^2} \quad (326)$$

where  $n$  is an integer.

Consider the case of the spin-flip transition of the electron. In the case of an exact balance between the Lorentzian force (Eq. (323)) and the electric force corresponding to the Hall voltage (Eq. (324)), each superconducting point mass of the electron propagates along a great circle where

$$E/B = v \quad (327)$$

where  $v$  is given by Eq. (6). Substitution of Eq. (6) into Eq. (327) gives

$$E/B = \frac{\hbar}{m_e r} \quad (328)$$

Eq. (328) is the condition for superconductivity in the presence of crossed electric and magnetic fields. The electric field corresponding to the Hall voltage corresponds to the electric energy term,  $E_{ele}$ , of the Poynting power theorem (Eq. (310)).

$$E_{ele} = \frac{1}{2} \int_0^{2\pi} \int_0^\pi \int_0^{r_1} \epsilon_o \mathbf{E} \cdot \mathbf{E} r^2 \sin \theta dr d\theta d\phi \quad (329)$$

The electric term for this superconducting state is derived as follows using the coordinate system shown in Figure 28.

The current is perpendicular to  $\mathbf{E}_r$ , thus there is no dissipation. This occurs when

$$e\mathbf{E} = e\mathbf{v} \times \mathbf{B} \quad (330)$$

or

$$E/B = v \quad (331)$$

The electric field corresponding to the Hall Voltage is

$$\mathbf{E} = \mathbf{v} \times \mathbf{B} \quad (332)$$

Substitution of Eq. (332) into Eq. (329) gives

$$E_{ele} = \frac{1}{2} \epsilon_o \int_0^{2\pi} \int_0^\pi \int_0^{r_1} (vB)^2 r^2 \sin \theta dr d\theta d\phi \quad (333)$$

The spin flip transition may be induced by the absorption of a resonant photon. The velocity is determined from the distance traversed by each point and the time of the transition due to capture of a photon resonant with the spin-flip transition energy. The current  $\mathbf{i}_\phi$  corresponding to the

Hall voltage and  $E_r$  is given by the product of the electron charge and the frequency  $f$  of the photon where the correspondence principle holds as given in the Photon Absorption section of Ref. [3].

$$i = ef \quad (334)$$

The resistance of free space for the propagation of a photon is the radiation resistance of free space  $\eta$ .

$$\eta = \sqrt{\frac{\mu_0}{\epsilon_0}} \quad (335)$$

The power  $P_r$  of the electron current induced by the photon as it transitions from free space to being captured by the electron is given by the product of the corresponding current and the resistance  $R$  which is given by Eq. (335).

$$P_r = i^2 R \quad (336)$$

Substitution of Eq. (334) and Eq. (335) gives

$$P_r = e^2 f^2 \sqrt{\frac{\mu_0}{\epsilon_0}} \quad (337)$$

It follows from the Poynting Power theorem (Eq. (310)) with spherical radiation that the transition time  $\tau$  is given by the ratio of the energy and the power of the transition [26].

$$\tau = \frac{\text{energy}}{\text{power}} \quad (338)$$

The energy of the transition which is equal to the energy of the resonant photon is given by Planck's equation.

$$E = \hbar\omega = hf \quad (339)$$

Substitution of Eq. (337) and Eq. (339) into Eq. (338) gives

$$\tau = \frac{hf}{e^2 f^2 \sqrt{\frac{\mu_0}{\epsilon_0}}} \quad (340)$$

The distance traversed  $\ell$  by the electron with an kinetic angular momentum change of  $\frac{\hbar}{2}$  is

$$\ell = \frac{2\pi r}{2} = \frac{\lambda}{2} \quad (341)$$

where the wavelength is given by Eq. (4). The velocity is given by the distance traversed divided by the transition time. Eq. (340) and Eq. (341) give

$$v = \frac{\lambda/2}{\tau} = \frac{\lambda/2}{\frac{hf}{e^2 f^2 \sqrt{\frac{\mu_0}{\epsilon_0}}}} = \frac{\sqrt{\frac{\mu_0}{\epsilon_0}} e^2}{2h} \lambda f \quad (342)$$

The relationship for a photon in free space is

$$c = \lambda f \quad (343)$$

The fine structure constant given by Eq. (319) is the dimensionless factor that corresponds to the relativistic invariance of charge.

$$\alpha = \frac{1}{4\pi} \sqrt{\frac{\mu_0}{\epsilon_0}} \frac{e^2}{\hbar} = \frac{1}{2} \sqrt{\frac{\mu_0}{\epsilon_0}} \frac{e^2 c}{\hbar} = \frac{\mu_0 e^2 c}{2\hbar} \quad (344)$$

It is equivalent to one half the ratio of the radiation resistance of free space,  $\sqrt{\frac{\mu_0}{\epsilon_0}}$ , and the hall resistance,  $\frac{\hbar}{e^2}$ . The radiation resistance of free space is equal to the ratio of the electric field and the magnetic field of the photon (Eq. (120)). Substitution of Eq. (343) and Eq. (344) into Eq. (342) gives

$$v = \alpha c \quad (345)$$

Substitution of Eq. (345) into Eq. (333) gives

$$E_{ele} = \frac{1}{2} \epsilon_0 \int_0^{2\pi} \int_0^{\pi} \int_0^{r_1} (\alpha c \mu_0 H)^2 r^2 \sin \theta dr d\theta d\phi \quad (346)$$

where

$$B = \mu_0 H \quad (347)$$

The relationship between the speed of light,  $c$ , and the permittivity of free space,  $\epsilon_0$ , and the permeability of free space,  $\mu_0$ , is

$$c = \frac{1}{\sqrt{\mu_0 \epsilon_0}} \quad (348)$$

Thus, Eq. (346) may be written as

$$E_{ele} = \frac{1}{2} \alpha^2 \int_0^{2\pi} \int_0^{\pi} \int_0^{r_1} \mu_0 H^2 r^2 \sin \theta dr d\theta d\phi \quad (349)$$

Substitution of Eq. (267) gives

$$E_{ele} = \alpha^2 \frac{2\pi \mu_0 e^2 \hbar^2}{3m_e^2 r_1^3} \quad (350)$$

The magnetic flux,  $\mathbf{B}$ , is quantized in terms of the Bohr magneton because the electron links flux in units of the magnetic flux quantum,

$$\Phi_0 = \frac{\hbar}{2e} \quad (351)$$

Substitution of Eqs. (311-321) gives

$$E_{ele} = 2 \left( \frac{2}{3} \alpha^2 \frac{\alpha}{2\pi} \mu_B B \right) \quad (352)$$

## Dissipated Energy

The  $\mathbf{J} \cdot \mathbf{E}$  energy over time is derived from the electron current corresponding to the Larmor excitation and the electric field given by Faraday's law due to the linkage of the magnetic flux of the fluxon during the spin-flip. Consider the electron current due the external field. The application of a magnetic field with a resonant Larmor excitation gives rise to a precessing angular momentum vector  $\mathbf{S}$  of magnitude  $\hbar$  directed from the origin of the orbitsphere at an angle of  $\theta = \frac{\pi}{3}$  relative to the applied magnetic field. As given in the Spin Angular Momentum of the Orbitsphere with  $\ell = 0$  section,  $\mathbf{S}$  rotates about the axis of the applied field at the Larmor frequency. The magnitude of the components of  $\mathbf{S}$  that are parallel and orthogonal to the applied field (Eqs (240a-240b)) are  $\frac{\hbar}{2}$  and  $\sqrt{\frac{3}{4}}\hbar$ , respectively. Since both the RF field and the orthogonal components shown in Figure 25 rotate at the Larmor frequency, the RF field that causes a Stern Gerlach transition produces a stationary magnetic field with respect to these components as described in the Boundary Condition for the Electron in a Magnetic Field are Met section. The corresponding central field at the orbitsphere surface given by the superposition of the central field of the proton and that of the photon follows from Eqs. (2.10-2.17) of Ref. [3] and given by Eq. (288):

$$\mathbf{E} = \frac{e}{4\pi\epsilon_0 r^2} \left[ Y_0^0(\theta, \phi) \mathbf{i}_r + \text{Re} \left\{ Y_\ell^m(\theta, \phi) e^{i\omega_n t} \right\} \mathbf{i}_y \delta(r - r_1) \right] \quad (353)$$

where the spherical harmonic dipole  $Y_\ell^m(\theta, \phi) = \sin \theta$  is with respect to the  $\mathbf{S}$ -axis. The dipole spins about the  $\mathbf{S}$ -axis at the angular velocity given by Eq. (6). The resulting current is nonradiative as shown in the Acceleration Without Radiation section. Thus, the field in the RF rotating frame is magnetostatic as shown in Figure 6 but directed along the  $\mathbf{S}$ -axis. Thus, the corresponding current given by Eq. (251) is

$$\mathbf{K}(\rho, \phi, z) = \frac{3}{2} \frac{e\hbar}{m_e r_n^3} \sin \theta \mathbf{A}_\phi \quad (354)$$

Next consider the Faraday's equation for the electric field

$$\oint_C \mathbf{E} \cdot d\mathbf{s} = -\frac{d}{dt} \int_S \mu_0 \mathbf{H} \cdot d\mathbf{a} \quad (355)$$

As demonstrated by Purcell [62], the velocity of the electron changes according to Lenz's law, but the change in centrifugal force is balanced by the change in the central field due to the applied field. The magnetic flux of the electron given by Eq. (262) is

$$\mathbf{B} = \mu_0 \mathbf{H} = \frac{\mu_0 e\hbar}{m_e r_1^3} (\mathbf{i}_r \cos \theta - \mathbf{i}_\theta \sin \theta) \quad \text{for } r < r_n \quad (356)$$

From Eq. (321), the magnetic flux  $B_{\mathbf{J} \cdot \mathbf{E}}$  of the fluxon is

$$\mathbf{B}_{\mathbf{J} \cdot \mathbf{E}} = \frac{\alpha}{2\pi} \frac{\mu_0 e\hbar}{m_e r_1^3} (\mathbf{i}_r \cos \theta - \mathbf{i}_\theta \sin \theta) = \frac{\alpha}{2\pi} \frac{\mu_0 e\hbar}{m_e r_1^3} \mathbf{i}_z \quad (357)$$

The electric field  $\mathbf{E}$  is constant about the line integral of the orbitsphere. Using Eq. (355) with the change in flux in units of fluxons along the z-axis given by Eq. (357) gives

$$\int_{-r_1}^{+r_1} \oint \mathbf{E} \cdot d\mathbf{s} dz = \int_{-r_1}^{+r_1} -\pi r^2 \frac{dB}{dt} dz \mathbf{i}_\phi \quad (358)$$

$$\begin{aligned} 2\pi \mathbf{E} \int_0^\pi r_1 \sin^2 \theta d\theta &= -\pi \frac{\Delta B}{\Delta t} r_1^2 \sin^3 \theta d\theta \mathbf{i}_\phi \\ &= -\pi r_1^2 \frac{2\Delta B}{3\Delta t} \mathbf{i}_\phi \end{aligned} \quad (359)$$

Substitution of Eq. (357) into Eq. (359) gives

$$\pi r_1 \mathbf{E} = -\pi r_1^2 \frac{2}{3} \frac{\alpha}{2\pi} \frac{\mu_0 e \hbar}{m_e r_1^3 \Delta t} \mathbf{i}_\phi \quad (360)$$

$$\pi r_1 \mathbf{E} = -\pi \frac{2}{3} \frac{\alpha}{2\pi} \frac{\mu_0 e \hbar}{m_e r_1 \Delta t} \mathbf{i}_\phi \quad (361)$$

Thus,

$$\mathbf{E} = -\frac{2}{3} \frac{\alpha}{2\pi} \frac{\mu_0 e \hbar}{m_e r_1^2 \Delta t} \mathbf{i}_\phi \quad (362)$$

The dissipative power density  $\mathbf{E} \cdot \mathbf{J}$  can be expressed in terms of the surface current density  $\mathbf{K}$  as

$$\int_V (\mathbf{E} \cdot \mathbf{J}) \Delta t dv = \int_S (\mathbf{E} \cdot \mathbf{K}) \Delta t da \quad (363)$$

Using the electric field from Eq. (362) and the current density from Eq. (354) gives

$$\begin{aligned} \int_V (\mathbf{E} \cdot \mathbf{J}) \Delta t dv &= \int_0^{2\pi} \int_0^\pi \left( \frac{2}{3} \frac{\alpha}{2\pi} \frac{\mu_0 e \hbar}{m_e r_1^2 \Delta t} \frac{3}{2} \frac{e \hbar}{m_e r_1^3} \sin^2 \theta \right) \Delta t r_1^2 \sin \theta d\theta d\phi \\ &= \frac{4}{3} \frac{\alpha}{2\pi} \frac{\pi \mu_0 e^2 \hbar^2}{m_e^2 r_1^3} \end{aligned} \quad (364)$$

Substitution of Eq. (321) into Eq. (364) gives

$$\int_V (\mathbf{E} \cdot \mathbf{J}) \Delta t dv = 2 \left( \frac{4}{3} \right) \left( \frac{\alpha}{2\pi} \right)^2 \mu_B B \quad (365)$$

### Total Energy of Spin-Flip Transition

The principal energy of the transition corresponding to a reorientation of the orbitsphere is given by Eq. (308). And, the total energy of the flip transition is the sum of Eq. (308), and Eqs. (321), (352), and (365) corresponding to the electric energy, the magnetic energy, and the dissipated energy of a fluxon treading the orbitsphere, respectively.

$$\Delta E_{mag}^{spin} = 2 \left( 1 + \frac{\alpha}{2\pi} + \frac{2}{3} \alpha^2 \left( \frac{\alpha}{2\pi} \right) - \frac{4}{3} \left( \frac{\alpha}{2\pi} \right)^2 \right) \mu_B B \quad (366)$$

$$\Delta E_{mag}^{spin} = g\mu_B B \quad (367)$$

where the stored magnetic energy corresponding to the  $\frac{\partial}{\partial t} \left[ \frac{1}{2} \mu_o \mathbf{H} \cdot \mathbf{H} \right]$  term increases, the stored electric energy corresponding to the  $\frac{\partial}{\partial t} \left[ \frac{1}{2} \epsilon_o \mathbf{E} \cdot \mathbf{E} \right]$  term increases, and the  $\mathbf{J} \cdot \mathbf{E}$  term is dissipative. The magnetic moment of Eq. (308) is twice that from the gyromagnetic ratio as given by Eq. (295). The magnetic moment of the electron is the sum of the component corresponding to the kinetic angular momentum,  $\frac{\hbar}{2}$ , and the component corresponding to the vector potential angular momentum,  $\frac{\hbar}{2}$ , (Eq. (304)). The spin-flip transition can be considered as involving a magnetic moment of  $g$  times that of a Bohr magneton. The  $g$  factor is redesignated the fluxon  $g$  factor as opposed to the anomalous  $g$  factor, and it is given by Eq. (366).

$$\frac{g}{2} = 1 + \frac{\alpha}{2\pi} + \frac{2}{3} \alpha^2 \left( \frac{\alpha}{2\pi} \right) - \frac{4}{3} \left( \frac{\alpha}{2\pi} \right)^2 \quad (368)$$

For  $\alpha^{-1} = 137.03604(11)$  [76]

$$\frac{g}{2} = 1.001\ 159\ 652\ 120 \quad (369)$$

The experimental value [23] is

$$\frac{g}{2} = 1.001\ 159\ 652\ 188(4) \quad (370)$$

The calculated and experimental values are within the propagated error of the fine structure constant. Different values of the fine structure constant have been recorded from different experimental techniques, and  $\alpha^{-1}$  depends on a circular argument between theory and experiment [39]. One measurement of the fine structure constant based on the electron  $g$  factor is  $\alpha_{g_e}^{-1} = 137.036006(20)$  [77]. This value can be contrasted with equally precise measurements employing solid state techniques such as those based on the Josephson effect [78] ( $\alpha_J^{-1} = 137.035963(15)$ ) or the quantized Hall effect [79] ( $\alpha_H^{-1} = 137.035300(400)$ ). A method of the determination of  $\alpha^{-1}$  that depends on the circular methodology between theory and experiment to a lesser extent is the substitution of the independently measured fundamental constants  $\mu_o$ ,  $e$ ,  $c$ , and  $h$  into Eq. (344). The following values of the fundamental constants are given by Weast [76]

$$\mu_o = 4\pi \times 10^{-7} \text{ Hm}^{-1} \quad (371)$$

$$e = 1.6021892(46) \times 10^{-19} \text{ C} \quad (372)$$

$$c = 2.99792458(12) \times 10^8 \text{ ms}^{-1} \quad (373)$$

$$h = 6.626176(36) \times 10^{-34} \text{ JHz}^{-1} \quad (374)$$

For these constants,

$$\alpha^{-1} = 137.03603(82) \quad (375)$$

Substitution of the  $\alpha^{-1}$  from Eq. (375) into Eq. (368) gives

$$\frac{g}{2} = 1.001\ 159\ 652\ 137 \quad (376)$$

The experimental value [23] is

$$\frac{g}{2} = 1.001\ 159\ 652\ 188(4) \quad (377)$$

The *postulated* QED theory of  $\frac{g}{2}$  is based on the determination of the terms of a *postulated* power series in  $\alpha/\pi$  where each *postulated* virtual particle is a source of *postulated* vacuum polarization that gives rise to a *postulated* term. The algorithm involves scores of *postulated* Feynman diagrams corresponding to thousands of matrices with thousands of integrations per matrix requiring decades to reach a consensus on the “appropriate” *postulated* algorithm to remove the intrinsic infinities. The remarkable agreement between Eqs. (376) and (377) demonstrates that  $\frac{g}{2}$  may be derived in closed form from Maxwell’s equations in a simple straightforward manner that yields a result with eleven figure agreement with experiment—the limit of the experimental capability of the measurement of  $\alpha$  directly or the fundamental constants to determine  $\alpha$ . In Chp. 1, Appendix II of Ref. [3], the Maxwellian result is contrasted with the QED algorithm of invoking virtual particles, zero point fluctuations of the vacuum, and negative energy states of the vacuum. Rather than an infinity of radically different QED models, an essential feature is that *Maxwellian solutions are unique*.

## ACKNOWLEDGMENT

Thanks to M. Nansteel for reviewing the manuscript and making useful suggestions.

## REFERENCES

1. F. Laloë, *Am. J. Phys.* **69** (6), 655 (2001).
2. G. Landvogt, *Int. J. Hydrogen Energy* **28**, 1155 (2003).
3. R. L. Mills, *The Grand Unified Theory of Classical Quantum Mechanics*, September 2001 Edition, BlackLight Power, Inc., Cranbury, New Jersey, Distributed by Amazon.com; January 2003 Edition posted at [www.blacklightpower.com](http://www.blacklightpower.com).
4. R. L. Mills, *Int. J. Hydrogen Energy* **25**, 1171 (2000).
5. R. L. Mills, *Int. J. Hydrogen Energy* **26**, 1059 (2001).
6. H. Margenau and G. M. Murphy, *The Mathematics of Physics and Chemistry* (D. Van Nostrand Company, Inc., New York, 2<sup>nd</sup> Edition, 1956) pp. 363–367.
7. H. J. Maris, *J. Low Temp. Phys.* **120**, 173 (2000).
8. C. A. Fuchs and A. Peres, *Phys. Today*, **53** (3), 70 (2000).
9. S. Peil and G. Gabrielse, *Phys. Rev. Lett.* **83**, 1287 (1999).
10. F. J. Dyson, *Am. J. Phys.*, **58**, 209 (1990).
11. J. Horgan, *Sci. Am.* **267** (1), 94 (1992).
12. H. A. Haus, *Am. J. Phys.* **54**, 1126 (1986).
13. R. L. Mills, “The Grand Unified Theory of Classical Quantum Mechanics,” Global Foundation, Inc. Orbis Scientiae entitled *The Role of Attractive and Repulsive Gravitational Forces in Cosmic Acceleration of Particles The Origin of the Cosmic Gamma Ray Bursts*, (29th Conference on High Energy Physics and Cosmology Since 1964) Dr. Behram N. Kursunoglu, Chairman, December 14–17, 2000, Lago Mar Resort, Fort Lauderdale, FL, Kluwer Academic/Plenum Publishers, New York, pp. 243–258.
14. R. L. Mills, *Int. J. Hydrogen Energy* **27**, 565 (2002).
15. D. A. McQuarrie, *Quantum Chemistry* (University Science Books, Mill Valley, CA, 1983), pp. 206-225.
16. J. Daboul and J. H. D. Jensen, *Z. Physik* **265**, 455 (1973).
17. T. A. Abbott and D. J. Griffiths, *Am. J. Phys.* **53**, 1203 (1985).
18. G. Goedecke, *Phys. Rev.* **135B**, 281 (1964).
19. P. Pearle, *Foundations Phys.* **7**, (11/12), 931 (1977).
20. L. C. Shi and J. A. Kong, *Applied Electromagnetism* (Brooks/Cole Engineering Division, Monterey, CA, 1983), pp. 170–209.
21. J. D. Jackson, *Classical Electrodynamics*, 2<sup>nd</sup> Edition, (John Wiley & Sons, New York, 1975), pp. 739-779.
22. D. A. McQuarrie, *Quantum Chemistry* (University Science Books, Mill Valley, CA, 1983), pp. 238-241.
23. R. S. Van Dyck, Jr. and P. Schwinberg, H. Dehmelt, *Phys. Rev. Lett.* **59**, 26 (1987).
24. M. Mizushima, *Quantum Mechanics of Atomic Spectra and Atomic Structure* (W.A. Benjamin, Inc., New York, 1970), p. 17.
25. J. D. Jackson, *Classical Electrodynamics*, 2<sup>nd</sup> Edition (John Wiley & Sons, New York, 1975), pp. 739–752.
26. J. D. Jackson, *Classical Electrodynamics*, 2<sup>nd</sup> Edition (John Wiley & Sons, New York, 1975), pp. 758–763.
27. E. M. Purcell, *Electricity and Magnetism* (McGraw-Hill, New York, 1965), pp. 156–167.
28. D. Clark, *J. Chem. Educ.* **68**, 454 (1991).
29. J. Gribbin, *New Scientist*, **153** (2066), 15 (1997).

30. I. Levine, et al., Phys. Rev. Lett. **78**, 424 (1997).
31. C. E. Moore, "Ionization Potentials and Ionization Limits Derived from the Analyses of Optical Spectra," Nat. Stand. Ref. Data Ser.-Nat. Bur. Stand. (U.S.), No. 34, 1970.
32. R. C. Weast, *CRC Handbook of Chemistry and Physics*, 58<sup>th</sup> Edition (CRC Press, West Palm Beach, Florida, 1977), p. E-68.
33. P. J. Bromberg, J. Chem. Phys., **50** (9), 3906 (1969).
34. J. Geiger, Z. Physik, **175**, 530 (1963).
35. A. Beiser, *Concepts of Modern Physics*, 4<sup>th</sup> Edition (McGraw-Hill Book Company, New York, 1978), pp. 2–10.
36. E. G. Adelberger, C. W. Stubbs, B. R. Heckel, Y. Su, H. E. Swanson, G. Smith and J. H. Gundlach, Phys. Rev. D **42** (10), 3267 (1990).
37. G. R. Fowles, *Analytical Mechanics*, 3<sup>rd</sup> Edition (Holt, Rinehart, and Winston, New York, 1977), pp. 154–155.
38. K. Hagiwara et al., Phys. Rev. D **66**, 010001 (2002); <http://pdg.lbl.gov/2002/s035.pdf>.
39. P. J. Mohr and B. N. Taylor, Rev. Mod. Phys. **72** (2), 351 (2000).
40. T. Van Flandern, Phys. Lett. A **250**, 1 (1998).
41. R. Cowen, Sci. News **153** (19), 292 (1998).
42. M. Chown, New Scientist, **154** (2081), 50 (1997).
43. B. Schwarzschild, Phys. Today, **51** (10), 19 (1998).
44. J. C. Mather and E. S. Cheng, Astrophys. J. Lett. **354** (May 10), L37–L40 (1990).
45. W. Saunders and C. Frenk, Nature **349** (6304), 32 (1991).
46. R. P. Kirshner, A. Oemler, Jr., P. L. Schechter and S. A. Shtetman, Astron. J. **88**, 1285 (1983).
47. V. de Lapparent, M. J. Geller and J. P. Huchra, Astrophys. J. **332**(9) 44 (1988).
48. A. Dressler, S. M. Faber, D. Burstein, R. L. Davies, D. Lynden-Bell, R. J. Terlevich and G. Wegner, Astrophys. J. **313**, L37-L42, (1987).
49. S. Flamsteed, Discover **16** (3), 66 (1995).
50. J. Glanz, Science **273** (5275), 581 (1996)
51. S. D. Landy, Sci. Am. **280** (6), 38 (1999).
52. W. L. Freeman, B.F. Madore and G.D. Illingworth, Nature **371** (6500), 757 (1994).
53. R. M. Wald, *General Relativity* (University of Chicago Press, Chicago, 1984), pp. 114–116.
54. P. J. E. Peebles and J. Silk, Nature **346** (6281), 233 (1990).
55. W. McC. Siebert, *Circuits, Signals, and Systems* (The MIT Press, Cambridge, Massachusetts, 1986), pp. 597-603.
56. J. Glanz, Science **279** (5355), 1298 (1998).
57. R. Cowen, Sci. News **153** (22), 344 (1998).
58. R. Cowen, Sci. News **154** (18), 277 (1998).
59. P. de Bernardis et al., Nature **404**, 955 (April 27, 2000); available at <http://www.physics.ucsb.edu/~boomerang>.
60. N. W. Halverson, E. M. Leitch, C. Pryke, J. Kovac, J. E. Carlstrom, W. L. Holzapfel, M. Dragovan, J. K. Cartwright, B. S. Mason, S. Padin, T. J. Pearson, M. C. Shepard, and A. C. S. Readhead, "DASI first results: a measurement of the cosmic microwave background angular power spectrum," arXiv:astro-ph/0104489, 30 April, (2001).
61. B. Holverstott, R. Mills, "Modeling the Orbitsphere," posted at [www.blacklightpower.com](http://www.blacklightpower.com).

62. E. M. Purcell, *Electricity and Magnetism* (McGraw-Hill, New York, 1965), pp. 370–375, 447.
63. R. L. Mills, “The Fallacy of Feynman’s Argument on the Stability of the Hydrogen Atom According to Quantum Mechanics,” submitted.
64. D. A. McQuarrie, *Quantum Chemistry* (University Science Books, Mill Valley, CA, 1983), pp. 238–241.
65. J. D. Jackson, *Classical Electrodynamics*, 2<sup>nd</sup> Edition (John Wiley & Sons, New York, 1975), p. 178.
66. G. R. Fowles, *Analytical Mechanics*, 3<sup>rd</sup> Edition (Holt, Rinehart, and Winston, New York, 1977), p. 196.
67. D. A. McQuarrie, *Quantum Chemistry* (University Science Books, Mill Valley, CA, 1983), pp. 206–221.
68. J. D. Jackson, *Classical Electrodynamics*, 2<sup>nd</sup> Edition (John Wiley & Sons, New York, 1975), pp. 194–197.
69. E. M. Purcell, *Electricity and Magnetism* (McGraw-Hill, New York, 1965), pp. 370–379.
70. J. D. Jackson, *Classical Electrodynamics*, 2<sup>nd</sup> Edition, John Wiley & Sons, New York, (1975), pp. 84–102; 752–763.
71. S. Patz, *Cardiovasc. Interven. Radiol.* **8** (25), 225 (1986).
72. E. M. Purcell, *Electricity and Magnetism* (McGraw-Hill, New York, 1965), pp. 361–367.
73. C. E. Gough, M. S. Colclough, E. M. Forgan, R. G. Jordan, M. Keene, C. M. Muirhead, A. I. M. Rae, N. Thomas, J. S. Abell and S. Sutton, *Nature* **326**, 855 (1987).
74. S. Das Sarma and R.E. Prange, *Science* **256**, 1284 (1992).
75. J. D. Jackson, *Classical Electrodynamics*, 2<sup>nd</sup> Edition (John Wiley & Sons, New York, 1975), pp. 582–584.
76. R. C. Weast, *CRC Handbook of Chemistry and Physics*, 68<sup>th</sup> Edition (CRC Press, Boca Raton, Florida, 1987–88), p. F-186 to p. F-187.
77. G. P. Lepage, “Theoretical advances in quantum electrodynamics,” International Conference on Atomic Physics, Atomic Physics, Proceedings, Singapore, World Scientific, **7**, (1981), 297.
78. E. R. Williams and P. T. Olsen, *Phys. Rev. Lett.* **42**, 1575 (1979).
79. K. v. Klitzing, G. Dorda and M. Pepper, *Phys. Rev. Lett.* **45**, 494 (1980).

Table I. The calculated electric (per electron), magnetic (per electron), and ionization energies for some two-electron atoms.

Atom	$r_1$ ( $a_o$ ) <sup>a</sup>	Electric Energy <sup>b</sup> (eV)	Magnetic Energy <sup>c</sup> (eV)	Calculated Ionization Energy <sup>d</sup> (eV)	Experimental Ionization [31-32] Energy (eV)
<i>He</i>	0.567	-23.96	0.63	24.59	24.59
<i>Li</i> <sup>+</sup>	0.356	-76.41	2.54	75.56	75.64
<i>Be</i> <sup>2+</sup>	0.261	-156.08	6.42	154.48	153.89
<i>B</i> <sup>3+</sup>	0.207	-262.94	12.96	260.35	259.37
<i>C</i> <sup>4+</sup>	0.171	-396.98	22.83	393.18	392.08
<i>N</i> <sup>5+</sup>	0.146	-558.20	36.74	552.95	552.06
<i>O</i> <sup>6+</sup>	0.127	-746.59	55.35	739.67	739.32
<i>F</i> <sup>7+</sup>	0.113	-962.17	79.37	953.35	953.89

<sup>a</sup> from Equation (137)

<sup>b</sup> from Equation (139)

<sup>c</sup> from Equation (140)

<sup>d</sup> from Equations (138) and (141)

Table II. The Maxwellian closed-form calculated and experimental parameters of  $H_2$ ,  $D_2$ ,  $H_2^+$  and  $D_2^+$ .

Parameter	Calculated	Experimental	Eqs. <sup>a</sup>
$H_2$ Bond Energy	4.478 eV	4.478 eV	12.251
$D_2$ Bond Energy	4.556 eV	4.556 eV	12.253
$H_2^+$ Bond Energy	2.654 eV	2.651 eV	12.220
$D_2^+$ Bond Energy	2.696 eV	2.691 eV	12.222
$H_2$ Total Energy	31.677 eV	31.675 eV	12.247
$D_2$ Total Energy	31.760 eV	31.760 eV	12.248
$H_2$ Ionization Energy	15.425 eV	15.426 eV	12.249
$D_2$ Ionization Energy	15.463 eV	15.466 eV	12.250
$H_2^+$ Ionization Energy	16.253 eV	16.250 eV	12.218
$D_2^+$ Ionization Energy	16.299 eV	16.294 eV	12.219
$H_2^+$ Magnetic Moment	$9.274 \times 10^{-24} \text{ JT}^{-1}$	$9.274 \times 10^{-24} \text{ JT}^{-1}$	14.1-14.7
	$\mu_B$	$\mu_B$	
Absolute $H_2$ Gas-Phase NMR Shift	-28.0 ppm	-28.0 ppm	12.362
$H_2$ Internuclear Distance <sup>b</sup>	0.748 Å	0.741 Å	12.238
	$\sqrt{2}a_o$		
$D_2$ Internuclear Distance <sup>b</sup>	0.748 Å	0.741 Å	12.238
	$\sqrt{2}a_o$		
$H_2^+$ Internuclear Distance <sup>c</sup>	1.058 Å	1.06 Å	12.207
	$2a_o$		
$D_2^+$ Internuclear Distance <sup>b</sup>	1.058 Å	1.0559 Å	12.207
	$2a_o$		
$H_2$ Vibrational Energy	0.517 eV	0.516 eV	12.259
$D_2$ Vibrational Energy	0.371 eV	0.371 eV	12.264
$H_2$ $\omega_e x_e$	$120.4 \text{ cm}^{-1}$	$121.33 \text{ cm}^{-1}$	12.261
$D_2$ $\omega_e x_e$	$60.93 \text{ cm}^{-1}$	$61.82 \text{ cm}^{-1}$	12.265
$H_2^+$ Vibrational Energy	0.270 eV	0.271 eV	12.228
$D_2^+$ Vibrational Energy	0.193 eV	0.196 eV	12.232
$H_2$ J=1 to J=0 Rotational Energy <sup>b</sup>	0.0148 eV	0.01509 eV	14.45
$D_2$ J=1 to J=0 Rotational Energy <sup>b</sup>	0.00741 eV	0.00755 eV	14.37-14.45
$H_2^+$ J=1 to J=0 Rotational Energy <sup>c</sup>	0.00740 eV	0.00739 eV	14.49
$D_2^+$ J=1 to J=0 Rotational Energy <sup>b</sup>	0.00370 eV	0.003723 eV	14.37-14.43, 14.49

<sup>a</sup> Ref. [3].

<sup>b</sup> The internuclear distances are not corrected for the reduction due to  $\bar{E}_{osc}$ .

<sup>c</sup> The internuclear distances are not corrected for the increase due to  $\bar{E}_{osc}$ .

Table III. Predicted harmonic parameters  $\ell$  and relative intensities  $I(n)$  as a function of peak  $n$ .

$n$	$\ell^a$	Angle ( $^\circ$ ) <sup>a</sup>	$I(n)^b$
1	197	0.91	1
2	591	0.30	0.50
3	788	0.23	0.33
4	985	0.18	0.25
5	1182	0.15	0.20
6	1379	0.13	0.17

<sup>a</sup> Eq. (225)

<sup>b</sup> Eq. (229)

Table IV. Summary of the results of the matrix transformations of the two orthogonal current loops to generate the orbitsphere.

Step	Initial Direction of Angular Momentum Components $(\hat{r} \times \hat{K})^a$	Final Direction of Angular Momentum Components $(\hat{r} \times \hat{K})^a$	Sign of $\Delta\alpha_r$	Sign of $\Delta\alpha_f$	Initial to Final Axis Transformation	$\mathbf{L}_{xy}$	$\mathbf{L}_z$
1	$\hat{x}, -\hat{y}$	$-\hat{x}, \hat{y}$	$+\Delta\alpha_x$	$+\Delta\alpha_y$	$+x' \rightarrow +y$ $+y' \rightarrow +x$ $+z' \rightarrow -z$	0	$\frac{\hbar}{4}$
2	$-\hat{x}, \hat{z}$	$-\hat{x}, \hat{z}$	$-\Delta\alpha_z$	$+\Delta\alpha_x$	$+z' \rightarrow -x$ $+x' \rightarrow -z$ $+y' \rightarrow -y$	$\frac{\hbar}{4}$	$\frac{\hbar}{4}$
Total						$\frac{\hbar}{4}$	$\frac{\hbar}{2}$

<sup>a</sup>  $\mathbf{K}$  is the current density,  $\mathbf{r}$  is the polar vector of the great circle, and “ $\hat{\phantom{u}}$ ” denotes the unit vectors  $\hat{u} \equiv \frac{\mathbf{u}}{|\mathbf{u}|}$ .

Figure 1. The orbitsphere is a two dimensional spherical shell of zero thickness with the Bohr radius of the hydrogen atom,  $r = a_H$ .

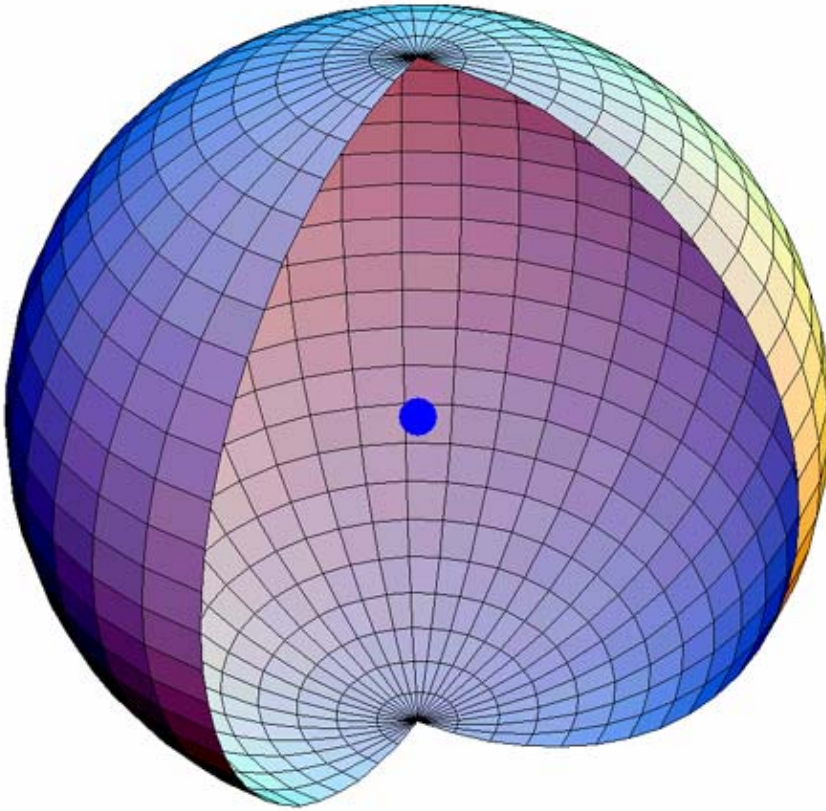
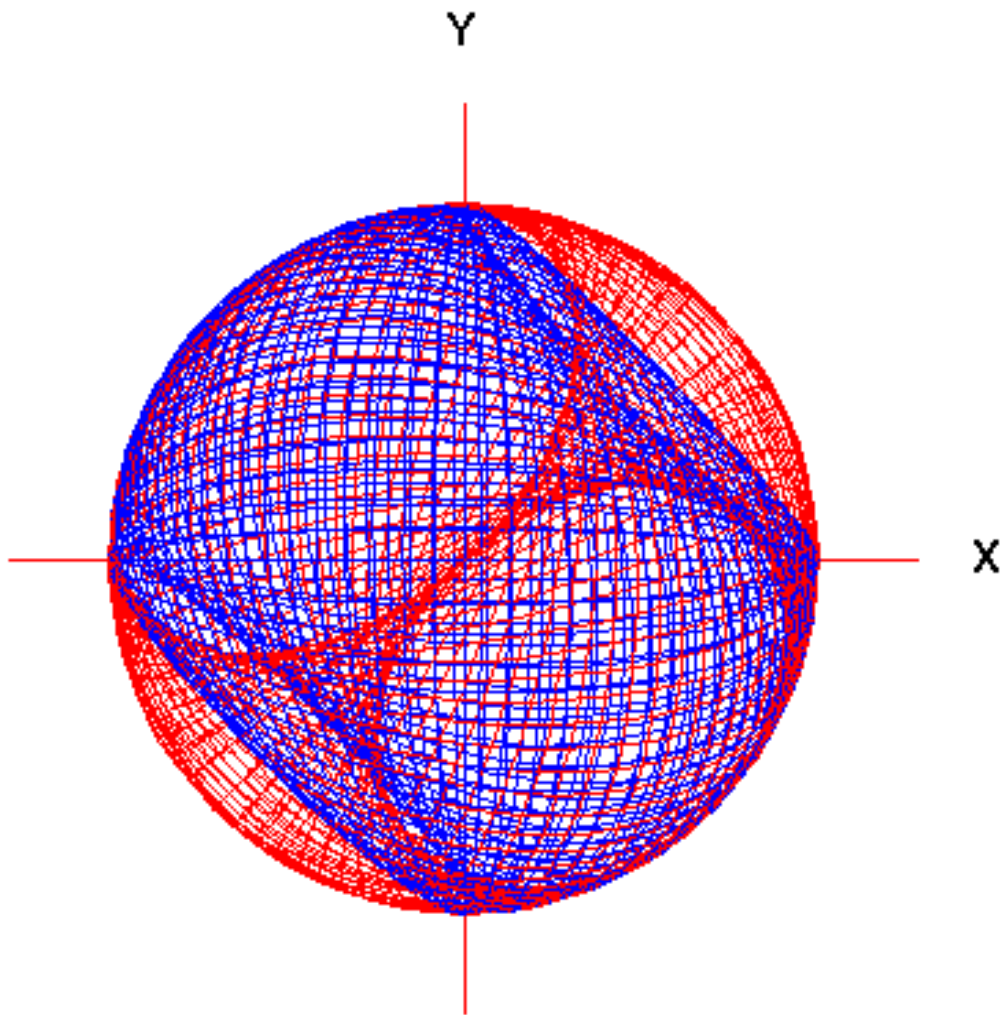


Fig. 2. The current pattern of the orbitsphere shown with 6 degree increments of the infinitesimal angular variables  $\pm\Delta\alpha_p$  and  $\pm\Delta\alpha_j$ , from the perspective of looking along the z-axis. The current and charge density are confined to two dimensions at  $r_n = nr_1$ . The corresponding charge density function is uniform.



**View Along the Positive Z Axis**

Fig. 3. The orbital function modulates the constant (spin) function (shown for  $t = 0$ ; three-dimensional view).

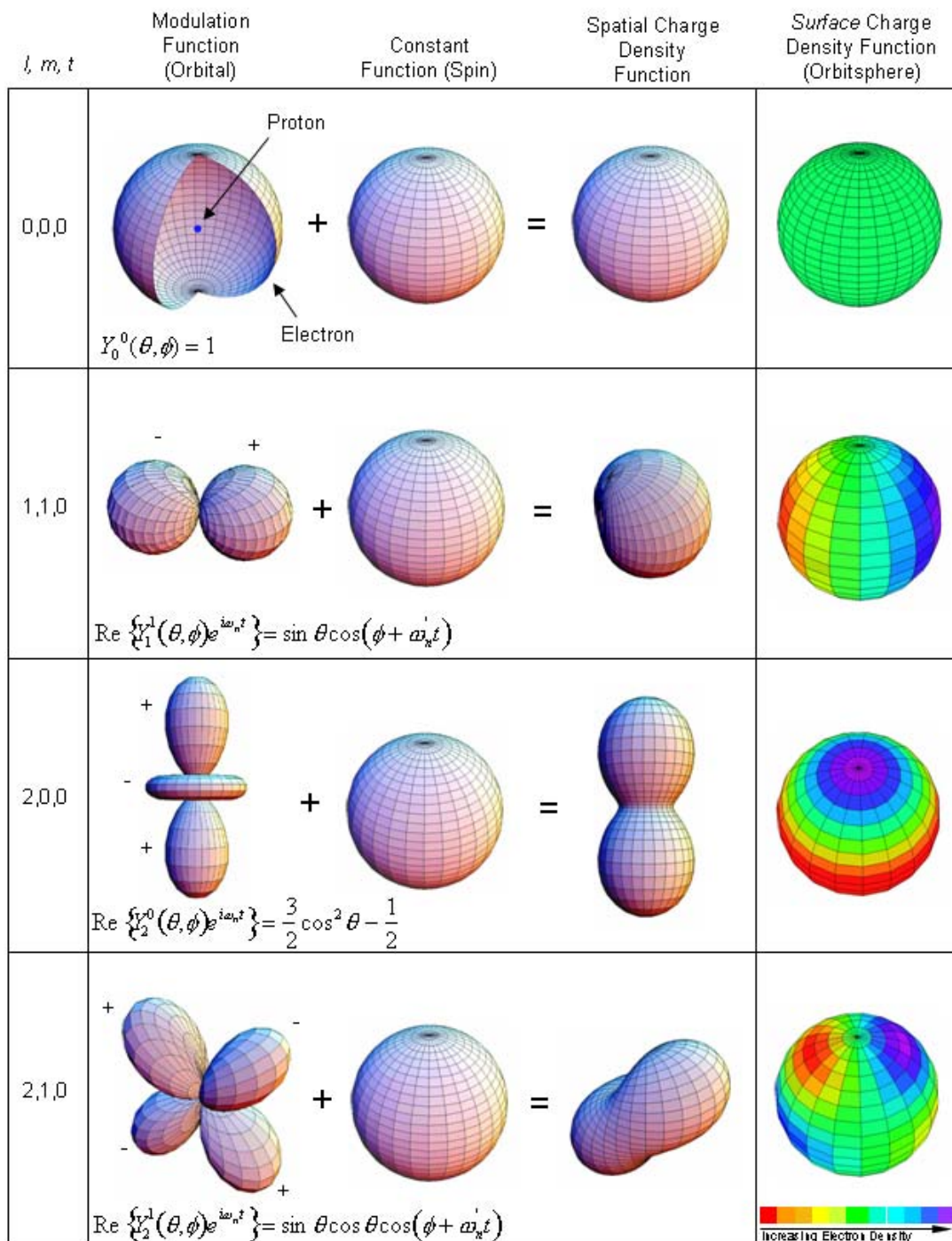


Fig. 4. The normalized radius as a function of the velocity due to relativistic contraction.

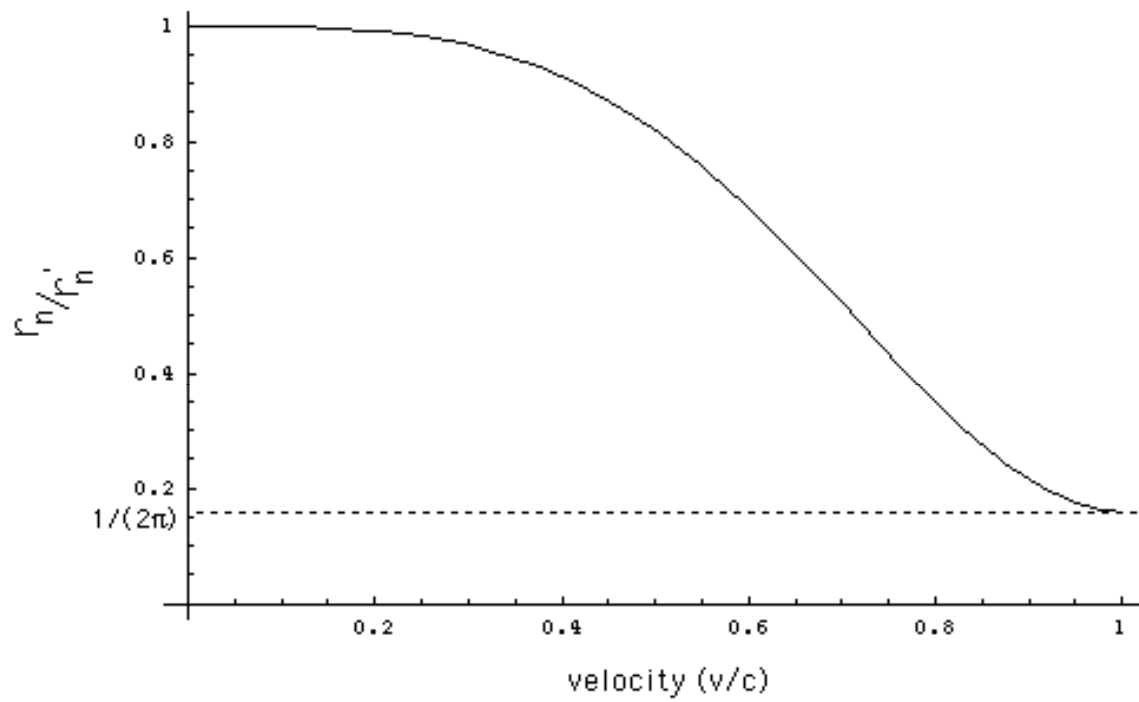


Fig. 5. Far field approximation.

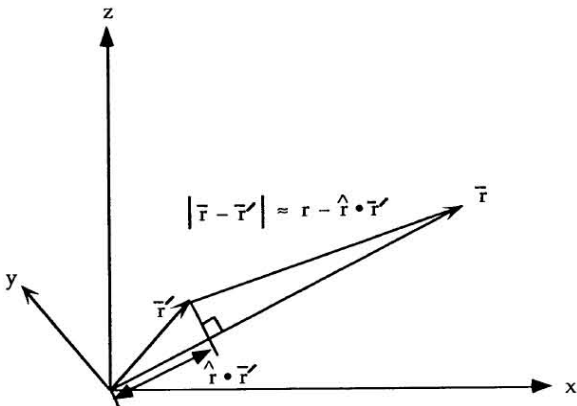


Fig. 6. The magnetic field of an electron orbitsphere (z-axis defined as the vertical axis).

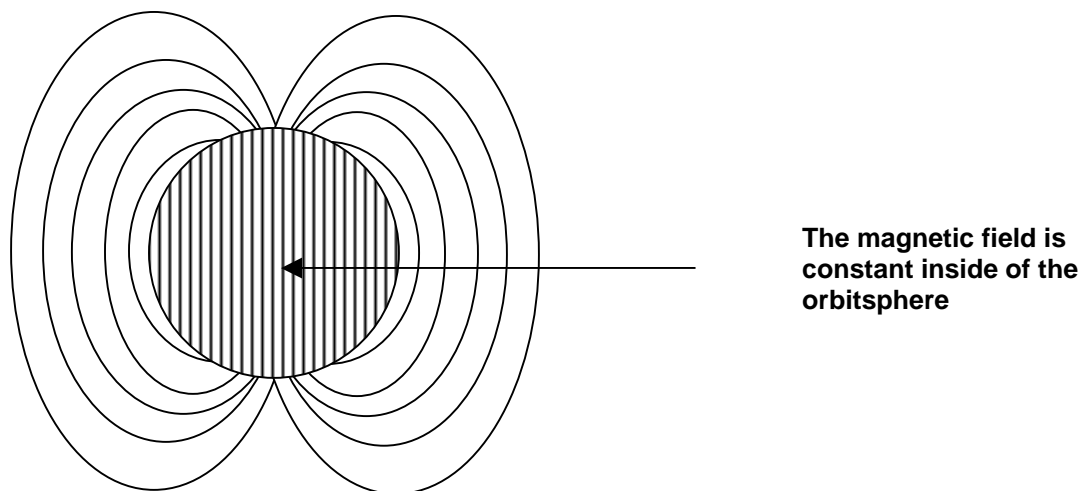


Fig. 7. Broadening of the spectral line due to the rise-time and shifting of the spectral line due to the radiative reaction. The resonant line shape has width  $\Gamma$ . The level shift is  $\Delta\omega$ .

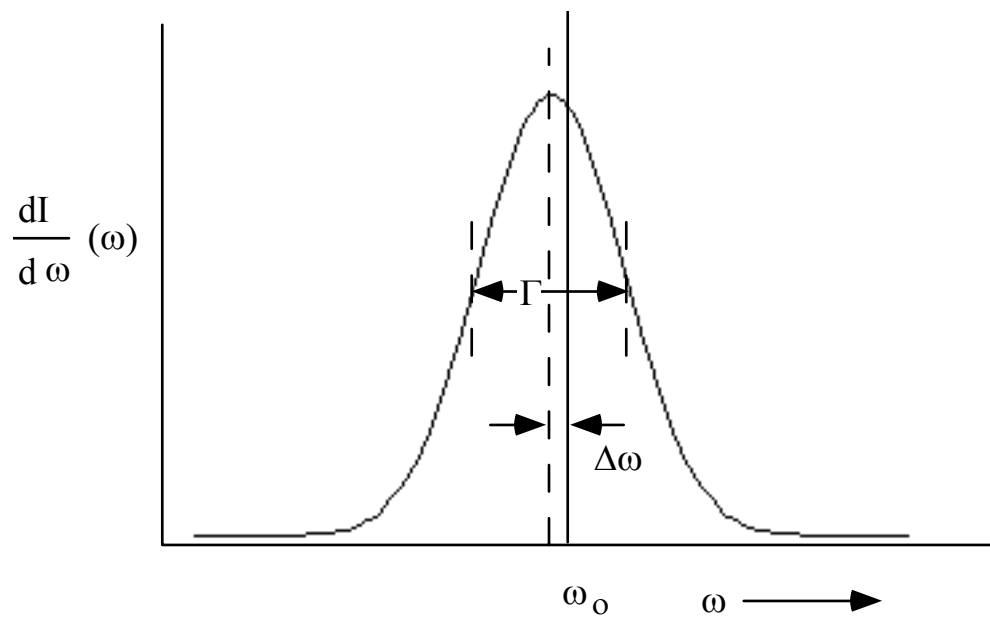


Fig. 8. The Cartesian coordinate system wherein the first great circle magnetic field line lies in the  $yz$ -plane, and the second great circle electric field line lies in the  $xz$ -plane is designated the photon orbitsphere reference frame of a photon orbitsphere.

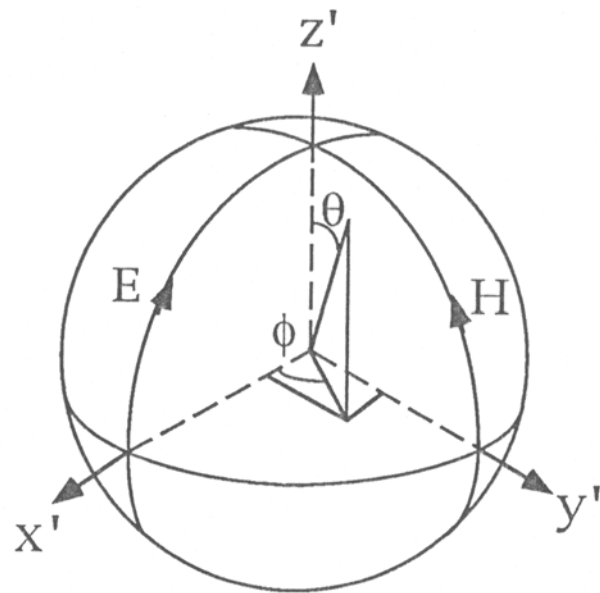
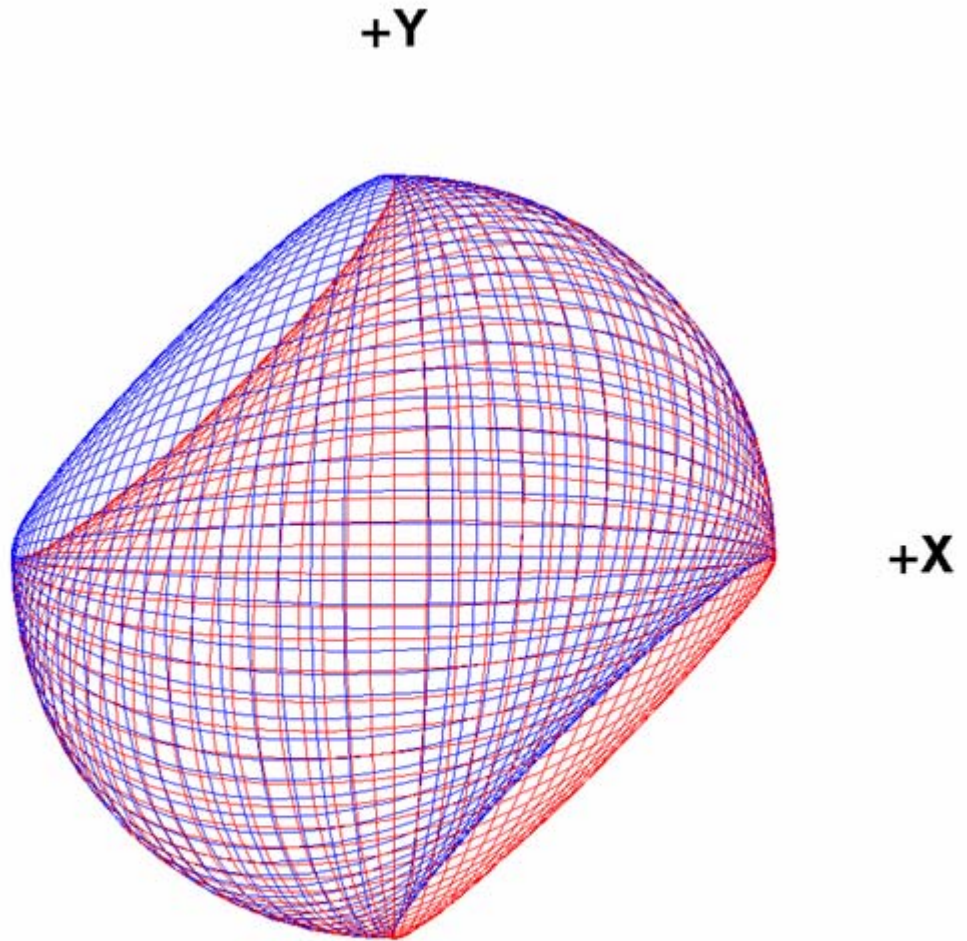


Fig. 9. The field line pattern from the perspective of looking along the z-axis of a right-handed circularly polarized photon.



**View Along the Positive Z Axis**

Fig. 10. The electric field of a moving point charge ( $v = \frac{4}{5}c$ ).

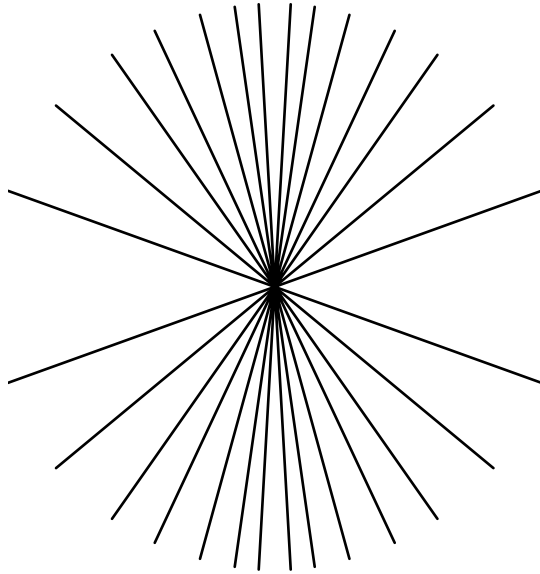


Fig. 11. The electric field lines of a right-handed circularly polarized photon orbitsphere as seen along the axis of propagation in the lab inertial reference frame as it passes a fixed point.

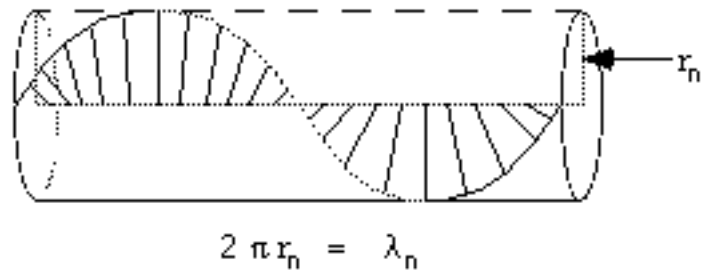
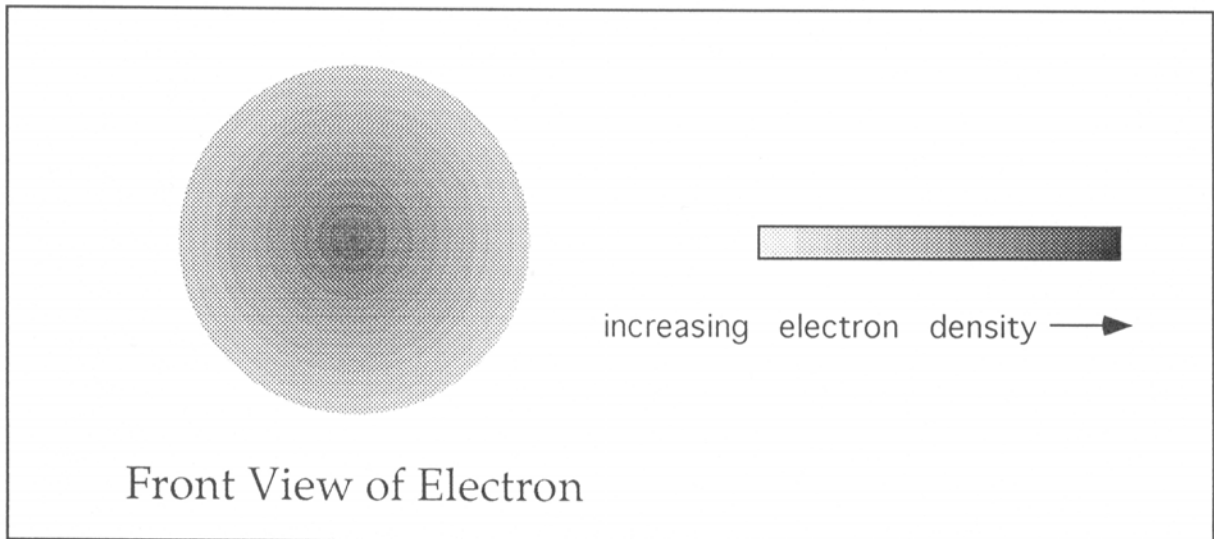


Fig. 12. The front view of the magnitude of the mass (charge) density function in the xy-plane of a free electron; side view of a free electron along the axis of propagation—z-axis.



$$\rho_0 = \frac{\hbar}{mv_z}$$

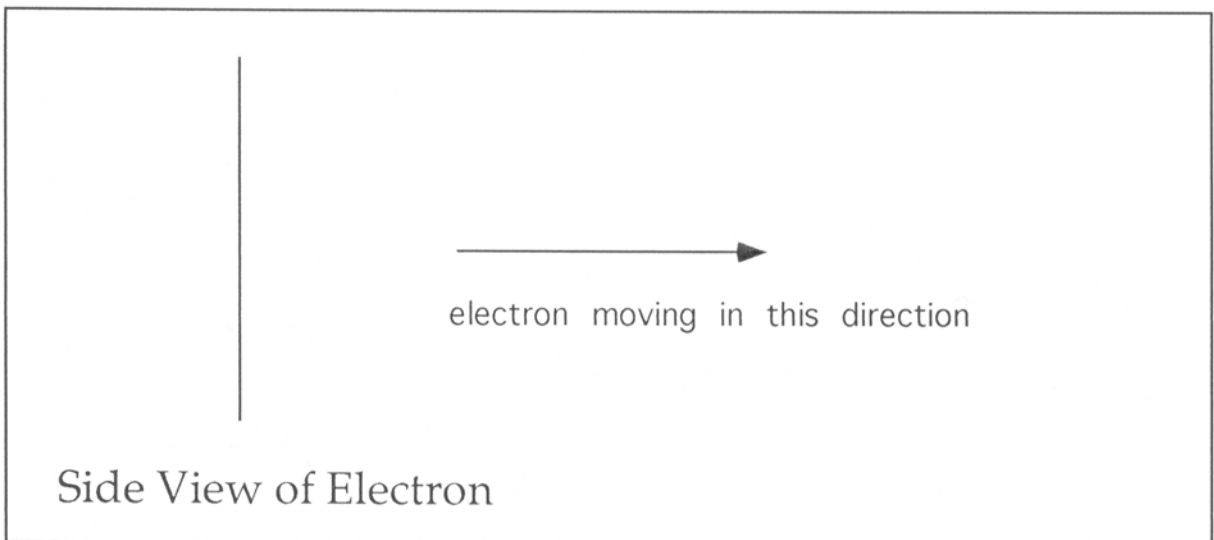


Fig. 13. The experimental results for the elastic differential cross section for the elastic scattering of electrons by helium atoms and a Born approximation prediction.

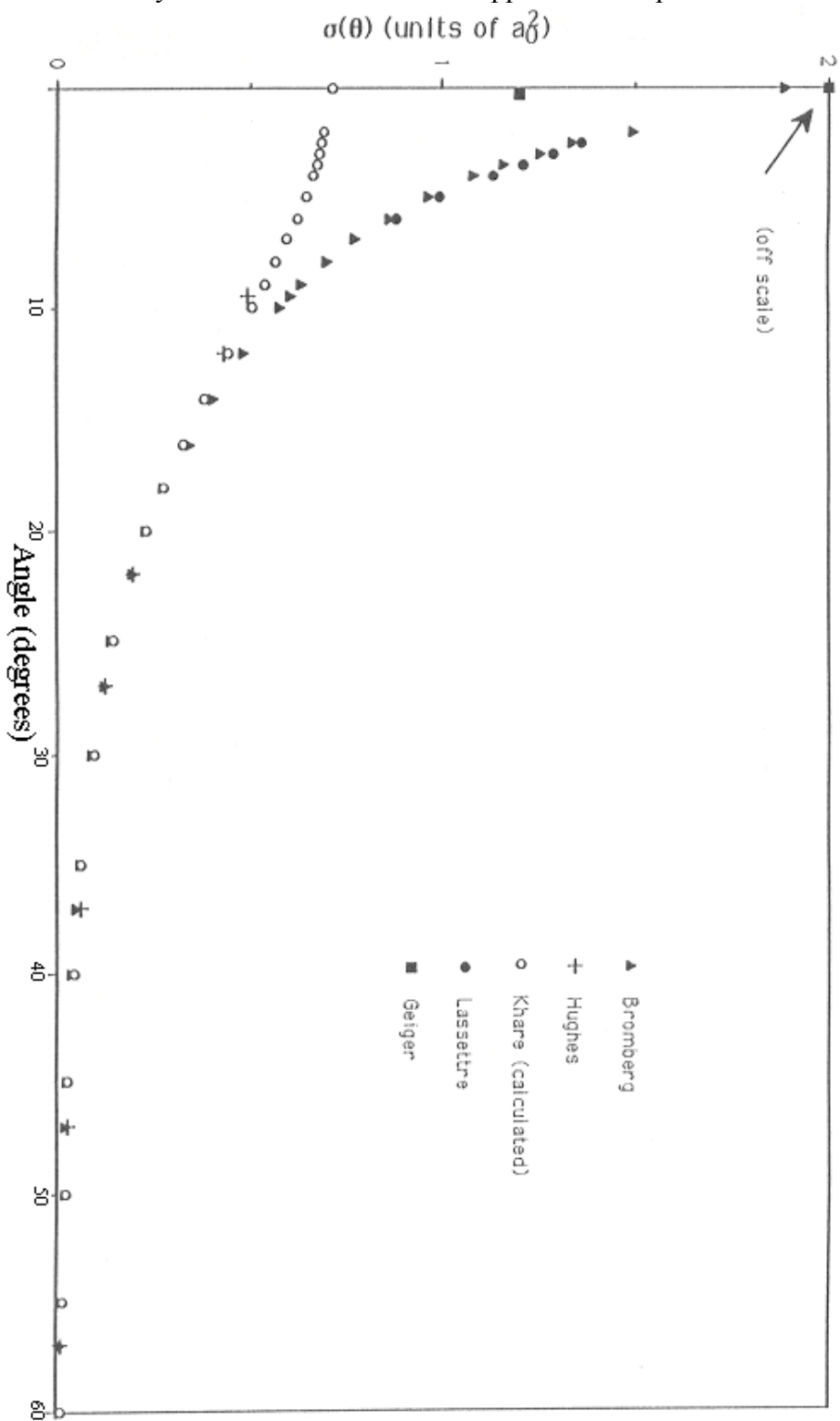


Fig. 14. The closed form function (Eqs. (146) and (147)) for the elastic differential cross section for the elastic scattering of electrons by helium atoms. The scattering amplitude function,  $F(s)$  (Eq. (145)), is shown as an insert.

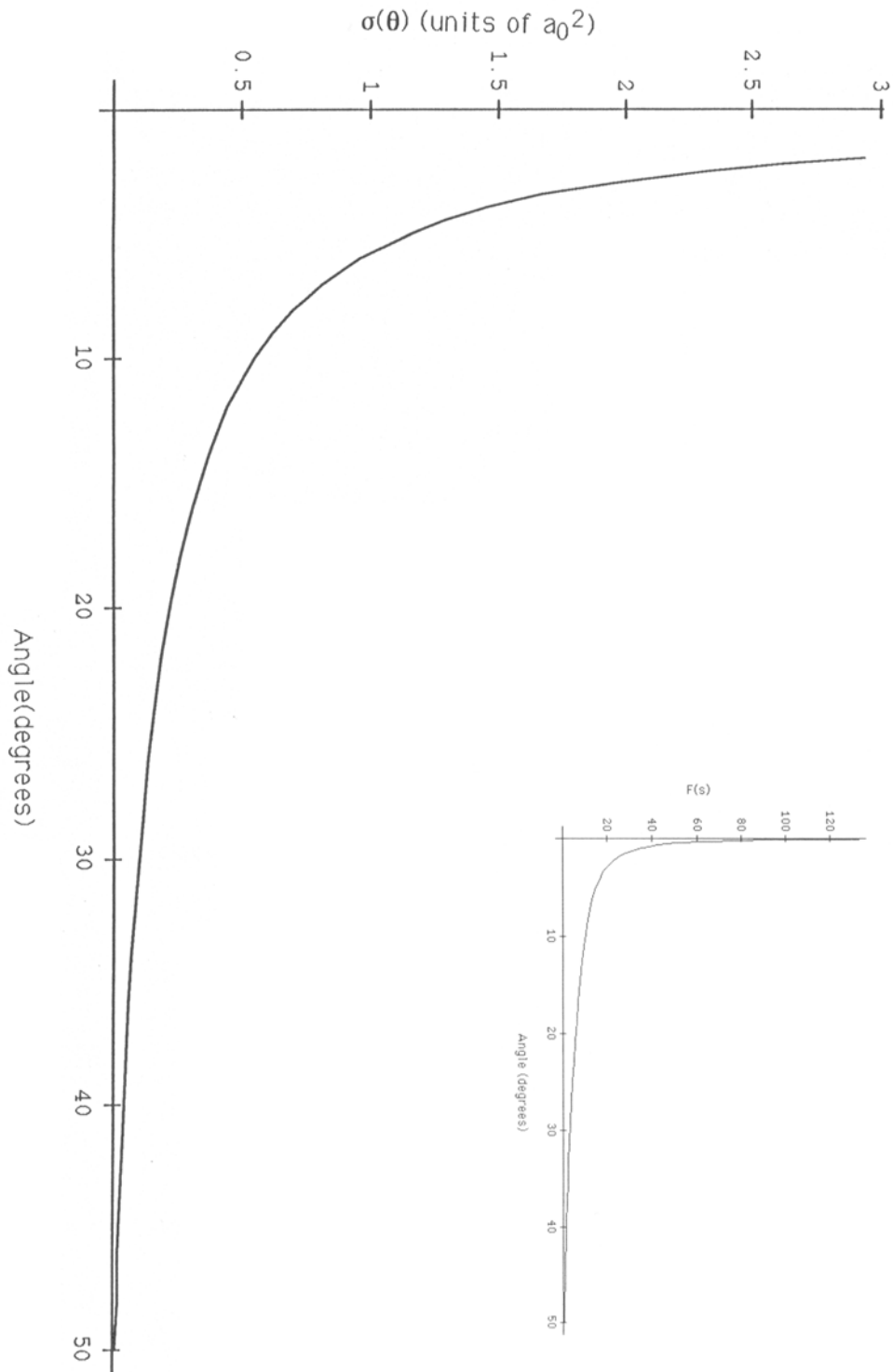


Fig. 15. The radius of the universe as a function of time.

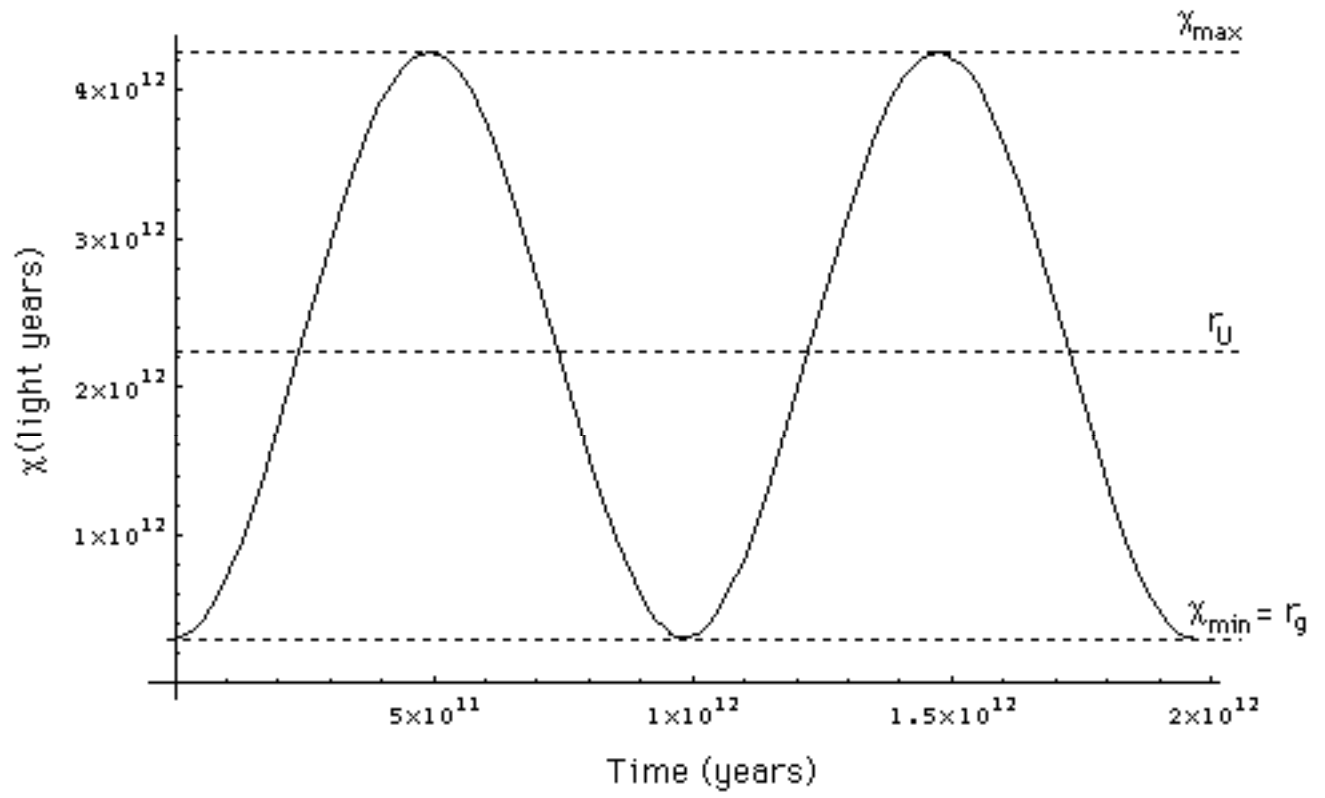


Fig. 16. The expansion/contraction rate of the universe as a function of time.

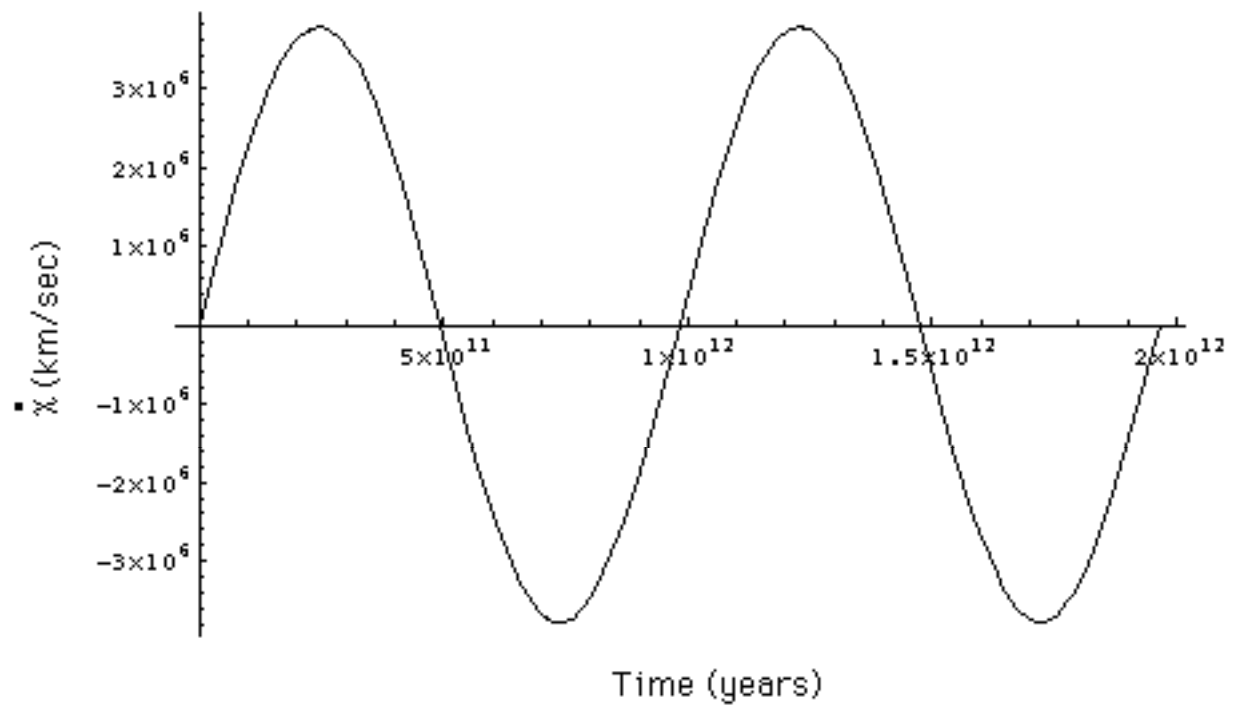


Fig. 17. The Hubble constant of the universe as a function of time.

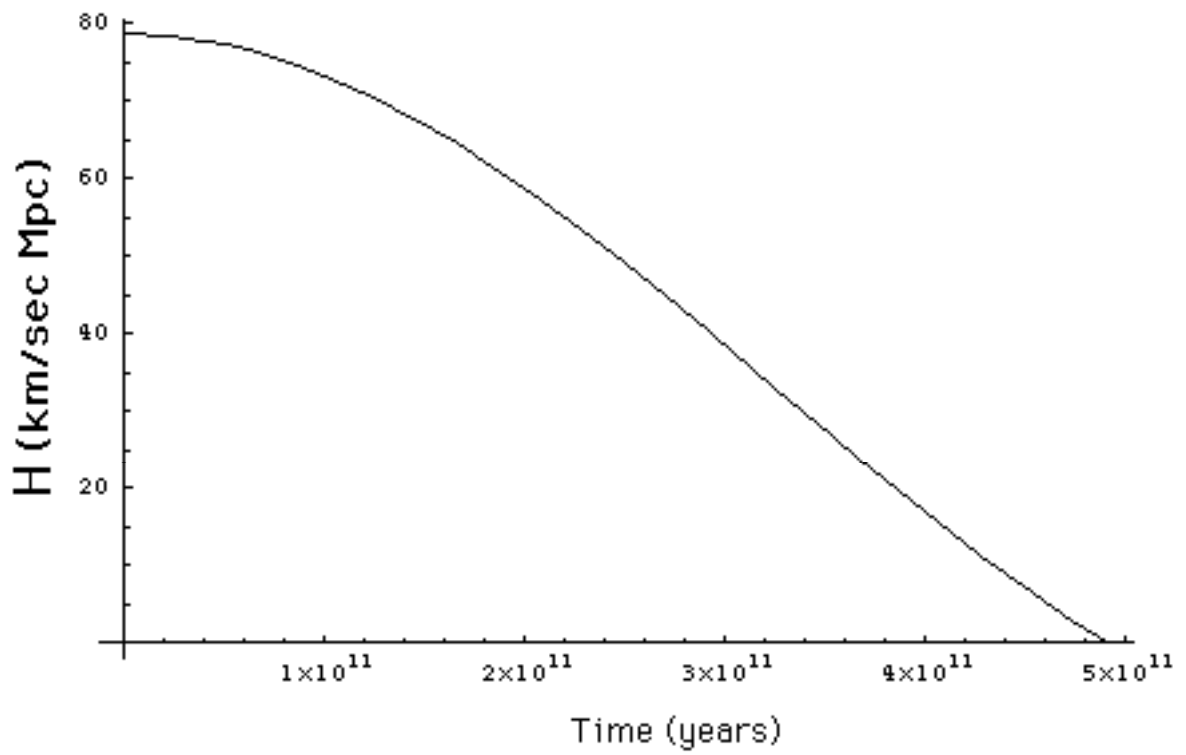


Fig. 18. The density of the universe as a function of time.

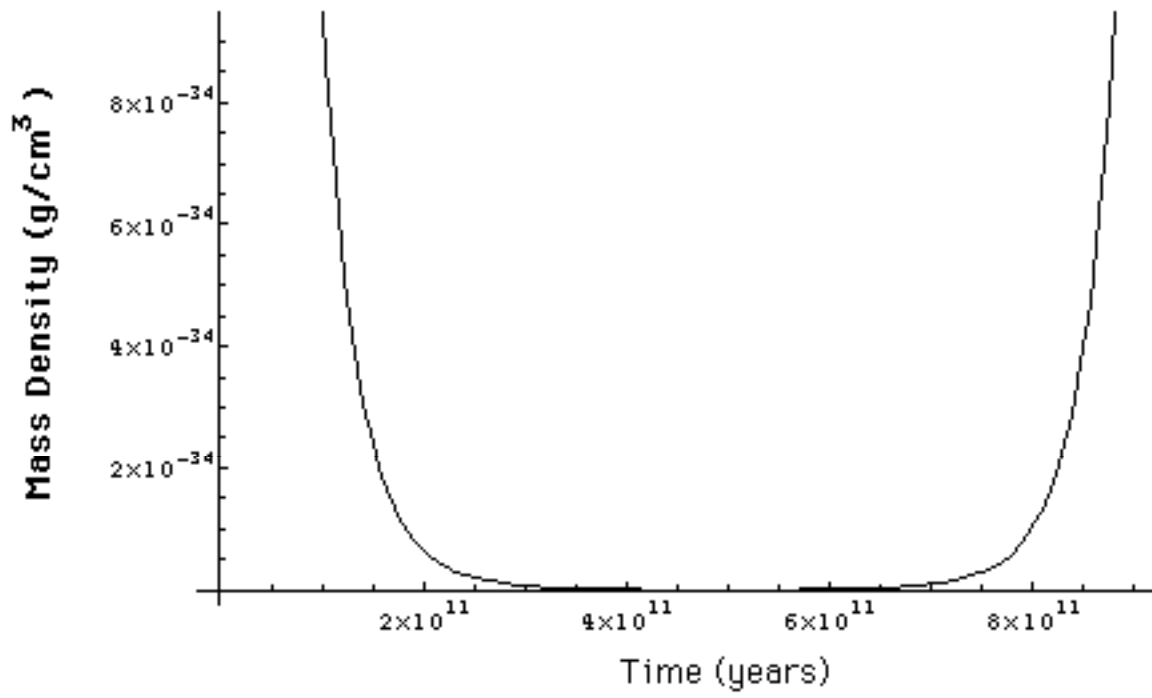


Fig. 19. The power of the universe as a function of time.

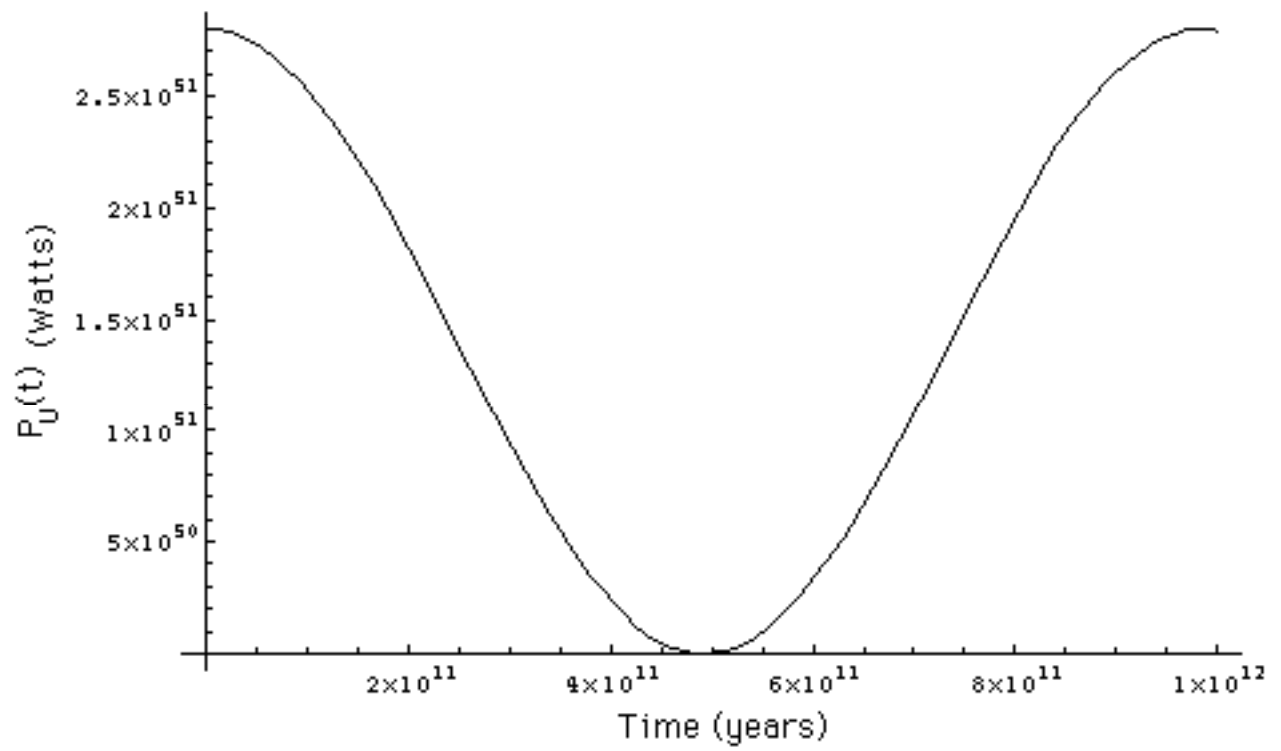


Fig. 20. The temperature of the universe as a function of time during the expansion phase.

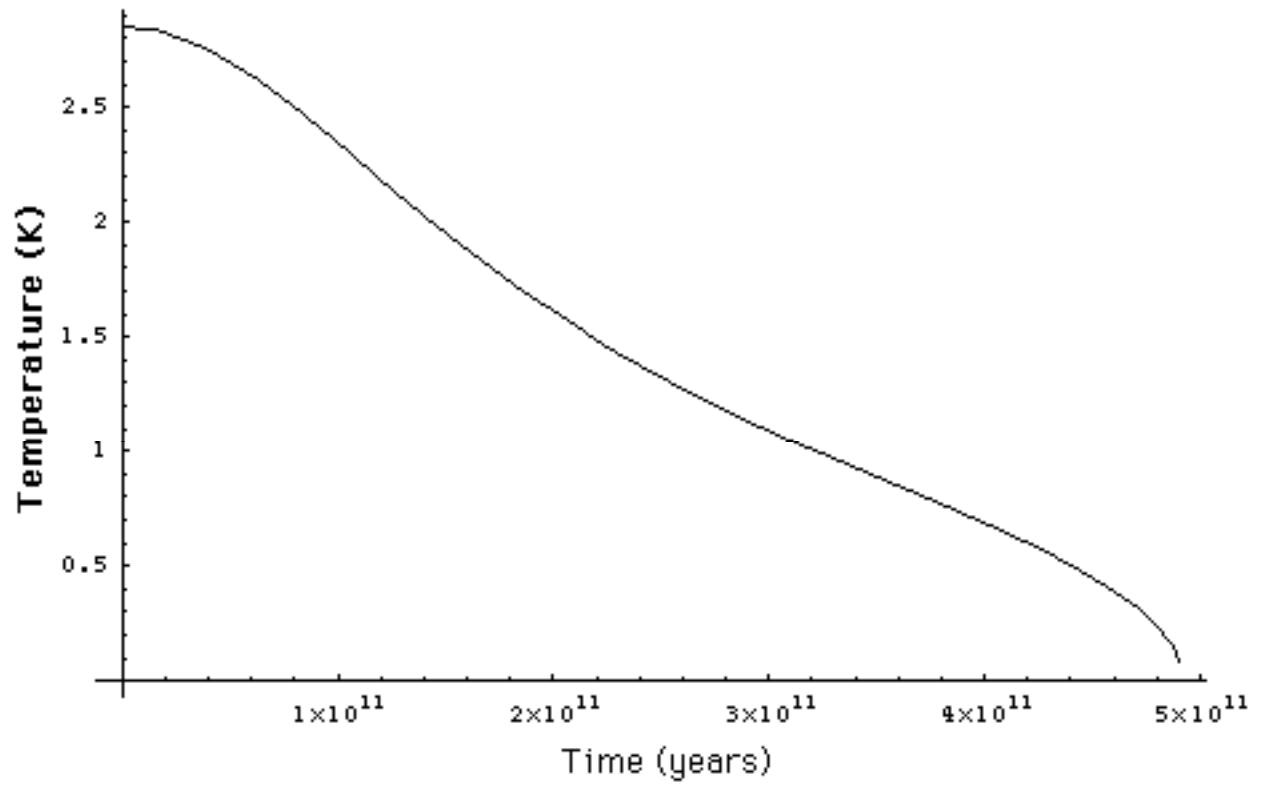


Fig. 21. The differential expansion of the light sphere due to the acceleration of the expansion of the cosmos as a function of time.

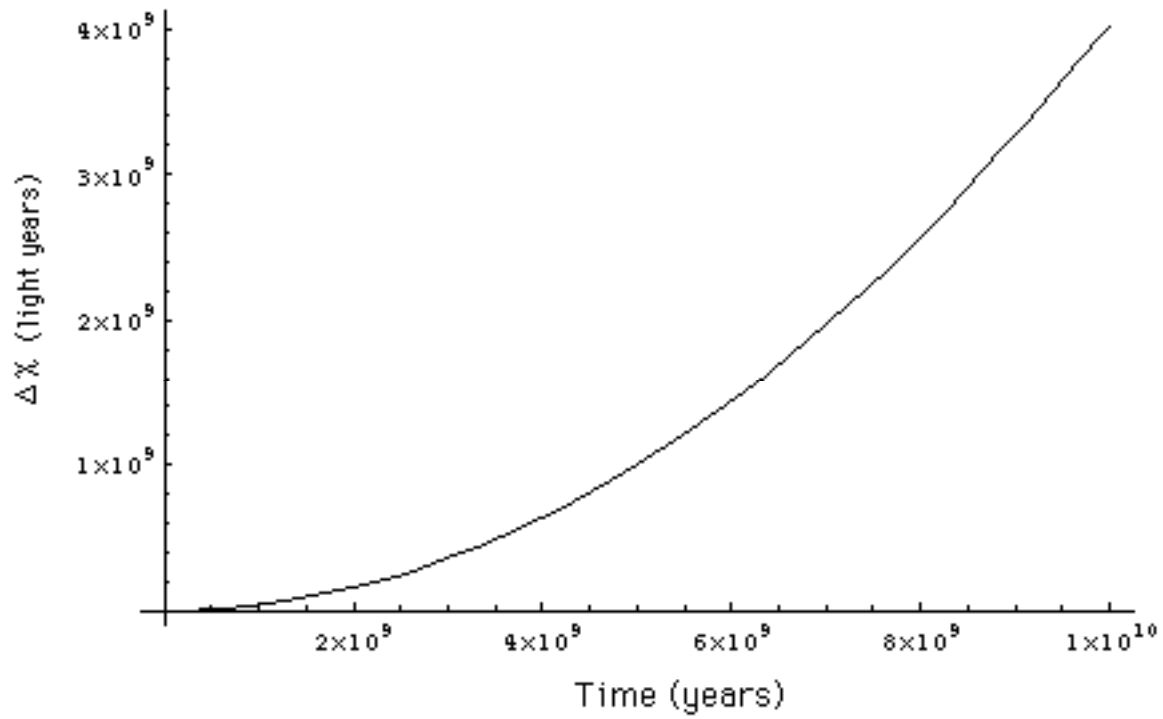


Fig. 22. Step One. Each point or coordinate position on the continuous two-dimensional electron orbitsphere defines an infinitesimal charge (mass)-density element which moves along a geodesic orbit comprising a great circle. Two such infinitesimal charges (masses) at points one (moving counter clockwise on the great circle in the  $y'z'$ -plane) and two (moving clockwise on the great circle in the  $x'z'$ -plane) of two orthogonal great circle current loops in the basis frame are considered as sub-basis elements to generate the current density corresponding to the spin quantum number,  $s = \frac{1}{2}$ ;  $m_s = \pm \frac{1}{2}$ . The  $xyz$ -system is the laboratory frame, and the orthogonal-current-loop basis set is rigid with respect to the  $x'y'z'$ -system that undergoes transformations to generate the elements of the electron current density function. The angular momentum of the orthogonal great circle current loops in the  $x'y'$ -plane is  $\frac{\hbar}{2\sqrt{2}}$ .

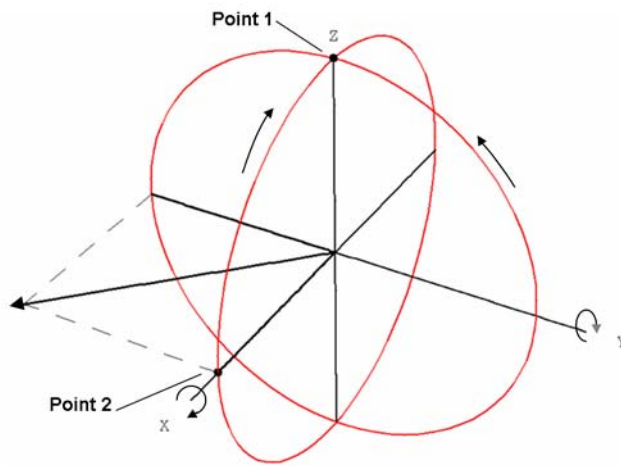


Fig. 23. Step Two. The orthogonal great circle basis set is rotated  $\Delta\alpha_x = \frac{\pi}{2}$  with respect to the basis set of Step One shown in Figure 22 the direction of the current of the loop in the  $y'z'$ -plane is reversed. Point one now moves clockwise on the great circle in the  $y'z'$ -plane, and point two moves counter clockwise on the great circle in the  $x'y'$ -plane. The angular momentum of the orthogonal great circle current loops in the  $-xz$ -plane is  $\frac{\hbar}{2\sqrt{2}}$  corresponding to each of the  $z$  and  $-x$ -components of magnitude  $\frac{\hbar}{4}$ .

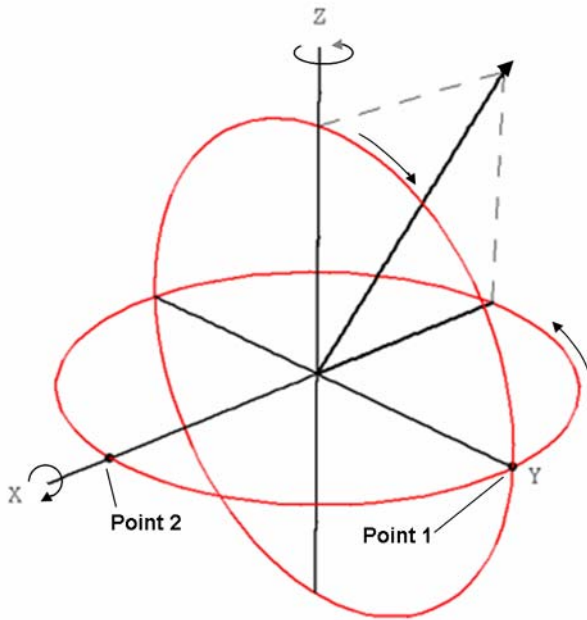


Fig. 24. The trajectory of the resultant angular momentum vector of the orthogonal great circle current loops of magnitude  $\frac{\hbar}{2\sqrt{2}}$  during Step One.

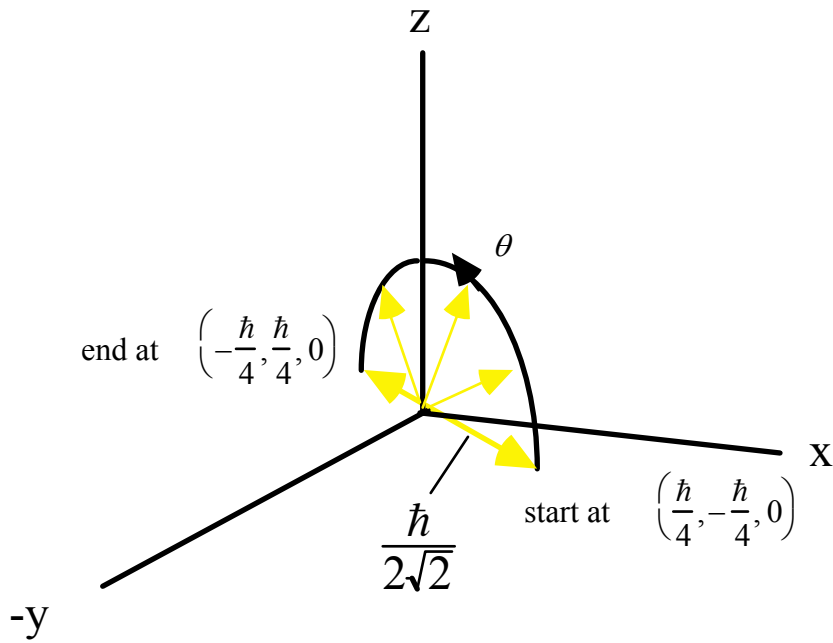


Fig. 25. The angular momentum components of the orbitsphere and  $\mathbf{S}$  in the rotating coordinate system  $X_R$ ,  $Y_R$ , and  $Z_R$  that precesses at the Larmor frequency about  $Z_R$  such that the vectors are stationary.

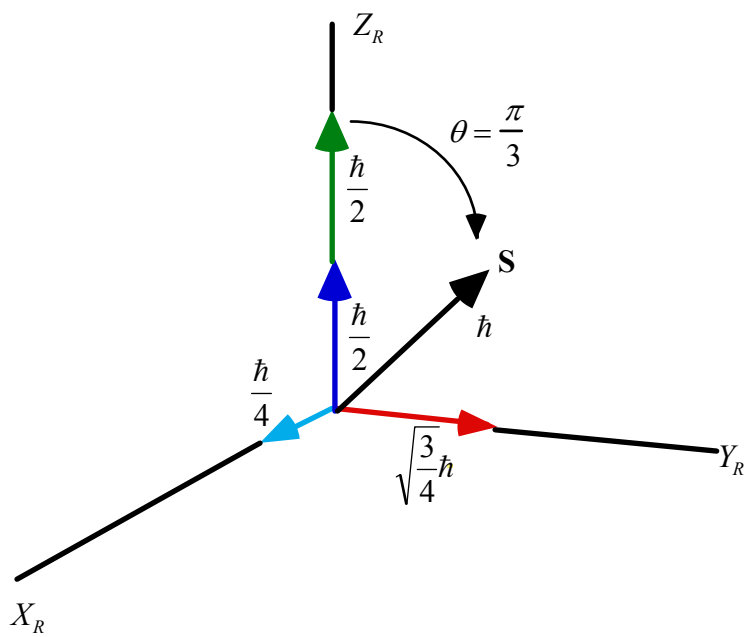


Fig. 26. The angular momentum components of the orbitsphere and  $\mathbf{S}$  in the stationary coordinate system.  $\mathbf{S}$  and the components in the  $xy$ -plane precesses at the Larmor frequency about the  $z$ -axis.

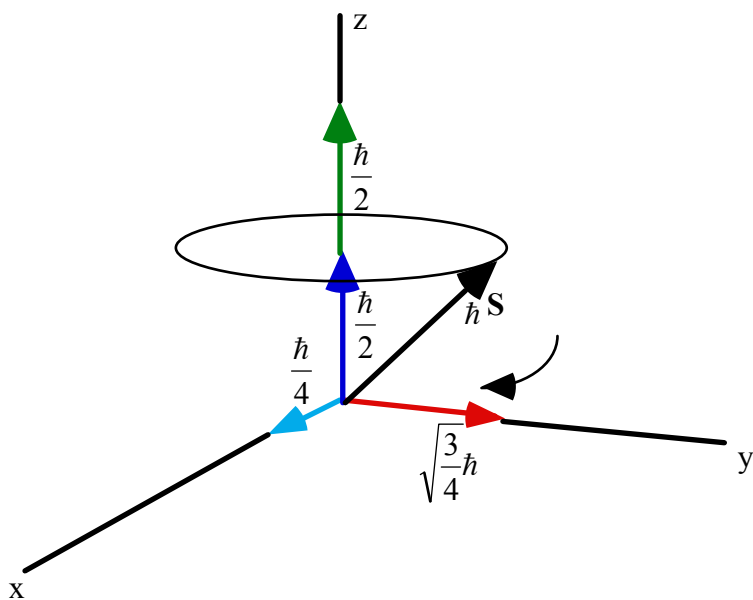


Fig. 27. Coordinate system of crossed electric field,  $\mathbf{E}_y$ , corresponding to the Hall voltage, magnetic flux,  $\mathbf{B}_x$ , due to applied field, and superconducting current  $\mathbf{i}_z$ .

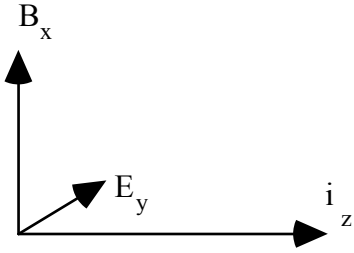


Fig. 28. Coordinate system of crossed electric field,  $\mathbf{E}_r$ , corresponding to the Hall voltage, magnetic flux,  $\mathbf{B}_\theta$ , due to applied field, and superconducting current  $\mathbf{i}_\phi$ .

